Coupling atmospheric dispersion model and geographical information systems : application to pesticide spray drift

N. Bozon

UNIVERSITÉ MONTPELLIER 2
SCIENCES ET TECHNIQUES

T H È S E

pour obtenir le grade de **DOCTEUR DE L'UNIVERSITE MONTPELLIER II**

Discipline	:	Mathématiques Appliquées
Formation Doctorale	:	Mathématiques
Ecole Doctorale	:	Information, Structures et Systèmes

présentée et soutenue publiquement le 6 juillet 2009 par

Nicolas BOZON

COUPLING ATMSOPHERIC DISPERSION MODEL AND GEOGRAPHICAL INFORMATION SYSTEMS: APPLICATION TO PESTICIDE SPRAY DRIFT

JURY

Pr. Bijan MOHAMMADI	, Univ. Montpellier II	, Directeur
Pr. Véronique BELLON-MAUREL	, Montpellier SupAgro	, Examinateur
Pr. Carole SINFORT	, Montpellier SupAgro	, Examinateur
Pr. Michel CUER	, Univ. Montpellier II	, Président
M. Sylvain LABBE	, Maison de la Télédetection	, Examinateur

RAPPORTEURS

Pr. Venkatesh RAGHAVAN	, Osaka City Univ. (jp)	, Rapporteur
Pr. Thierry JOLIVEAU	, Univ. Jean Monnet	, Rapporteur

Á Géraldine,
A ma soeur et à mes parents

Remerciements

Je ne saurais assez remercier le Pr.Bijan Mohammadi pour m'avoir proposer ce sujet de thèse ainsi que pour la qualité de l'encadrement scientifique qu'il m'a fournit durant ces trois années. Je n'oublierai jamais cette collaboration qui m'a permis d'évoluer et de préparer l'avenir.

Merci à la Région Languedoc Roussillon et au Cemagref d'avoir financer ce travail, et de m'avoir fournit des conditions de travail agréables ainsi que des moyens suffisants pour pouvoir atteindre les objectifs que je m'étais fixé .

Je remercie vivement le Pr.Véronique Bellon-Maurel et le Pr.Carole Sinfort pour leur soutien tout au long de ce travail. Je remercie également Sylvain Labbe pour ses conseils et ses idées avisées en géomatique. Je remercie aussi le Dr.Bernard Bonicelli et Bernadette Ruelle, ainsi que l'ensemble du personnel de l'UMR ITAP du Cemagref de Montpellier avec qui il fût très agréable de travailler.

Je remercie tous les membres du jury d'avoir accepté de juger ce travail ; qu'ils trouvent ici l'expression de ma profonde reconnaissance. Je remercie spécialement le Pr.Venkatesh Raghavan d'avoir bien voulu traverser la planète pour assister à ma soutenance. Sa venue à Montpellier a constitué la première étape d'une collaboration de recherche qui s'annonce prometteuse. Un grand merci également au Pr.Thierry Joliveau pour avoir juger mon travail et procurer des remarques constructives. Merci aussi au Pr.Michel Cuer de l'Université Montpellier 2 d'avoir accepter de présider ma soutenance.

Un grand merci également à René-Luc D'Hont et Michael Douchin de la société 3LIZ pour leur soutien et leur aide en SIG ainsi qu'en programmation.

Je salue le Dr.Ryad Bendoula aka " Le Coach " et le remercie grandement pour le soutien méthodologique et pyschologique qu'il m'a procuré, ainsi que pour les bonnes rigolades que l'on a pu avoir ensemble. Un merci spécial au Dr.Vincent Géraudie aka " Grand Maître " pour sa bonne humeur et sa joie de vivre, ainsi que pour m'avoir supporté dans le bureau pendant ces trois ans. Merci aussi à tous les autres copains du laboratoire !

Merci à mon amie Géraldine d'avoir accepter cette période d'éloignement géographique et d'avoir cru en moi. Je remercie enfin ma famille, André, Jacqueline et Floriane à qui je dois beaucoup. Merci de m'avoir soutenu et encourager jusqu'au bout.

Aknowledgments

I could not thank Pr.Bijan Mohammadi enough for proposing this phD subject and for the high qualtiy scientific direction he provided to me. I will never forget this collaboration which made me evolve and prepare the future.

Thanks to the Region Languedoc Roussillon and to Cemagref for funding this work, and for providing an excellent working environment as well as sufficent fundings for me to reach the objectives I had planned.

I also strongly thank Pr.Véronique Bellon-Maurel and Pr.Carole Sinfort for their help. Thanks to Sylvain Labbe for the acute ideas and advices about geomatics he provided. I also want to thank Dr.Bernard Bonicelli and Bernadette Ruelle, as well as all the UMR ITAP staff from Cemagref of Montpellier. It was really pleasant to work with all of them.

I thank every member of the jury for accepting to judge my work. A special thank goes to Pr.Venkatesh Raghavan who has accepted to report this work and to cross the planet for attending my presentation. His trip to Montpellier was the first step of a promising reseacrh collaboration. Thanks also to Pr.Thierry Joliveau for judging my work and providing interesting remarks. Thanks to Pr.Michel Cuer from University of Montpellier 2 who chaired my presentation as the president.

A big thank to René-Luc D'Hont and Michael Douchin from the 3LIZ company for their help in GIS and programming.

I also want to thank Dr.Ryad Bendoula aka " Le Coach " for the methodological and psychological help he provided. Thanks for the good times we had together. A special thank to Dr.Vincent Géraudie aka " Grand Maître " for his buoyancy and joie de vivre, and for bearing me at office during these three years. Thanks to all the friends from the lab.

I thank my friend Géraldine for accepting this long time away and for beliving in me. Thanks to my family, André, Jacqueline and Floriane to whom I owe a lot. Thank you for supporting me all along this work.

Contents

Introduction (fr.) 1

Introduction (en) 6

I Coupling atmospheric dispersion modeling and GIS 11

1 Atmospheric dispersion modeling 13
- 1.1 Atmospheric layers . . . 13
  - 1.1.1 Atmospheric boundary layer . . . 13
  - 1.1.2 Planetary surface layer . . . 14
  - 1.1.3 Wind flows within the PSL . . . 15
- 1.2 Atmospheric dispersion modeling . . . 16
  - 1.2.1 Atmospheric dispersion models . . . 16
  - 1.2.2 General ADM structure . . . 17
  - 1.2.3 Main parameters affecting ADM . . . 18
  - 1.2.4 Conclusion . . . 19

2 GIS assets and limitations for ADM 20
- 2.1 GIS fundamentals . . . 20
  - 2.1.1 Definitions . . . 20
  - 2.1.2 GIS data models . . . 21
- 2.2 GIS and ADM cross-cutting thematics . . . 23
  - 2.2.1 Coordinate systems . . . 23
  - 2.2.2 Scales . . . 24
  - 2.2.3 Time . . . 25
  - 2.2.4 Conclusion . . . 25

3 Coupling ADM and GIS 26
- 3.1 Coupling techniques . . . 26
  - 3.1.1 Isolated applications . . . 26
  - 3.1.2 The loose coupling . . . 26
  - 3.1.3 The tight coupling . . . 27
  - 3.1.4 Full integration . . . 27
- 3.2 Review of existing ADM/GIS couplings . . . 27

3.2.1 CFD based couplings . . . 27
3.2.2 GIS based couplings . . . 28
3.2.3 Conclusion on ADM/GIS couplings . . . 30

II Spatial modeling of pesticide atmospheric dispersion 31

4 Pesticide spray drift modeling 33
4.1 Problem formulation . . . 33
4.1.1 Context . . . 33
4.1.2 Past research . . . 34
4.2 Drift-X model principles . . . 34
4.2.1 An alternative to the use of CFD . . . 34
4.2.2 Assumptions and hypothesis . . . 35
4.2.3 A reduced order modeling approach . . . 36
4.3 Transport and non-symmetric geometry . . . 37
4.3.1 Non-symmetric geometry . . . 37
4.3.2 Calculation of migration times . . . 39
4.3.3 Generalized plume solutions . . . 40
4.3.4 Flow field . . . 41
4.4 Conclusion . . . 42

5 Scale changes implementation into Drift-X 43
5.1 Introduction . . . 43
5.2 Multi-level construction . . . 43
5.2.1 Integral data . . . 45
5.2.2 Multilevel correction for ground variations . . . 45

6 Numerical results 51
6.1 Simple simulations . . . 51
6.2 Topographic impact . . . 54
6.3 Sensitivity to DEM resolution . . . 56
6.4 Multi-leveled simulations . . . 59
6.4.1 Scalable simulations . . . 59
6.4.2 Multi-leveled pesticide cloud . . . 60

7 The Drift-X simulation platform 62
7.1 Fortran ADM . . . 62
7.1.1 The Drift-X inputs . . . 63
7.1.2 The Drift-X outputs . . . 64
7.2 Open source geospatial software for ADM . . . 64
7.2.1 Quantum GIS API . . . 64
7.2.2 Drift-x plugin development . . . 65
7.3 The multi-level algorithm implementation . . . 67
7.3.1 Scales and extents . . . 67
7.3.2 Limitations and perspectives . . . 67

7.4 Standard GIS formats rendering . . . 68
7.4.1 Vector representations . . . 68
7.4.2 Raster representation . . . 70
7.4.3 Drift-X plugin GUI . . . 71

III Neffiès watershed: A case study **73**

8 A typical southern French wine-growing area **75**
8.1 The geographic context of the study area . . . 75
8.2 The Life Aware project . . . 77
8.3 Avalaible datasets . . . 77
8.3.1 Geospatial data . . . 78
8.3.2 Meteorological data . . . 78

9 Linking Drift-X to real-time agro-meteorological database **79**
9.1 The Aware PostGIS database . . . 79
9.1.1 Spraying applications as a relational database . . . 79
9.1.2 Spraying applications statistics . . . 80
9.2 Using PostGIS from Drift-X plugin . . . 82
9.2.1 Neffiès dedicated Drift-X plugin . . . 82
9.2.2 Querying PostGIS from Python . . . 82

10 Drift-X for pesticide exposure risk assessment **84**
10.1 Simultaneous Drift-X simulations . . . 84
10.1.1 Input parameters . . . 84
10.2 Using GRASS GIS for exposure risk assessment . . . 86
10.2.1 GRASS GIS presentation . . . 86
10.2.2 Land use data description . . . 86
10.2.3 Intersecting CLC and Drift-X raster layers . . . 87
10.2.4 Zonal statistics . . . 87

Conclusion (en) **90**

Conclusion (fr) **94**

List of figures **99**

List of Acronyms **102**

Bibliography **107**

Résumé - La pollution atmosphérique par les pesticides issus de la viticulture est un problème environnemental majeur affectant aussi bien la santé humaine que l'équilibre des écosystèmes. La modélisation de la dispersion atmosphérique et l'usage des systèmes d'information géographique peuvent permettre de quantifier spatialement la pollution atmosphérique sur le territoire. Cette thèse est fondée sur le couplage d'un modèle de dispersion atmosphérique des pesticides et d'un système d'information géographique, destiné à prédire et cartographier la pollution atmosphérique après les traitements phyto-sanitaires. L'introduction des modèles numériques de terrains et des changements d'échelle dans la modélisation à complexité réduite sont présentés et illustrés. La plateforme de simulation numérique découlant du couplage prend la forme d'un plugin au logiciel Quantum GIS, explorant ainsi le potentiel des SIG libres dans l'implémentation de modèles physiques complexes. La plateforme est finalement utilisée sur un bassin versant viticole du Sud de la France, et un scénario d'analyse des risques de pollution est proposé.

Mots-clés: *Couplage, Dispersion atmosphérique, Pesticides, Viticulture, Modélisation à complexité réduite, Système d'Information Géographique, Modèle Numérique de Terrain, Quantum GIS, SIG libre.*

Abstract - Atmospheric pollution due to agricultural pesticide for viticulture is a major concern today, regarding both public health, sustainable agriculture and ecosystems quality monitoring. Atmospheric dispersion modeling and the use of geographic information systems allow us to spatially quantify the atmospheric pollution on a given area. This thesis is based on the coupling of an atmospheric dispersion model and a geographic information system, in order to predict and map atmospheric pollution after pesticide spraying applications. Implementations of digital elevation models and scale changes into the reduced order modeling are described and illustrated. The resulting simulation platform is presented as a Quantum GIS software plugin, thus exploring the Open Source GIS capabilities to implement complex physical models. The platform is finally used on a typical Souther French wine-growing area, and a pollution risk analysis scenario is proposed.

Key-words: *Coupling, Atmospheric dispersion, Pesticide, Viticulture, Reduced order modeling, Geographic Information Systems, Digital Elevation Model, Quantum GIS, Open Source GIS*

Nicolas BOZON

Cemagref Montpellier - UMR ITAP
351, rue Jean François Breton
34196 Montpellier Cedex 5 (France)
email: nicolas.bozon@gmail.com

Introduction

La pollution atmosphérique par les pesticides d'origine agricole est un problème environnemental majeur affectant aussi bien la santé humaine que l'équilibre des écosystèmes. Ce sujet a d'ailleurs été mis de l'avant lors du Grenelle de l'environnement en 2007, lorsque le gouvernement proposa de réduire de moitié les applications de pesticides, démontrant ainsi la prise de conscience publique grandissante à propos des risques liés aux pesticides. Bien que l'usage systématique des pesticides soi taujourd'hui remis en question par des alternatives telles que la protection intégrée des cultures (PIC) ou l'agriculture biologique, les produits phytosanitaires représentent une source importante de pollution atmosphérique et leurs effets négatifs sont prouvés.

En effet, les pratiques agricoles modernes sont fondées sur l'utilisation massive de pesticides pour controler la qualité et le rendement des récoltes. Ceci est particulièrement le cas en viticulture qui est l'une des cultures les plus consommatrice de pesticides après les céréales [1]. Les progrès de la protection du vignoble et les nouvelles solutions chimiques ont contribué à l'augmentation des récoltes et assurer des rendements réguliers aux viticulteurs.

La plupart des vignobles francais sont concernés par l'utilisation de pesticides. Ainsi, la France est le troisième utilisateur de pesticide dans le monde et présente la plus grande consommation en Europe, avec un volume total de 76,100 tonnes de matières actives vendues en 2004, et un taux de consommation approchant les 5,4 kg/ha pour la même année selon le raport mené par le Cemagref et l'INRA [2]. La même étude souligne que la viticulture francaise occupe 0.860 Mha soit moins de de 4% de la surface agricole utile, mais représente près de 20% de la consommation nationale de pesticides [2].

En effet, *Vitis vinifera* est soumise à plusieures maladies cryptogamiques comme le Mildiou *(Plasmopara viticola)*, l'oïdium *(Uncinula necator)* ou la pourriture grise *(Botrytis cinerea)*, pouvant provoquer d'importants dommages. Les pieds de vigne sont très sensibles aux espèces invasives et ont besoin d'etre traités avec des méthodes de pulvérisation et des produits spécifiques. Ces derniers se répendent ensuite dans l'environnement notamment par dérive atmosphérique qui représente un des vecteurs de contamination majeur.

La dispersion atmosphérique des pesticides peut être expliquée simplement comme suit. Les produits phytopharmaceutiques sont appliqués sur la vigne à l'aide d'un pulvérisateur, qui est une machine agricole permettant de diffuser les pesticides en assurant la

pénétration du produit dans la végétation. Le pulvérisatur est habituellement porté ou tracté par un tracteur comme le montre la figure 1.

Figure 1: Pulvérisateur typique utilisé dans les vignobles du sud de la France

Les pesticides se diffusent ensuite dans plusieures directions pendant que le pulvérsiateur traite la parcelle. Une part atteind la végétation, une autre part est déposée au sol, et le reste s'éleve au dessus de la parcelle et est transportée par le vent. Ceci provoque la formation d'un nuage de pesticides (figure 2) se dispersant dans l'environnement [3].

Figure 2: Nuage de pesticides observé tôt le matin à Neffiès (34)

De nombreuses études agro-météorologiques s'intéressent à la dérive des pesticides et à son impact sur l'environnement. Certaines d'entre elles sont établies à l'échelle micro

et permettent d'analyser la dispersion en champ proche ou les flux de pesticide au sein d'une parcelle cultivée [4]. Les études en champs proches tendent à devenir de plus en plus précises grâce notamment à l'utilisation de la dynamique des fluides assistée par ordinnateur (CFD), qui permet par exemple d'étudier l'optimistation de la taille des gouttes en utilisant des modèle de buses en 3D [5], ou encore de quantifier les flux d'air au sein des rangs de vignes en se basant sur des modèles 3D de végétation [6]. D'autres études permettent d'estimer la volatilisation post-traitement des pesticides [7], et de quantifier par exemple les quantités de produits s'élevant au dessus de la parcelle [8]. Ces travaux sont généralement validés grâce à des simulations en soufflerie et/ou par des expériences au champ afin de pouvoir comparer les résultats des modèles numériques avec des jeu de données réels.

Ainsi, la connaissance de la dispersion des pesticides en champs proche est de plus plus précise et permet aux scientifiques de caractériser les émissions de pesticides dans la couche limite atmosphérique pendant et après les traitements [9]. Ceci constitue un atout majeur pour la modélisation du transport des pesticides à plus grande distance, car les résultats validés des modèles à petite échelle peuvent être utilisés comme données d'entrée dans les différents modèles de dispersion atmosphérique disponibles. Bien que de nombreux modèles soient efficaces sur de petits domaines (quelques mètres carrés), seulement quelques uns sont adaptés et validés pour des domaines plus larges (quelques kilomètres carrés), et les simulations de dérive des pesticides ne sont que rarement menées à l'échelle du bassin-versant. Cela constitue notre interêt de recherche principal sur lequel la problématique est construite.

Des outils modernes tels que la télédétection et les systèmes d'information géographique (SIG) ont procuré de nouvelles dimensions à la gestion des ressources naturelles et la prévention des risques, et il est aujourd'hui globalement accepté que la géomatique a un important rôle à jouer dans le zonage agricole [10], le développement de l'agriculture durable mais aussi dans les études agro-météorologiques. L'idée de coupler un modèle de dispersion atmosphérique avec les SIG est donc justifiée pour améliorer la précision et l'étendue des simulations de dérive des pesticides.

Les technologies géomatiques sont devenues des outils essentiels pour combiner différentes couches d'informations géospatiales et statistiques, permettant ainsi de simuler certaines intéractions avec processus physiques complexes [11] comme la dispersion atmosphérique. De plus, les SIG et la modélisation de la dispersion atmosphérique présentent de nombreuses similarités concernant leurs modèles de données, qui sont tous deux basés sur les systèmes de coordonnées et les notions d'échelles temporelles et spatiales. Les équations de dispersion et de transport font intervenir de nombreux paramètres soumis à d'importantes variations spatio-temporelles [12] qui affectent fortement le comportement des nuages de pesticides. La dimension spatiale est donc primordiale dans la modélisation atmosphérique, mais représente aussi le paradigme des SIG [13]. Ces derniers représentent donc des outils idéaux pour formaliser, analyser et visualiser les variations spatiales de la dispersion atmosphérique.

Toutefois, on observe une certaine incompatibilité entre la difficulté des SIG à simuler dynamiquement certains processus physiques [14], et les méthodes de modélisation utilisées par les mathématiciens ou les physiciens pour mener des analyses environnementales qui ne supportent que rarement les données et les analyses géospatiales [15]. Le concept de couplage découle de ce constat et s'avère nécessaire tant pour les experts en modélisation [16] de manière à adapter leurs modèles à la réalité géographique des zone d'études, que pour les géomaticiens afin de tirer profit des modèles dans les analyses spatiales et statistiques des phénomènes complexes.

L'objectif scientifique de cette thèse est de développer un cadre méthodologique pour le couplage d'un modèle de dispersion atmosphérique et d'un SIG selon la méthode de couplage "fort" [17, 18]. Ce dernier permet de faire communiquer les deux systèmes par l'utlisation des modèles numériques de terrains (MNT) comme source de donnée commune, et de mettre en place des échanges de données bilatéraux. Cela implique premièrement de modéliser la dispersion atmosphérique et de l'adapter à un environnement SIG, puis de prendre en compte les changements d'échelles présentés par le processus de dispersion atmosphérique, grâce à une nouvelle approche méthodologique. Le couplage proposé doit allier la force des SIG pour la gestion des informations spatiales et le pouvoir des mathématiques appliquées pour modéliser des phénomènes complexes. Un objectif sous-jacent est de coupler le modèle de dispersion et le SIG techniquement, en construsiant un logiciel SIG capable de générer des simulations géoréferencées de la dispersion atmosphérique.

La première partie de cette étude est intitulée "Coupling ADM and GIS" et est composée de trois chapitres. Le premier entend rappeler des notions fondamentales tant par rapport à la modélisation de la dispersion atmosphérique et qu'au fonctionnement des SIG, puis de souligner les nombreux liens possibles entre les deux disciplines, notamment grâce à une revue bibliographique des couplages existants.

La seconde partie intitulée "Spatial modeling of atmospheric dispersion" regroupe quatre chapitres. La modélisation de la dispersion atmosphérique est d'abord présentée et les concepts mis en oeuvre détaillés, notamment à propos de l'approche à compléxité réduite qui a été utilisée. Les changements d'échelle sont ensuite modélisés à travers une construction multi-niveaux, de manière à prendre en compte la dispersion atmosphérique de la parcelle au bassin-versant. Les résultats du modèle et de sa version multi-echelle sont ensuites exploités au sein du troisième chapitre qui regroupe des résultats numériques variés. L'influence topographique sur la dispersion et la sensibilité du modèle à la résolution des MNT sont notamment approfondies. Différents types de MNT et plusieures projections cartographiques sont utilisés afin de démontrer la souplesse du modèle. Enfin, le dernier chapitre présente la plateforme de simulation Drift-X, qui couple le modèle de dispersion réalisé avec le Système d'Information Géographique Quantum GIS. Cet aspect technique du couplage aborde des éléments de programmation SIG, et démontre notamment comment les Modèles Numériques de Terrain (MNT) sont utilisés pour faire communiquer les deux systèmes dans le sens d'un couplage fort.

La dernière partie entend exploiter le couplage dans le cadre d'une étude de cas centrée sur le bassin versant de Neffiès, qui constitue une zone viticole typique du sud de la France. Le contexte géographique de la zone et l'ensemble des données spatiales et météorologiques disponibles sont présentées dans le premier chapitre. L'exploitation d'une base de données agro-météorologique par le modèle Drift-X et la mise en oeuvre de simulations sur la base de données topographiques et météorologiques réelles sont ensuite détaillées dans un second chapitre. Le lien avec la base de données ont permis d'identifier un scénario qui sera utilisé dans le troisième et dernier chapitre, à travers une analyse des risques d'exposition à la pollution au sein de l'environnement proche du nuage de dispersion. Des données d'occupation du sol de référence sont notamment utilisées et mise en relation avec les sorties de Drift-X, de manière à proposer des cartes de risques simplifiées.

Cette thèse et certains des résultats qu'elle contient ont donnée lieu aux distinctions, communications et publications suivantes:

- Bozon, N. and Mohammadi B. "***2008 Geo-Grenelle Award***". Institut Géographique National. 20th edition of the Geo-Evenements conferences - April 8th, 9th and 10th, 2008

- Bozon, N. and Mohammadi B. "*GIS-based atmospheric dispersion modelling*". Free and Open Source Software for Geospatial, FOSS4G 2008 - Cape Town (SA) - September 29th - October 4th, 2008.

- Bozon, N. and Mohammadi, B. "*GIS based atmopsheric dispersion modelling Forecasting the pesticide atmospheric spray drift from a vineyard plot to a watershed.*". Applied Geomatics. Vol.1. Springer, 2009, accepted.

- Bozon, N., Mohammadi, B. and Sinfort, C. "*Similitude and non symmetric geometry for dispersion modelling*". Proceeding of STIC and Environment 2007. 5th edition. e-sta Vol.5, number 2, 2007.

- Bozon, N., Mohammadi, B. and Sinfort, C. "*A GIS-based atmospheric dispersion model*". Proceeding of STIC and Environment 2009. Hermès, 2007, in revision process.

Introduction

Atmospheric pollution due to agricultural pesticide is a major concern today, regarding both public health, sustainable agriculture and ecosystems quality monitoring. This topic by the way belonged to the 2007 French "Grenelle de l'Environnement" highlights, as the government proposed to halve pesticide use within the next ten years, demonstrating the increasing public awareness of risks implied by pesticide. Despite the systematic use of pesticide is being called into question by several alternatives such as biological agriculture or Integrated Pest Management (IPM), chemicals still represent an important source of atmospheric pollution, and their undesirable adverse effects on the environment are proven.

Indeed, modern agricultural practices are based on the massive use of phytopharmaceutical products to control crops quality and quantity. This is particularly true about viticulture, which is one of the most pesticide consuming culture after cereals [1]. Advances in vineyards protection and new chemical solutions have contributed to increasing yields and to ensuring regular quality production to agricultural exploitations. Chemical control products have proved to be extremely efficient and allow the pesticide penetration within canopies.

Most French vineyards are concerned by the use of fertilizers and pesticide. As a matter of fact, France ranks third in the world for pesticide consumption and is the leading user in Europe, with a total volume of 76,100 tonnes of active substances sold in 2004, and a corresponding consumption rate approaching 5,4 kg/ha for the same year, according to the collective scientific expertise from Cemagref and INRA research centers [2]. The same study highlights that French viticulture occupies about 0.860 Bha which amounts to less than 4% of the french utilized agricultural area (UAA), but uses 20% of the total national pesticide counsumption [2]. This situation is not due to excessive quantities applied on vineyards in one application, but rather to the numerous applications carried all along the growth and ripeness phases of cultures.

Indeed, *Vitis vinifera* is prone to several crytogamic diseases such as Mildiou *(Plasmopara viticola)*, Oïdium *(Uncinula necator)* or Gray mold *(Botrytis cinerea)*, that can lead to important damage. Vine stocks are very sensitive to invasive species such as fungies, and need to be massively treated using specific spraying methods and dedicated pesticide. The latter then spread in the environment in many ways, and atmospheric spray drift represents one of the major vector of contamination.

Atmospheric dispersion of pesticide can be basically explained as follows. Phytopharmaceutical products are usually spread over the plots using a sprayer, which is an agricultural machine allowing to spray pesticide over large areas. It is most of the time towed or suspended from a tractor, as shown in figure 3.

Figure 3: Typical sprayer used in southern French vineyards

Sprayed pesticides then spread in several directions while the sprayer runs through the vineyards. Some of it reaches the vine leaves and grapes, some reaches the ground and run-off on soils and the rest leaves the plot to be transported by the wind. This forms a pesticide cloud, as shown by figure 4, that is prone to dispersion and depositing in the environment [3].

Figure 4: Early morning pesticide cloud observed at Neffiès (34)

Many agro-meteorological studies are focusing on the spray drift process and on its impacts on the environment. Some of them are established at the micro-scale level and provide some knowledge on the near-field atmopsheric dispersion process, or on the pesticide flows within a cultivated plot [4]. Near-field studies tend to become very accurate using Computational Fluid Dynamics (CFD) principles, focusing for example on droplets size optimization using spraying nozzle 3D models [5], or modeling 3D plant models to best quantify airflows within the plant rows [6]. Other studies allow to estimate the post-treatment volatilization of pesticide species [7], and to quantify their atmospheric concentrations above vineyards [8]. Those studies are most of the time validated using wind tunnel devices or field experiments in order to compare models numerical results with measured value datasets.

Thus, the near-field spray drift modeling becomes more and more accurate and enables scientists to characterize pesticide emissions to the air during and after the treatments [9]. This is a major asset to model the long-range transport of pesticide, as the results of validated micro-scaled models can be used as input data in the different atmospheric dispersion models available. Despite the fact that many models prove to be efficient on small domains (i.e a few square meters), only a few are adapted and validated for larger areas (i.e a few square kilometers) and simulations of atmospheric spray drift are seldom performed at the watershed scale. It is the interest of our research and the issue on which our problem question is based.

As modern tools such as satellite remote sensing and Geographical Information Systems (GIS) have been providing newer dimensions to effectively monitor and manage natural resources, and as it has been well conceived in the last decades that GIS has a great role to play in agricultural zoning [10], sustainable agriculture development but also agro-meteorology applications, the idea of coupling ADM and GIS to enhance our work came up quite early in order to forecast pesticide spray drift on larger domains.

GIS technology has thus become an essential tool for combining various map and statistical data in models that simulate the interactions of complex natural systems [11] such as atmospheric dispersion. Moreover, GIS and ADM present many similarities in the concepts of their data model, which are both based on coordinate systems, scale and time. ADM equations are bringing many parameters into play which are most of the time influenced by spatial and temporal variations [12]. These strongly affect the dispersion and transport of pesticide clouds. The spatial dimension is thus essential in ADM, but also represents the GIS paradigm [13]. The last mentioned therefore represent ideal tools to formalize, analyze and visualize the atmospheric dispersion models spatial variations.

However, we can observe a kind of incompatibility between GIS lack of capabilities to simulate certain physical processes dynamically [14], and the modeling methods used by mathematicians or physicians to perform environmental simulations that rarely support spatial datasets and analysis [15]. The coupling concept stems from this observation and turns out necessary both for modelers [16] to apply their models in the landscape

geographic reality and for GIS experts to take advantage of advanced models in spatial and statistical analysis of complex physical processes.

The scientific objective of this thesis is to develop a methodological framework for coupling an atmospheric dispersion model with GIS according to the "tight" coupling approach [17, 18]. The latter tends to make two different systems communicate through the use of DEM layers as a common data source, and to implement bilateral parameters transfer. This implies first to model the pesticide atmospheric dispersion in a GIS environment, and then to manage the scale changes presented by the atmopsheric dispersion process, thanks to a new methodological approach. The intended coupling must gather the GIS ability to manage spatial information and the power of applied mathematics. An underlying objective is to achieve the coupling technically, by building a GIS-based software able to perform georeferenced atmospheric dispersion simulations.

The first part of this study is called "Coupling ADM and GIS", and is composed of three chapters. The first one aims to recall both ADM and GIS fundamentals and to underline the many possible links between the two, and notably contains a review of existing such couplings. The second chapter aims to present the retained reduced-order modeling approach regarding pesticide atmospheric transport and to provide a detailed description of the resulting model. The third chapter finally adds some technical specifications on effective GIS-based coupling and the use of Digital Elevation Models (DEM) as a cross-platform data source.

The second part is called "Spatial modeling of atmospheric dispersion" and gathers four chapters. The first one presents the Drift-X atmospheric dispersion model and the concepts it is based on, notably regarding the reduced order approach it uses and some of its simplifications. Scale changes implementation are presented in the second chapter. A multi-leveled construction is proposed and coupled with GIS, in order to account for the whole dispersion process, from the vineyard plot to the watershed. Simple and multi-leveled simulations resulting from the modeling are then presented in the third chapter. GIS based numerical results are performed using several DEM types according to several cartographic projections, in the aim to highlight the flexibility of the coupling. The topographic impact on the atmospheric dispersion process but also the model's sensitivity to DEM resolution are notably detailed. The last chapter finally explores the open source GIS capabilities for scripting and enhancing the presented model, and focuses on its coupling with the Quantum GIS API. The resulting software is presented as a Quantum GIS plugin and illustrated through several code snipets. The development side of the coupling notably show how DEM layers are used as a cross-platform datasource, tending to a tight coupling approach.

The last part finally gathers the different sides of the coupling through a case study carried out in the Neffiès watershed which is a typical southern French wine-growing area. Geographic context and the available geospatial and meteorological datasets are presented in the first chapter. The use of an agro-meteorological within the Drift-X model is then

proposed in order to set up simulations with realistic topographies and meterological data. This allowed to identify a scenario which is used in the last chapter. Reference landuse data layers are notably used in interaction with the Drift-X outputs, in order to propose a simplified risk analysis using basic geostatistical methods.

This thesis and the presented results gave rise to the following distinctions, communications and publications:

- Bozon, N. and Mohammadi B. "***2008 Geo-Grenelle Award***". Institut Géographique National. 20th edition of the Geo-Evenements conferences - April 8th, 9th and 10th, 2008

- Bozon, N. and Mohammadi B. "*GIS-based atmospheric dispersion modelling*". Free and Open Source Software for Geospatial, FOSS4G 2008 - Cape Town (SA) - September 29th - October 4th, 2008.

- Bozon, N., Mohammadi, B. and Sinfort, C. "*Similitude and non symmetric geometry for dispersion modelling*". Proceeding of STIC and Environment 2007. 5th edition. e-sta Vol.5, number 2, 2007.

- Bozon, N., Mohammadi, B. and Sinfort, C. "*A GIS-based atmospheric dispersion model*". Proceeding of STIC and Environment 2009. Hermès, 2007, in revision process.

- Bozon, N. and Mohammadi, B. "*GIS based atmopsheric dispersion modelling Forecasting the pesticide atmospheric spray drift from a vineyard plot to a watershed.*". Applied Geomatics.Springer, 2009, accepted.

Part I

Coupling atmospheric dispersion modeling and GIS

Chapter 1

Atmospheric dispersion modeling

This chapter aims first to recall some general meteorology aspects and to provide some basic knowledge on the atmosphere structure and on wind physical processes. The atmospheric boundary layer (ABL) and the planetary surface layer (PSL) where atmospheric dispersion occurs are presented in the first section, because the surface effects they entail, such as turbulent mixing, strongly influence atmospheric dispersion.

Atmospheric dispersion modeling (ADM) is then introduced in the second section. The general goals of atmospheric dispersion models are described and an atmospheric dispersion model structure is proposed. The main parameters affecting ADM will finally be itemized in particular as regards pollutant emissions, winds and topography.

1.1 Atmospheric layers

The Earth's atmosphere is usually divided into five layers from the surface to space, namely troposphere, stratosphere, mesosphere, thermosphere and exosphere as shown on figure 1.1. In this work, we will focus on the troposphere which is the lowest layer of the atmosphere, where atmospheric dispersion processes of our interest are taking place. Indeed, most meso-scaled atmospheric dispersion processes like pesticide spray drift occurs near the ground within the lowest part of the troposphere called the atmospheric boundary layer, which is described below.

1.1.1 Atmospheric boundary layer

The ABL, also known as planetary boundary layer or peplosphere, consists of the lowest area of the troposphere and its behavior is strongly influenced by its contact with the Earth's surface. It is stretched from the surface up to 1 to 2.5 km depending on the surface's topography, and presents a high level of turbulence. Indeed, in this layer physical quantities such as flow velocity, temperature or moisture display rapid fluctuations (turbulences), and flow fields located near the surface are encountering obstacles that reduce the wind speed, and so introduce random vertical and horizontal velocity components in the direction of the main flow . These turbulences produce strong vertical mixing between the air from the flow field and the one originating from its bordering layers.

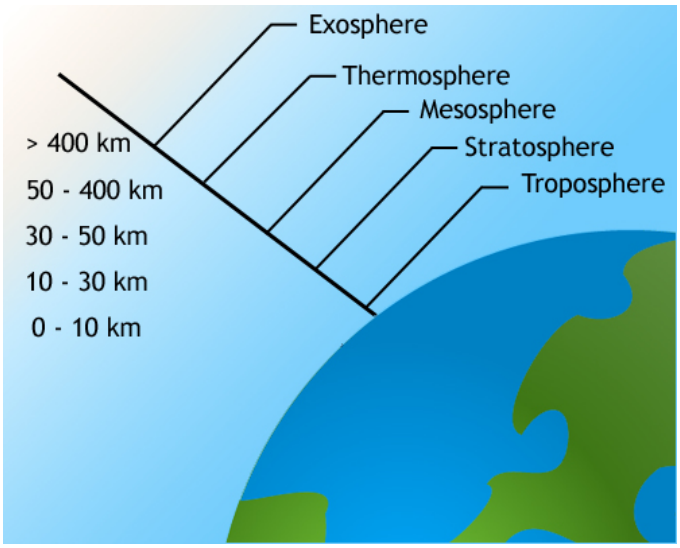

Figure 1.1: Atmospheric layers

The upper part of the ABL is called the Ekman layer and presents a force balance between the pressure gradient force, the Coriolis force and the turbulent drag. The solution to Ekman's equations generally overstates the magnitude of the horizontal wind field because it does not account for the velocity shear in the surface layer. Splitting the boundary layer into the surface layer and the Ekman layer (see figure 1.2) generally yields more accurate results.

Above the ABL is the "free atmosphere" , as shown by figure 1.2, where the wind is approximately geostrophic (i.e parallel to the isobars) while within the PBL the wind is affected by the surface drag and turns across the isobars. The free atmosphere is usually considered as non turbulent, or only intermittently turbulent.

1.1.2 Planetary surface layer

The Planetary Surface Layer (PSL) refers to the lowest part of the ABL previously defined. It is the more turbulent part of the ABL. It is characterized by constant vertical fluxes of heat and momentum between the Earth's surface and the ABL above it. The surface layer corresponds to the region where surface effects are dominating. It can be divided into three main parts :

- The inertial sublayer is the upper part of the PSL , where wind profiles obey to semi-logarithmic laws. (between 10 and 100 meters)
- The roughness sublayer is the medium part of the PSL, where wind profiles are mechanically and thermally influenced by nearby surface elements. (between 1 and 10 meters)
- The viscous sublayer is the lower part of the PSL , where wind profiles are as quasi-linear as the viscous forces are dominant (between 0 and 1 meter)

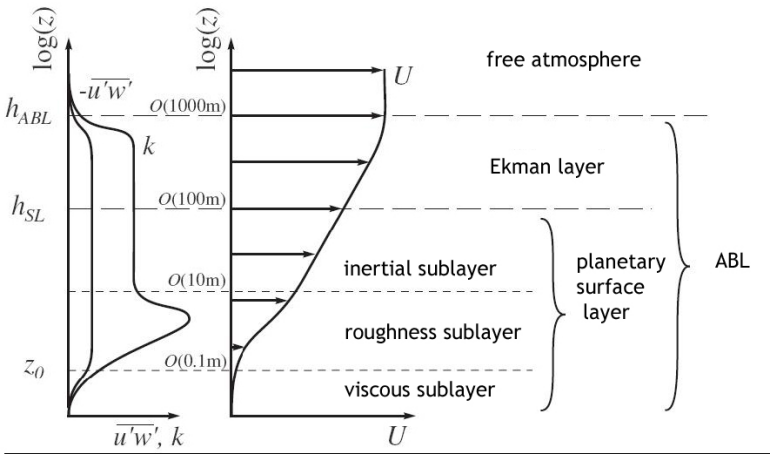

Figure 1.2: ABL and BSL layers

1.1.3 Wind flows within the PSL

Wind defines the air flow that composes the atmosphere. Many different kinds of winds exist and meteorologists usually classify them according to their spatial scale, their speed, the type of forces they are resulting in and also the geographic regions where they occur. In the PSL, due mainly to aerodynamic drag, there is a wind gradient in the wind flow just a few hundred meters above the earth's surface. Wind speed increases with increasing height above the ground, starting from zero due to the no-slip condition presented by the viscous sub-layer. The flow near the surface encounters obstacles that reduce the speed of wind, and introduce random vertical and horizontal velocity components at a right angle to the main direction of the flow.

This turbulence causes vertical mixing between the air moving horizontally at one level and the air at those levels immediately above and below it, which is important in dispersion of pollutants. The reduction in velocity near the surface is related to surface roughness, so wind velocity profiles are quite different from one terrain type to another. Local topography and especially complex terrains slow down the movement of the air near the surface, thus reducing wind velocity. As an example, over a city or rough terrain, the wind gradient effect could cause a reduction of 40% to 50% of the geostrophic wind speed aloft while over open water, the reduction may be only 20% to 30% [19].

As the complete study of the PSL winds represents a full-fledged meteorologic discipline and that many research programs are carried, we can simply notice that wind processes are complex near the surface and that micro-scaled turbulences cannot be always measured due to uncertainty and strong variability. We will see later that small eddies and local winds are difficult to model and most of the time imply important simplifications in the calculation of wind flows.

1.2 Atmospheric dispersion modeling

Atmospheric dispersion modeling is an essential tool in air quality management because it provides a relationship between source terms locations (i.e where discharges to the air occur) and observed adverse effects on the environment and the neighborhood. ADM is nowadays recognized as a full-fledged mathematical discipline, because its use has significantly grown up in the last decades, primarily due to the multiplication of dispersion phenomenons resulting from industrial development and the ensuing atmospheric pollution drops. ADM is now applied to other problematics such as agricultural spray drift, facing the huge rise of the use of pesticide worldwide.

Atmospheric dispersion models refers to the mathematical simulation of air pollutants dispersion in the ambient atmosphere. They are intimately related to numerical simulations as most models are performed with computer programs that solve the mathematical equations and algorithms which simulate the pollutant dispersion. As atmospheric dispersion is complex and because air pollution cannot be measured in every place it occurs, models are used to simplify and simulate the dispersion of air pollutants from emission sources, and to to predict the downwind concentrations or depositions on a given area.

1.2.1 Atmospheric dispersion models

Many different types of models exist, as shown by the quite extensive technical literature referring to ADM and mesoscale meteorology. Probably several hundreds of models [3] has been developed since the former Bosanquet and Pearson air pollutant plume dispersion equations that were formalized in the thirties. From simple Gaussian plume models to Lagrangian particle models, and from Eulerian grid models to hybrid ones through more recent Large Eddy Simulations (LES) and Direct Numerical Simulations (DNS), advances in Computational Fluid Dynamics (CFD) and computer hardware and software have led to a variety of solutions to model atmospheric dispersion.

Inspite simulations of complex fluid flows tend to become more and more accurate, only approximate solutions can be achieved using ADM due to uncertainty of meteorological and chemical parameters in the first hand, and to a series of constraints related to input data acquisition or calculation costs in the second hand. As no model can exactly suit any dispersion process at any scale, the choice of a model according to the definition of the problem requires serious prior thinking. This can be achieved by examining the following points:

- The importance of the properties of the compound to be modeled
- The mathematical principles to be used in order to best fit reality
- The consequences of assumptions and simplification on the intended results
- The definition of the required accuracy of outputs according to the former problem
- The selection of the appropriate vertical, horizontal, and temporal scales

- The availability and precision of meteorological and emissions inputs
- The definition of calculation costs and the needed computer hardware and software

All these questions can find answers both through a thorough knowledge of miscellaneous aspects of the problem to be modeled and of its physics, and through appropriates choices made thanks to literature and the reference ADM frameworks. A mine of information can be find in reference books such as [20], [21] and [22]. Models classification and advice about mathematical criteria can also be find in ADM dedicated reports and thesis such as [12], [23], [24] and [25].

1.2.2 General ADM structure

Whatever its type, an atmospheric dispersion model requires a set of input data to produce outputs that describe the wind flow behavior and the pollutant concentration. Current practical air pollution modeling systems gather several essential components organized through functional levels that can be summarize as the following [23] :

- **A set of inputs and parameters** that describe the general meteorology:
  - Meteorological data such as wind speed and direction, amount of atmospheric turbulence (stability class) or ambient air temperature...
  - Emissions parameters such as source location and height, source diameter or emission velocity...
  - Surface roughness, ground elevation and location, height and width of any obstacles...
- **A set of assumptions and approximations** that simplify narrow down the physical situation to an idealized situation, keeping the most important features. For example:
  - The pesticide cloud advects downwind with reduced turbulence
  - The pollutant does not undergo chemical reactions while it is transported
  - The dispersion process occurs within an idealized atmospheric boundary layer over flat terrain
- **A set of mathematical relations** and auxiliary conditions that describe the idealized physical system. Two equations types are commonly used:
  - Balance equations which are based on thermodynamics principles, chemical kinetics and transport equations
  - Constitutive equations which determine the value of physico-chemical parameters and some aspects of the physical parametrization.
- **A set of algorithms** and programming classes that solve the equation system. It is usually composed of two main components:

- A computer program able to solve equations such as Fortran or more recently object-oriented languages such as C++
- A graphical user interface which allows to setup the inputs and visualize the outputs in an easy way.

1.2.3 Main parameters affecting ADM

Such as the complexity of ADM has been generally presented, three input parameters appear to be essential in any modeling and it is useful to better acquaint ourselves with their definitions as they will be used later in this work. Atmopsheric dispersion and air quality are not only related to the emmited quantity of pollutant at the source term, but depend above all on the meteorological and morphological properties of the environment surrounding the source term. Therefore, emissions, winds and topography are more thouroughly explained below, as those three parameters will be used to model pesticide atmospheric spray drift.

Emissions

The term "emission" generally designates the discharge of a substance into the air. Talking about environmental emissions, it both names to the quality and the quantity of pollutants released by the source term. Regarding the pesticide spray drift study, it often refers to the emission factor, which can be defined as the average emission rate of pesticide for a given sprayer, relative to the intensity of spraying applications. Emissions are also qualified according the type of source term, namely mobile sources such as a sprayer moving within a plot and fixed source or "point source" such as an industrial chimney. However we will see later that mobile sources can be equated as point sources depending on the complexity of their movements.

Winds

Wind defines the flow of air molecules in motion. Winds can be classified according to numerous properties, notably their scale on which we are focusing here. Pesticide spray drift modeling most of the time involves mesoscale winds, those which act on a local scale such as prevailing winds, and microscale winds which blow on distances of only about ten to hundreds meters and are essentially unpredictable. The latter refer to every turbulences that occur at the bottom the atmospheric boundary layer (ABL), in other words near the Earth surface. Wind data accuracy and wind field calculations play a crucial role in ADM as they represent the main vector transporting emissions. They represent an huge source of uncertainty, as many micro-scale winds cannot be described properly.

Topography

Topography currently names the Earth surface shape and its features description. It specifically involves the recording of relief or terrain, the three-dimensional quality of the surface, and the identification of specific landforms. Topography is useful to determine the precise position of any feature or any point in terms of both a horizontal coordinate

system such as latitude and longitude, and a vertical frame such as altitude. In modern usage, this involves generation of elevation data in digital form which are described in the next section. Topographic data is another important input parameters for ADM, as elevation values strongly modify wind fields calculations, and therefore influence the pesticide clouds movements and trajectory.

1.2.4 Conclusion

Mesoscale wind flow and atmospheric dispersion modeling tend to become more and more accurate thanks to the advances in fluid mechanics and to the use of CFD tools. However, the PSL wind processes are uncertain and their modeling implies to proceed to simplifications, as micro turbulences and some aspect of the turbulent mixing cannot be predicted precisely. Moreover, the finer the scale on which the calculation is performed, the more numerous wind measurement are required to calculate and sometime validate accurate wind flows.

The variety of the available atmospheric dispersion models has been introduced, and we must retain that the choice of a modeling approach must be done according to the scales in which the dispersion occurs, the required accuracy for the model's outputs and the availability of wind and emission datasets. Several other important constraints must be examined such as the implied calculation costs or the possible ways to tend to the model validation. Such choices and hypothesis regarding our concern are exposed in section 4.2.2.

This chapter has finally allowed us to identify emissions, winds and topography as the three main parameters of any atmospheric dispersion modeling. These will especially studied in order to propose a vineyard pesticide spraying applications dedicated dispersion model, in conjunction with the conceded choices and hypothesis.

Chapter 2

GIS assets and limitations for ADM

ADM is characterized by numerous specific parameters, making it quite a challenging and rather new field of spatial modeling [26]. Although geomatics and its underlying disciplines are known to be powerful for analyzing and mapping environmental processes, only a few studies focus on possible links between ADM and Geographic Information Systems (GIS).

This section aims to point out geospatial assets and limitations for ADM by first recalling some GIS fundamentals and then identifying cross-cutting thematics in the second hand. Given that several terms are specifically used all along this thesis, it is wise to remind the reader of their definitions before going on the heart of the matter.

2.1 GIS fundamentals

2.1.1 Definitions

Geomatics

Let us first define the term "Geomatics" which is the mother discipline of GIS since the early seventies. It based on the contraction of the words "Geography" and "Informatics" and can be defined as the numerical and computational side of geography. Geomatics is a multidisciplinary science which includes tools and techniques used in land surveying, remote sensing, GIS, but also Global Positioning Systems (GPS) and other related forms of Earth mapping. Geomatics refers to the wide field of geographic information science which integrates acquisition, modeling, analysis, and management of spatially referenced data. It is based on the scientific frameworks of computer and information systems science but also on the principles of geodetics including for example geoids and coordinate systems.

Geographic Information System

A Geographic Information System (GIS) can be defined as a set of hardware, software, data, organizations and individuals which make it possible to store, analyze, produce and represent geographic data. A GIS is able to references real-world spatial data elements (also called geometries or features) to a coordinate system, and provides therefore

a numerical representation of the earth surface and its related spatial processes. These features are usually separated into different layers which refers to several data types (vector or raster datasets) and also to different geometry types (points, lines, polygons). GIS layers are also commonly created according to several thematics (e.g. agricultural plots, water bodies, forests, built areas...) [27].

Digital Elevation Model

A digital elevation model (DEM) is a digital representation of ground surface topography or terrain. It is also widely known as a digital terrain model (DTM). A DEM can be represented as a raster layer (a grid of squares) or as a triangular irregular network (TIN) layer. A gridded DEM represents the terrain surface as a regular lattice of points elevation [28], whereas a TIN is a vector based representation of the terrain surface, made up of a network of vertices, with associated coordinates in three dimensions (x,y,z), connected by edges to form a triangular tessellation. DEMs and TINs are often used in Geographic Information Systems, and are the most common basis for digitally-produced relief maps and 3D rendering and visualization.

2.1.2 GIS data models

As already said in the GIS definition, the spatial components of geographic data can be represented by three data types: points, lines and areas. In addition to this, spatial data can be represented in a GIS according to two very different data models: either as rasters or vectors. These are succinctly described bellow.

The vector model

- A point is defined by a single pair of coordinate values. A point normally represents a geographic feature that is too small to be represented as a line or area. For example, a city or an agricultural plot can be represented as a point depending on the scale of the map on which it is be shown.

- A line is defined by an ordered list of coordinate pairs defining the points through which the line is drawn. Linear feature include contour lines, roads or streams for example. At most mapping scales these features will retain their linear form, although the degree of detail and generalization will vary with scale. A line is a synonym for an arc in GIS vocabulary.

- An area is defined by the lines that make up its boundary. Areas are also named as polygons or multi-polygons. Examples of such geographic features include for example ocean basins or lakes but also smaller features such as plots or buildings. When shown on maps at a very small scale these features may also eventually become points.

The raster model

The raster data model is an abstraction of the real world where the basic unit of data (points, lines and areas) is represented using a matrix of cells or 'pixels'. The raster model uses the grid-cell data structure where the geographic area is divided into cells identified by rows and columns. The following information must be known when using raster data:

- Grid extent (number of rows and columns)
- Grid resolution (size of grid cell)
- Georeferencing information (e.g. corner coordinates, projection and datum)

In the simplest form, each cell contains a value for the element. Any cell not containing a feature would have the value of "0", sometime called "no-data".

The comparison of vector and raster models

The main difference between the two data models can be explained graphically with the following figure

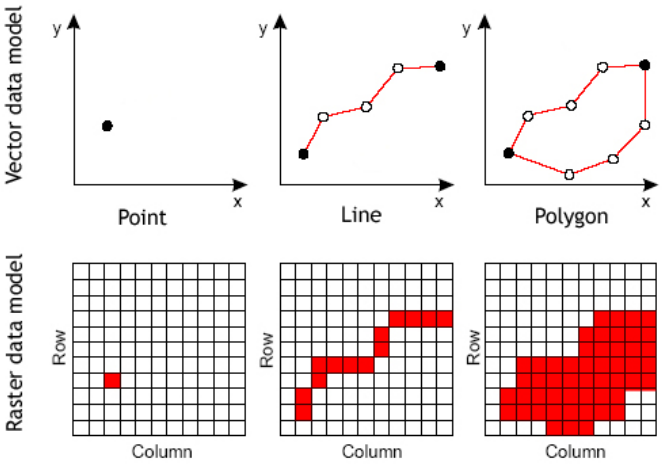

Figure 2.1: GIS Vector and Raster data models

The raster model presents a simpler data structure so that spatial analyses procedures are easier than with vector data. It is also efficient for scanned maps and remotely sensed information from satellite layers. However, raster data are graphically less pleasant depending on the pixel size and raster algebra outputs may be used with precautions for cartography. Furthermore, raster data are more complex to reproject than vectors and presents some limitations regarding the representation of topological relationships. Raster datasets also require bigger resources and disk space on computers for their storage.

The vector model is based on a more complex data structure as it handles several geometry types such as point, lines and polygons but also multi-point, multi-lines and multi-polygons. Topological relationships are thus easier to represent and to take into account for advanced spatial analysis. Vector datasets can be represented in their full resolution without any modification which enables to strongly zoom on vector layers and get more precision. Moreover, vector data are generally a smaller size and can be easily stored in spatial relational database management systems.

2.2 GIS and ADM cross-cutting thematics

ADM basics and GIS fundamentals have been recalled and we can now focus on possible links between the two disciplines. Indeed, cross-cutting thematics appear to be relevant both for spatial modeling of atmospheric dispersion and for the technical coupling, especially regarding coordinates systems, scales and time.

2.2.1 Coordinate systems

Coordinate systems are used both by mathematicians and geographers and constitute the base of space representation for atmospheric dispersion models and GIS applications. Many ADM systems are based on three dimensional Cartesian coordinate system that provide the three physical dimensions of space (length, width, and height) according to a frame gathering the *x*, the *y* and *z-axis* whereas most GIS use spherical coordinate systems based on ellipsoids and angles calculation to determine latitude (φ) and longitude (λ) values. The main differences between the two coordinate systems cited above are shown by figure 2.2.

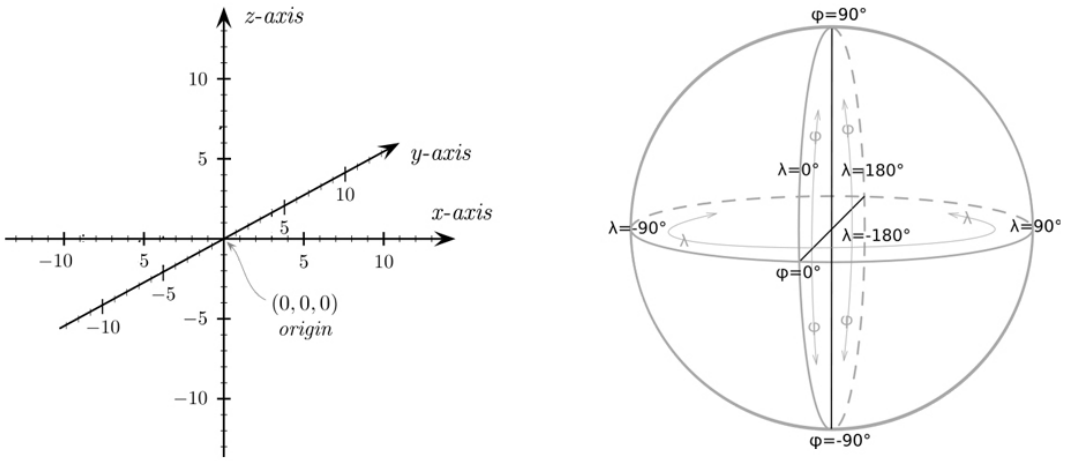

Figure 2.2: Cartesian (left) and Geographic (right) coordinate systems

Although GIS can display absolute *x,y,z* triplets, this is not a correct way to produce maps and location based analysis. Indeed, as geographic coordinate systems represent the surface of the Earth on a plane, a suitable map projection is needed in order to represent

Gaussian coordinates according to a coordinate system that best respect the reality of the Globe. Each projection preserves or approximates basic metric properties such as shapes, areas, distances and scales [29]. The purpose of the map and the place it represents determine which projection should be use to build the map and minimize distortion.

Given that atmospheric dispersion models are often designed to produce Cartesian x,y,z formated outputs, and that GIS supports by nature many projection types and matching coordinates transformation algorithms, we can easily conclude that both aspects should be able to communicate with each other through input/output processing. This would allow one to make use of ADM outputs in a geographic coordinate system and so to obtain a pesticide cloud in the "digital reality" of its landscape. More details on this concept are given in sections 7.1 and 7.2.2.

2.2.2 Scales

Scale has several meanings that are important to detailed, as it is once again used in different ways by atmospheric modelers and geographers. GIS community commonly differentiates four connotations for scale, as suggested by Quattrochi and Goodchild in [30]. The *cartographic scale* first refers to the size on the map divided by the size on the real world, which induces that small-scaled maps represents large areas [31]. The *geographic scale* is used to define the spatial extent of the study area. As for the *operational scale*, it describes the scale at which a phenomenon operates. A fourth definition of scale is linked to *resolution*, which can be defined as the smallest differentiable part of a spatial dataset and is helpful to define finer and coarser scales. For example, DEMs which present the smallest pixel size are of finer scale.

According to physicians, scale refers to the size and the spatial extent (also called domain) of physical processes. As an example, *micro-scale* (occurs over distances from 2mm to 2km), *meso-scale* (from 2 to 2000km) and *macro-scale* (500 to 10000km) are well-known terms and commonly used to describe local to global atmospheric and meteorologic phenomenons. However, some phenomena like atmospheric dispersion operate on several scales [32] that have to be taken into account in their modeling scheme. Multi scaled models are thereby needed in pesticide ADM, for example to make a canopy flow model, a volatilization model and a transport model interact, and so to model the whole process at best. Scale variations are an important research topic and many ADM studies are focusing on it to couple validated models operating from micro to meso scales, or to enhance existing atmospheric models as presented in [33].

ADM uses therefore both geographic and operational scales to determine the validity and the efficiency of a particular model. The coupling of ADM and GIS also implies to adapt a model's inputs/outputs to the cartographic scale, and to find the best way to map processes within a GIS environment. Resolution also presents several interesting issues regarding the use of DEM as input data in order to take realistic topographies into account. Scale and scale changes are therefore major interests for both the GIS and ADM communities, and this topic is more widely detailed and exploited in part 5.

2.2.3 Time

Time and temporality are also essential to many GIS applications. Although the concept of storing attribute information to spatial objects within a GIS is relatively a basic task, adding the time support raises new difficulties [34]. Temporal GIS applications are subject to numerous researches in the spatial modeling communities because many GIS based projects lack of linkage between space and time. Working with temporal GIS layers is a new challenging issue as it could greatly enhance spatial information in many cases, as regards about environmental spatial analysis.

Atmospheric dispersion models are also largely based on time. First, emissions and meteorological datasets are generally presented as time-series that often have to be processed to be used for ADM. Then, temporal scales also matter in the representativity of transport models as both the chemical and physical properties of a pesticide cloud are time-dependent and can be strongly modified depending on the date/time of the observation. Therefore, many models deal with the migration times of particles which makes it possible to know the fate of pesticide clouds or even the concentrations at a given moment, or for a given period.

ADM is time-dependent by nature and so it integrates time series and migration times in calculations, whereas GIS do not support temporality in their basic data models. Despite this apparent incompatibility, several attempts are being made to design temporal GIS databases and to support dynamic phenomenon natively into GIS as underlined by Wilson and Burrough in [35]. The premises of "4D-GIS" and geospatial virtual reality have started, but time is not a native feature of GIS, and this is a huge limitation to render dynamic physical processes such as pesticide atmospheric dispersion.

2.2.4 Conclusion

This chapter has recalled some of the GIS fundamentals in order to point out their assets for ADM. DEM have been described as they will be widely use for the intended coupling, as well as the vector and raster model that will both be employed, notably regarding pesticide clouds rendering within GIS.

GIS and ADM cross-cutting thematics have been highlighted and coordinate systems, scales and time now appear to be the base of our coupling. These three general concepts will be used all along the study in conjunction with the identified ADM most important parameters (namely emissions, winds and topography) both for the modeling and the technical coupling.

Chapter 3

Coupling ADM and GIS

Both ADM and GIS basics have been succinctly described. This chapter now aims to present available and validated techniques for coupling ADM and GIS. This enumeration of coupling techniques is then followed by a non-exhaustive review of existing ADM/GIS couplings. This review tackles both CFD based and GIS based couplings and allows us to reach conclusions on ADM/GIS couplings methods both for ADM and GIS scientific communities.

3.1 Coupling techniques

Nyerges proposed a conceptual framework for coupling external spatial based models and GIS [36], composed of four categories with increasing intensity of coupling. These are described in many coupling reviews examples, and sometimes reduced to only two categories (tight and loose coupling), referring to the traditional basic methods for coupling computer models [37].

3.1.1 Isolated applications

The model and the GIS are running on separate hardware and software environments and the data transfer between the two is done "manually" by the user. This does not represents a proper coupling, but a simple way to load the model's outputs in the GIS, subjected to data formats and projection processing. All the required steps appear to be quite cumbersome for the user.

3.1.2 The loose coupling

The loose coupling describes an approach where integration interfaces are developed with minimal assumptions between the GIS and the external model, thus reducing the risk that a change in one application will force a change in the another one. In other words, we can define loose coupling as a programming method according to which systems are linked by a communication network but ruled by their own functional logic [14]. This implies some input and output data flows and so most of the time it implies some file

formatting and format conversion. The loose coupling is used in many examples of GIS-based coupling due to its rather easy setup.

3.1.3 The tight coupling

The tight coupling refers to the approach according which models or softwares are gathered in a single system and are dependent upon each other, thus avoiding the inputs/outputs processing. In the case of GIS-based coupling, this means that the model and the GIS are working with specific shared modules such as specific functions or databases. The data models of the GIS and the model may still be different but automated data transfer is possible through a standardized graphical user interface. This method improves the coupling as the user needs to pay attention to the data integrity, but such couplings are more complex to build than loose coupling as it requires much more programming.

3.1.4 Full integration

In this approach, GIS and models are sharing the same data model through a common interface which greatly improves the interaction between GIS and models. It is even more extended than coupling, as the model often represents a native GIS class that has to be developed. Fully integrated GIS-based applications have not been many so far because they imply important programming tasks due to the limitations of the GIS or the model. However, once the integration is effective, it becomes easier to add new functionalities, since an Application Programming Interface (API) can be proposed.

3.2 Review of existing ADM/GIS couplings

3.2.1 CFD based couplings

Many atmospheric dispersion models are based on the use of CFD softwares to solve equations and to perform simulations over meshed domains. Despite the fact that such solutions are providing accuracy at any scales and simulations of more and more complex atmospheric dispersion processes, they do not natively support the GIS data model and cannot handle geospatial datasets in calculations. However, a few studies have experimented the introduction of GIS data into CFD based models in order to take advantage of topographic GIS data formats such as contours or raster DEM. These studies have been carried out in the field of urban ADM and have not been adapted for pesticide ADM yet.

A recent example of CFD/GIS integration is the work of Wong and al. who published an evaluation on data format conversion for integrating CFD models and GIS. The main goal of this study is to show how efficient is GIS data in CFD models and how sensitive the CFD results are to different GIS data formats. Atmospheric release simulations were performed using the FEFLO-URBAN CFD model which performs very large eddy simulations (VLES), on top of raster and contours topographic data as well as building data. One of the conclusion is that the raster format gave satisfying results compared to contours data [38].

Another case study of CFD based coupling presents the possible interactions between CFD software and ArcView GIS. In this work, ArcView and its Avenue programming capabilities are used to extract the coordinates and heights of buildings from the GIS data layers of a given urban area [39]. Those results are then sent to the CFX © software as input data in order to construct the geometry for atmospheric dispersion simulations on realistic built areas.

Such examples show that GIS data model can be embedded on powerful CFD platforms, but mainly using isolated applications or the loose coupling approach. As ADM studies most of the time require the use of proprietary CFD softwares such as Fluent ©, but that it would be too to complex to perform to their coupling with a whole GIS API, the tight coupling approach could be reached using GIS formats libraries. For example, GDAL/OGR could be integrated to the Gambit © geometry pre-processor as a GIS formats translator module. This way, standard DEM layers but also vector objects could be readen directly by Fluent © software.

3.2.2 GIS based couplings

Several studies have already lead to ADM/GIS based couplings that present loose, tight or integrated approaches. Those works are most of the time adapted for a specific study area according limited spatial and temporal conditions [40]. Such couplings are also often based on particular GIS environments and are not necessarily integrated into decision support systems (DSS) for preventing pesticide atmospheric pollution risks [41]. The following non-exhaustive review takes an interest in couplings using proprietary GIS such as ESRI © products in the first hand, and underlines the open source GIS capabilities in the second hand.

One of the more advanced project is called SPRAYTRAN [42] and is dedicated to predict the drift and deposition of pesticide from aerial spray applications. This GIS-based Lagrangian dispersion model was developed by the U.S. Department of Agriculture Forest Service (USDAFS). It uses the AGDISP model for the pesticide near-field emissions calculation [43] and the CALPUFF model which uses AGDISP outputs to calculate the long term transport of pesticide clouds [42]. The two models are coupled with GIS according a tight approach, and encapsulated into a single Windows © executable that works as an ESRI ArcGIS © extension. The SPRAYTRAN user thus dispose of a rather complex multi fenestrated software to setup both source terms characteristics and meteorological conditions, and the resulting pesticide plume is directly mapped into the GIS interface.

Several other loose coupling using ESRI © softwares and ADM have been carried. For example, the Distrital Francisco José de Caldas University developed an alternative analysis of air pollutants in Bogotá by coupling a Gaussian plume model formalized as a macro-commanded spreadsheet with ArcGis Geostatistical Analyst ©, in order to rapidly produce air pollution estimation maps [44]. Another coupling case study is presented by the work of Larry Koffman who developed an ArcView © extension to facilitate the

conversion of ASCII outputs coming from an external Lagarangian Plume model within the GIS software [45].

Another interesting project was led by the Kazakhstan Space Research Institute about the application of Gaussian plume models for air pollution simulation at instantaneous emissions. In this last example, a Gaussian model is transcribed in Fortran language and communicates with the ArcInfo © software through GIS formated inputs and outputs exchanges. This coupling allows to quickly compute Gaussian plumes and to map the concentrations fields at a chosen moment [46].

Other loosely coupled systems based on ESRI © technologies exist and the growing number of such couplings led to an ESRI initiative in collaboration with UCAR, NCAR, Unidata, NOAA, and several other key organizations called the ArcGIS © Atmospheric Data Model [47]. This is a working dialog between ESRI and the atmospheric sciences community regarding atmospheric data representation and analysis challenges. The scope of this program is to build a common data model that helps to address the needs of the atmospheric community, and provides direction for ESRI software and tool development. Atmospheric data encompass a very large array of data objects, with many available in a variety of data formats. The ultimate goal of the ArcGIS © Atmospheric Data Model is to represent each of these data objects in a uniform manner, allowing their superposition and combined analysis in the ArcGIS © desktop environment. The use of XML importers and exporters has notably been identified as a potential solution to provide an interoperable data model [47]. Such solutions would thus provide a native GIS-based atmospheric model which would avoid the actual necessary coupling between GIS and models.

Furthermore, we can observe strong capabilities of open source GIS such as GRASS GIS or Quantum GIS regarding the ADM/GIS coupling. The latter offer object-oriented open source libraries that provides flexibility and extensibility of GIS application development, as every algorithm is accessible. These benefits are largely met through the modular system provided by open source GIS, that makes program extensions development easier and so the tight or integrated couplings methods possible. This has potential applications in many disciplines that strive to couple numerical computing with geographic data analysis.

Several external environmental models have been integrated into GRASS GIS, as pointed out by Dassau and al. in [48]. A tell-tale example is the Trento University research on atmospheric dispersion, which gave birth to the r3.isosurf plugin for GRASS GIS. This is an integrated GRASS script that allows to calculate local thermally driven slope winds using DEM layers and complex fluid mechanic equations [49]. The results can then be mapped in 3D [50] within GRASS GIS.

3.2.3 Conclusion on ADM/GIS couplings

This non exhaustive review of literature allows us to point out several conclusions on ADM/GIS couplings. Regarding first the coupling types, it is clear that most couplings are performed by embedding or integrating atmospheric dispersion models into existing GIS, rather than using GIS datasets into CFD platforms. A few examples show that GIS data layers can greatly improve the accuracy when used as base mesh in CFD softwares, but this imply numerous preprocessing tasks and requires important resources. Moreover, most CFD based couplings are carried out over urban areas and street canyons according to specific air measurement, and no such example applied to pesticide spray drift was found in the literature.

Regarding GIS based couplings, we can affirm that several projects have managed to use atmospheric dispersion models into GIS applied to pesticide spray drift and air pollution risk analysis in both rural and urban areas. The loose coupling method is prevailing and the "proprietary GIS / external ADM program" tandem is the most mastered configuration. Several tight or integrated approaches have nevertheless been underlined, notably using open source GIS libraries and atmospheric models that were turned into native GIS classes.

We can finally conclude that ADM and GIS communities can greatly take advantage of working together in order to enhance spatial modeling of atmospheric dispersion and to make meso-scale meteorology models and GIS become closer. Huge researches have already started on the meteorological and GIS datasets compatibility, but also regarding the integration of dynamic processes according to time and scales into environmental GIS applications.

Part II

Spatial modeling of pesticide atmospheric dispersion

Chapter 4

Pesticide spray drift modeling

Current research on pesticide atmospheric dispersion modeling carried out by the UMR ITAP at the Montpellier Cemagref Lab in collaboration with the Research Mathematics and Modeling Institute of University Montpellier 2 is explained in this chapter. A simplified formulation of the problem is first proposed in order to expose the context of pesticide spray drift modeling. The Drift-X model and the original reduced-order approach it is based on are then detailed in order to setup the intended mathematical modeling. The latter focuses on pesticide cloud long-range transport from the vineyard to the watershed scales. Thus, the transport equations and the principles of non-symmetric geometry that are used are introduced.

4.1 Problem formulation

4.1.1 Context

Pesticide spray drift modeling is necessary to forecast both the movement of a pesticide cloud from a vineyard plot and its fate in the surrounding environment. Indeed, field and wind tunnel experiments are difficult and time-consuming [9, 51] and do not allow to analyze all the phenomena linked to pesticide dispersion. In this context, numerical simulation models can significantly help and complete experiments, as they allow scientists to test several processes using observation measurements, and sometime to design some physical models from simulations.

Many studies focus on near-field spray drift and provide good results, as mentioned in the introduction of this study. Long-range transport analysis is by contrast rather challenging to study because terrain experiments have to be setup on larger areas and would involve installing anemometers and air sensors on several square kilometers, and then proceeding first to flow field reconstruction based on long time-series wind measurements in the first hand, and then with numerous chemical analyses of air samples. As such projects are not possible yet, the numerical modeling of long-range transport appeared as a good and useful idea. The proposed modeling thus focuses on pesticide cloud dispersion after phytotreatments and uses near-field spray drift modeling results as input data, as detailed in the next section.

4.1.2 Past research

Past research has treated the problem of pesticide emission and dispersion, and proposed the coupling of models from the local scale (i.e. emission and near-field distribution including spray nozzle and canopy flow modeling) to the global scale (i.e. the Gaussian plume modeling). In this approach, a local model provides the inlet conditions for the levels above. Main assets of this local to global modeling is to avoid the solution of partial differential equations using model reduction. This is based on adapting search spaces for the solution of a given model using a priori information.

More precisely, a near field (to the spraying device) search space is built by using experimental observations and the Turbulent Jets theory. This combines a local spray drift model with a simplified canopy model [23]. The local spray drift model takes spraying characteristics into account such as the total pesticide quantity available in the tank, the injection velocity of the spraying nozzle, the number of rows treated at the same time by the spraying device, whereas the canopy model accounts for the number and height of the vine rows and defines vegetation parameters by determining the characteristics of a mean row. Several other essential parameters are taken into account in the combined model, namely the starting point of the sprayer, the direction it takes after the first row and of course its speed during the spraying application.

Once this local solution is known, the amount of pesticide leaving th eplot to the atmosphere is evaluated using analytical integration of the governing equations. A priori local information is once again included during this analytical solution looking for special solutions. This modeling is detailed in Dr.Brun's PhD thesis [23]. The resulting quantity of pesticide from this local model is then considered as leaving up the vineyard plot from its centroid. This amount of species is finally considered as candidate for long-range transport over a specified domain and according to a given flow field.

4.2 Drift-X model principles

4.2.1 An alternative to the use of CFD

Accurate wind datasets are difficult to acquire over large areas and long time-series but required by most CFD models. Some of the eolian processes included in pesticide atmospheric dispersion are also to complex to be solved by numerical simulations at that stage, due to their uncertainty and variability. Furthermore, CFD tools appear to be quite long to use for simulations, as both input data and domain geometry have to be pre-processed through the use of several softwares. Their use necessitate quite expensive hardware and software and most of all involves very long calculation costs.

Given that wind data are quite poor for our concern and that a large set of assumptions has to be done to model the whole dispersion process at different spatial and temporal scales, the use of CFD tools to solve our problem was ill-advised. In relation to the

necessary accuracy and because calculation costs have to stay low in order to perform fast simulations, an original alternative to the use of CFD is therefore proposed.

Drift-X model is a probabilistic simplified Gaussian atmospheric dispersion model able to forecast pesticide spray drift after the treatment, from the plot to the watershed. The model operates within a domain of a several square kilometers, corresponding to a typical southern French small wine-growing area.

Drift-X is based on a reduced-order modeling approach to flow field reconstruction with a small number of measurements, as well as to Gaussian plume transport over realistic topographies and unsteady wind flows. The main goal of Drift-X is to provide the mean tendency of a pesticide cloud after spraying applications, by forecasting the wind field and the pesticide concentrations for a permanent state.

4.2.2 Assumptions and hypothesis

This section details the choices regarding the assumptions and the hypothesis that have been done for the modeling, leading to a simplified atmospheric dispersion process.

Pesticide emissions

- The vineyard's inner dispersion is simplified. It could be enhanced but it is used as a "black box" in this study.

- The quantity of pesticide that is candidate for transport is considered as leaving the plot from its centroïd, at the given height of 2,5 m.

- The pollutant is considered as "neutral" and will not undergo chemical reactions while it is transported.

Pesticide cloud transport

- The flow field is constructed using a small number of points, and is so subject to uncertainties.

- The plume advects downwind and spreads out in the horizontal and vertical directions.

- The resulting concentration values are forecasted for a permanent state after the spraying application.

- The resulting concentration can be calculated as atmospheric concentrations values for a given height, or as deposited quantities at the ground elevation. The interaction with the soil is not included in the modeling.

4.2.3 A reduced order modeling approach

Let us first define formally what we mean by reduced order modeling. Considering the calculation of a state variable:

$$F(V(p)) = 0$$

$V(p)$ is function of independent variables p. Our aim is to define a suitable search space for the solution $V(p)$ instead of considering a general function space. This former approach corresponds to the finite element methods, for instance when we look for a solution V_h expressed in some finite dimensional subspace $S_N(\{W_i, i = 1, .., N\})$:

$$V_h = \sum_{i=1}^{N} v_i^{opt} W_i$$

S_N is generated by the functional basis chosen $\{W_i, i = 1, .., N\}$. As an example, we can consider W_i as polynomial of degree one ($W_i \in P^1$) on each element of a discrete domain called 'mesh'. v_i^{opt} denotes the values of the solution on the nodes of the mesh:

$$v_i^{opt} = argmin_{v_i} \|V - V_h\|_F, \quad i = 1, .., N$$

Hence, V_h is the projection of $V(p)$ over S_N. $\|.\|_F$ is a norm involving the state equation. In this approach, the quality of the solution is monitored either by the mesh size (i.e. $N \to \infty$) and/or the order of the finite element (i.e. $W_i \in P^m$ with m increasing for higher accuracy) [52]. If the approach is consistent, the projected solution tends to the exact solution when $N \to \infty$ or $m \to \infty$. In all cases, the size of the problem is large $1 \leq N < \infty$.

In a low-complexity approach, we approximate $V(p)$ by its projection $\tilde{V}$ over a subspace $\tilde{S}_n(\{w_i, i = 1, .., n\})$ that is not generated by polynomial functions anymore. We rather consider $\{w_i, i = 1, .., n\}$ as a family of solutions ('snapshots') of the initial full model $(p \to V(p))$:

$$\tilde{V} = \sum_{i=1}^{n} \tilde{v}_i^{opt} w_i$$

$$v_i^{opt} = argmin_{v_i} \|V - \tilde{V}\|_F, \quad i = 1, .., n$$

The cost of the two proposed methods depends on the cost of the solution of the minimization problems. For the reduced order approach to be efficient, we aim therefore $n \leq N$ [53]. This is only possible if the w_i family is well suited to the problem, in which case we can also expect a more accurate solution despite the small size of the problem.

4.3 Transport and non-symmetric geometry

Let us consider the situation of a source releasing a time dependent quantity $c_{inj}(t)$ into the atmosphere at a given location. In other words, $c_{inj}(t)$ represents the quantity of pesticide released by the sprayer at a given x/y position. Our goal is to develop a low-complexity model to represent the dispersion of this quantity. The primary factors influencing the dispersion of a neutral plume are advection by the wind and turbulent mixing.

The simplest model of this process is to assume that the plume advects downwind and spreads out in the horizontal and vertical directions. Hence, the distribution of a passive scalar c, emitted from a given point and transported by a uniform plane flow filed U along x coordinate, can be represented by:

$$c(x, y, z) = c_c(x) f(\sqrt{y^2 + z^2}, \delta(x)) \tag{4.1}$$

where

$$c_c(x) \sim exp(-a(U)x)$$

and

$$f(\sqrt{y^2 + z^2}, \delta(x)) \sim \exp(-b(U, \delta(x))\sqrt{y^2 + z^2})$$

c_c is the behavior along the central axis of the distribution and $\delta(x)$ characterizes the thickness of the distribution at a given x coordinate. An analogy exists with plane or axisymmetric mixing layers and neutral plumes where δ is parabolic for a laminar jet and linear in turbulent cases [54, 55].

$a(.)$ is a positive monotonic decreasing function and $b(.,.)$ is positive, monotonic increasing in U and decreasing in δ. In a uniform atmospheric flow field, this solution can be used for the transport of c^+ above.We would like now to generalize this solution in a non-symmetric metric defined by migration times based on the flow field and so to treat the case of variable flow fields.

4.3.1 Non-symmetric geometry

Let us now explain how the travel time-based metric is built. In a symmetric geometry approach, the distance function between two points A and B verifies the following:

$$d(A, B) = 0 \Rightarrow A = B \tag{4.2}$$

$$d(A, B) = d(B, A) \tag{4.3}$$

$$d(A, B) \leq d(A, C) + d(C, B) \tag{4.4}$$

But the distance function can be non uniform with anisotropy (the unit spheres being ellipsoids). In a chosen metric $\mathcal{M}$ the distance between A and B is given by:

$$d_{\mathcal{M}}(AB) = \int_0^1 \left({}^t\overrightarrow{AB}\mathcal{M}(A + t\overrightarrow{AB})\overrightarrow{AB} \right)^{1/2} dt \tag{4.5}$$

where $\mathcal{M}$ is positive definite and symmetric in symmetric geometries. With $\mathcal{M} = I$, the Euclidean geometry can be recovered and variable $\mathcal{M}$ makes it possible to account for anisotropy and non uniformity of the distance function.

Anisotropy can easily be illustrated with an European travel time based driving map, as shown in figure 4.1, which is a good example of an anisotropic geometric representation of a territory. However, the geometry is still symmetric in this case (as we suppose it takes the same time to drive from A to B than from B to A) and relations hold[1]

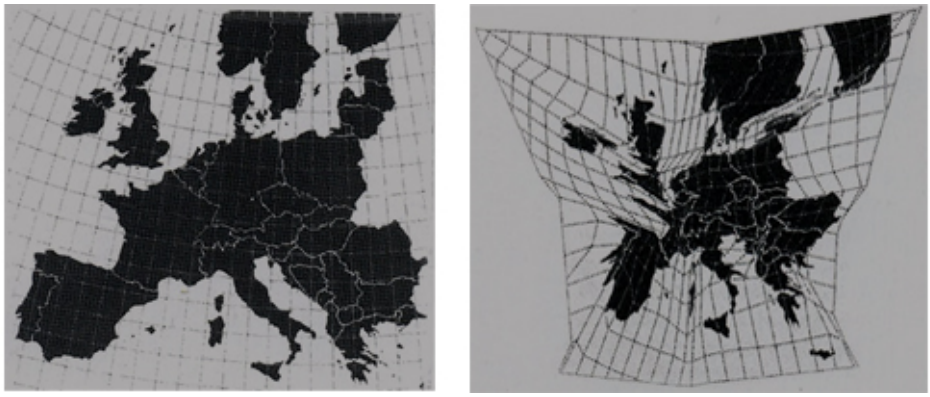

Figure 4.1: Map of European territory (left) and its distorted isochronic representation (right) based on driving travel times.

.

The mentioned symmetry is not natural for many applications. Considering once again the example of the driving map, everybody can experiences everyday that driving from A to B is not equivalent than driving from B to A during rush hours. We would like therefore to go one step further considering non symmetric geometries. Let us now consider the following definition of the distance function:

If A is upwind with respect to B then

$$d(B, A) = \infty \quad \textit{and} \quad d(A, B) = \int_A^{B^\perp} ds/u = T_{AB} \tag{4.6}$$

[1]This approach is also suitable for adaptive sampling and mesh adaptation [56, 57, 58]. Linking the metric to the Hessian of the variable, the metric permits to equi-distribute the interpolation error over a given sampling or mesh and for this former monitor the quality of the solution.

T_{AB} is the migration time from A to $B^{\perp}$ along the characteristic passing by A. u is the local velocity along this characteristic and is by definition tangent to the characteristic. $B^{\perp}$ denotes the projection of B over this characteristic in the Euclidean metric. In order to guarantee non-degenerency of d (i.e. $d(A,B) = 0 \Rightarrow A = B$), we require $B^{\perp} \neq A$. We assume that the characteristic issued from A is unique and so avoids sources and attraction points in the flow field. In case of non uniqueness of this projection, we would rather choose the direction of the projection which best satisfies the constraint ($\vec{u}.\nabla c = 0$) in B. Finally, we define A being upwind with respect to B if there exists no $B^{\perp}$. This definition of distance does not verify the triangular inequality. The inequality holds if C is upwind with respect to A or if B is upwind with respect to C.

4.3.2 Calculation of migration times

Our approach based on travel time aims to provide the solution at a given point without having to calculate the whole solution. Being in point B, we need an estimation of the migration time from the source in A to B.

The construction of characteristics is avoided using an iterative polynomial definition for a characteristic $s(t) = (x(t), y(t), z(t)), t \in [0,1]$, and by starting from a third order polynomial function verifying for each coordinate:

$$P_n(0) = x_A, P_n(1) = x_B, P'_n(0) = u^1_A, P'_n(1) = u^1_B \quad \text{(same for } y \text{ and } z) \tag{4.7}$$

If $P'_n(\zeta) \neq u^1(x = P_n(\zeta))$ this new point should be assimilated by the construction increasing by one the polynomial order. $\zeta \in]0,1[$ is chosen randomly. The migration time is computed over this polynomial approximation of the characteristic. The approximation $B^{\perp} = B$ is introduced here, which means the characteristic passing by A must pass exactly by B, which is unlikely. In a uniform flow, this means we suppose the angle between the central axis and $\vec{AB}$ is small (cosine near 1).

A correction factor of $2/3 = 0.636$ must therefore be introduced on the calculated times. This is the stochastic averaged cosine value for a white noise for angles between 0 and π. Once d is calculated by this procedure one needs to define $d^{\perp}_E$ which is unknown as $B^{\perp}$ is unknown. It has been decided to approwimate $d^{\perp}_E \sim d_E(B, B^*)$ where B^* is the projection of B over the vector $\vec{\overline{u}}$ the averaged velocity along the polynomial characteristic.

This approach gives satisfactory results for smooth atmospheric flow fields, which corresponds to our situation as phytotreatments are not performed when the weather is too windy (e.g. for winds stronger than $5m/s$, according to French regulation on pesticide spraying applications). This also results in the polynomial construction above gives satisfaction with low order polynomials.

4.3.3 Generalized plume solutions

Once this distance is built, we finally assume that the distribution of a passive scalar transported by a variable flow field $\vec{u}$ can be written as:

$$c(x, y, z) = c_c(d) f(d_E^{\perp}, \delta(d)) \tag{4.8}$$

where $d_E^{\perp}$ is the Euclidean distance in the normal direction local to the characteristic at $B^{\perp}$ along direction $BB^{\perp}$. This can be seen on figure 4.3, and compared with the former plume calculated with an uniform flow field on a traditional cartesian metric presented in figure 4.2.

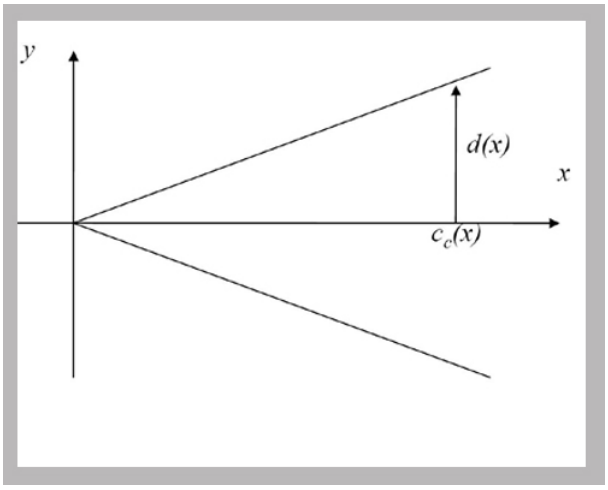

Figure 4.2: Sketch of the plume model in a cartesian metric for a uniform flow field

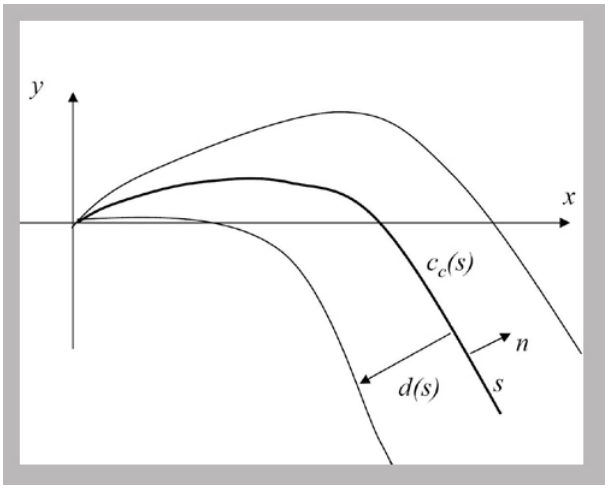

Figure 4.3: Sketch of the plume in a travel-time based metric for a rotating flow field

4.3.4 Flow field

It first should be reminded that realistic configurations most of the time provides very poor information on the atmospheric flow details, compared to the accuracy we would like to obtain for the transport. As an example, the flow will be described probably by less than one point by several square kilometers. We consider that the ground flow field is built from observation data as solution of the following system:

$$\vec{\tilde{u}}_H = -\nabla\phi, \quad -\Delta\phi = 0, \tag{4.9}$$

under constraint that

$$-\nabla\phi(x_j) = \vec{u}_{obs}(x_j), \quad j = 1, .., n_{obs}$$

where ϕ is a 2D scalar potential and n_{obs} the number of observation points. One particularity of the present application is that the number of observations is small and that the distance between two observation points is large. The observations are close to the ground at $z = H$ and this construction gives a map of the flow near the ground. If one assumes $\vec{u}_{obs}$ is divergence free, the solution to equation 4.9 at a point x can be seen as

$$\vec{\tilde{u}}_H(x) \sim \vec{u}_H(x) = \sum_{j=1}^{n_{obs}} \lambda_j(x)\vec{u}_{obs}(x_j), \quad 0 \leq \lambda_j(x) \leq 1 \tag{4.10}$$

where $\lambda_j(x)$ are barycentric functions such as

$$\sum_{j=1}^{n_{obs}} \lambda_j(x) = 1, \quad \text{and} \quad \lambda_j(x_i) = \delta_{ij}$$

In order to account for error in measurements $\vec{u}_{obs}$, a kriging construction can also be used [59, 60]. If one assumes $\vec{u}_H$ to behave as a stochastic variable, and supposing its mean and covariance being those of $\vec{u}_{obs}$, the kriging predictor $\vec{u}_H$ minimizes the variance of the prediction error: $\varepsilon = \vec{\tilde{u}}_H - \vec{u}_H$.

The main reasons to avoid numerical solving of the partial differential equation (PDE) are that one needs to use a mesh free technique, but also because available information is poor (making numerical solution unrealistic) and that one can observe noise in measurements. The plane velocity map $\vec{u}_H$ can be completed in the vertical direction using generalized wall functions [61, 62]. These can be written as:

$$(\vec{u}.\vec{\tau})^+ = (\vec{u}.\vec{\tau})/u_\tau = f(z^+) = f(zu_\tau/\nu)$$

where $\vec{\tau} = \vec{u_H}/\|\vec{u_H}\|$ is the local tangent unit vector to the ground in the direction of the flow and we assume that $(\vec{u}.\vec{n}(z = H) = 0)$ if $\vec{n}$ is the normal to the ground $(\vec{n} = (0, 0, -1)$ (with no topography variations). This is a non linear equation that provides the friction velocity,u_τ, knowing $(\vec{u}.\vec{\tau})_H$. It is used to define the horizontal velocity $\vec{u}.\vec{\tau} = u_\tau f(z^+)$ for $z > H$.

This construction gives two components of the flow and the divergence free condition implies that the third component is constant and therefore vanishes as it is supposed as zero at $z = H$. This construction could be improved but appear as sufficient for the required level of accuracy .

4.4 Conclusion

The reduced order modeling approach has been described and the Drift-X model presented. The Gaussian plume model has been applied on a simple way and modified according to non-symmetric geometry principles, in order to setup a travel-time based metric for the transport of passive scalars. The generalized plume solution as been adapted for rotating smooth flow fields calculation with a small number of measurement points.

Moreover, the topographic values have been taken into account in the transport model. Indeed, the z value of the Gaussian model is provided by DEM layers pixel values, leading to simulations over realistic topographies. The ground variations between those values are then calculated with the $\delta(x)$, which provides good results for medium to large topographic variations. The topographic impact on the flow field and dispersion is more detailed in section 6.2.

Facing the uncertainty of PSL wind flows and the lack of available wind datasets, a set of physical assumptions have to done in order to model the atmospheric transport of pesticide, that have been detailed in section 4.2.2. The lack of wind measurement also strongly oriented the modeling to be mesh free and to be built without solving any PDE. This approach has been presented as an interesting alternative to the use of CFD tools, and greatly improves the calculation costs which must stay law for the perspective of coupling the model with a GIS software and to perform fast dispersion simulations.

According to the modeling approach and the cited constraints, the Drift-X model is especially suited to model large topographic and wind variations. The flow field calculation is thus subjected to errors as both micro turbulences and small ground effects are not taken into account. However, these errors can be quantified mathematically and are considered as acceptable regarding the required accuracy for the Drift-X outputs.

Chapter 5

Scale changes implementation into Drift-X

5.1 Introduction

The Drift-X model has been presented and we would like now to account for the scale changes presented by the atmospheric dispersion. This chapter propose a multi-leveled construction of the dispersion that splits the domain into several "scales" and resamples the outputs resolution. Both the wind flow vectors and the topographic values are interpolated to the finer scale. The extent of latter can be set up just around the treated plot but also for example on a relevant topographic feature or on a particular place we want to reach a better accuracy.

In realistic configurations, simulations need to be carried out over several square kilometers domains. At the same time, one needs to be able to account for local topography variations with details provided every few meters. We saw previously that wind measurements are most of the time available on very coarse grids with only two measurements points usually being distant of several kilometers. Because of these constraints, it is unrealistic and inefficient to perform the whole simulation with a metric topographic accuracy. We would rather like to somehow account for large scale variations of topography on a coarse level simulation and include gradually the details of the ground variations near the main points of interest.

5.2 Multi-level construction

To perform this task, one recursively applies the modeling described above on a cascade of embedded rectangular homothetic domains $\omega^i, i = 0, ...,$ with $\omega^0 = \Omega$ the full domain. For the sake of simplicity, and also because this is rich enough for spraying applications, the construction is deliberately limited to rectangular configurations. Figure 5.1 shows a simple representation of this construction where information is transferred from coarse to fine levels on corners. No information is transferred at that stage from fine to coarse. Indeed, we emphasizes that the grids correspond to the locations where topographic data

are available. As mentioned before, our approach is mesh free in the sense that no meshes is used for calculation. Only evaluated information on wind and concentration are stored at these locations. The total wind field is expressed as:

$$\vec{U}_H = \sum_{i=0}^{n_{level}} \vec{u}^i \chi(\omega^i) \tag{5.1}$$

where $\vec{u}^0 = \vec{u}_H$ is calculated in equation 4.9) for the coarser level and $\chi(\omega^i)$ is the characteristic function for the subdomain on which level i is defined. In other words, the correction is equal to zero outside ω^i. n_{level} is the total number of levels used. For $i > 1$, velocity restriction from level $i-1$ to i is evaluated using equation 4.9 with the observation point being the information at the four corners q_j of a rectangle, as described bellow:

$$\vec{u}^i = -\nabla\phi^i, \quad -\Delta\phi^i = 0, \quad \phi^i(q_j) = \phi^{i-1}(q_j), \quad j = 1, .., 4$$

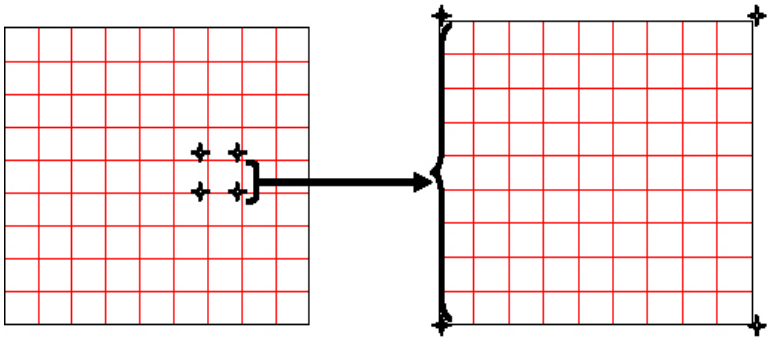

Figure 5.1: Sketch of the multi-leveled construction

Once again one can take advantage of the linearity of the operator, to use a similar decomposition for $\vec{u}^i$ than for $\vec{u}^0$ where the observation quantities are becoming the values at the corners of the homothetic restriction:

$$\vec{u}^i(x) = \sum_{j=1}^{4} \lambda_j(x) \vec{u}^{i-1}(q_j) \tag{5.2}$$

Where

$$\sum_{j=1}^{4} \lambda_j(x) = 1, \quad \text{and} \quad \lambda_j(x_i) = \delta_{ij}, \quad i, j = 1, .., 4$$

If $\vec{u}^{i-1}$ is divergence free, then this construction guarantees that

$$\int_{\partial\omega^i} \vec{u}^i . \vec{n}^i dS = \int_{\partial\omega^i} \vec{u}^{i-1}|_{\partial\omega^i} . \vec{n}^i dS = 0$$

Hence, the velocity restriction in ω^i remains divergence free and is compatible with the overall field. In the simulation presented here, three levels have been used to link $\Omega = \omega^0 \sim 10km^2$ to the $\omega^2 \sim 10m^2$.

Once velocity restriction is defined, the concentration restriction is defined as follow:

$$c^i = \sum_{j=1}^{4} \lambda_j(x) c^{i-1}(q_j) \tag{5.3}$$

This construction guarantees that the total mass in ω^i fits the entering quantity [1]:

$$\int_{\omega^i} c^i dV = \int_{\partial\omega^i} c^i (\frac{\vec{u}^i}{\|\vec{u}^i\|}.\vec{n}^i) dS$$

5.2.1 Integral data

Once the species distribution $c(x, y, z)$ is found and that the total injected quantity in time interval $[0, T]$ is known, one can assumes:

$$K = \int_0^T c_{inj}(t) dt$$

Various quantities can be computed. For instance, one can have an estimation of the amount of species which has reached the ground using:

$$C_g(x, y) = \int_{z \leq z_0} c(x, y, z) dz$$

or estimate the quantity still in the atmosphere beyond a distance R_0 from the source, using:

$$C_a = K - \int_{R \geq R_0} C_g(x, y) dV$$

$R = \sqrt{x^2 + y^2}$ corresponds to the radius from source. To improve the species presence prediction, the model above could for example be coupled with some volatilization models, that provide the leaving quantities from soil to ambient air under evaporation or leaching. These models include three processes: migration in a soil column, molecular diffusion in the viscous sub-layer, and transportation in ambient air. This former again calls for the present modeling.

5.2.2 Multilevel correction for ground variations

Multi-level correction

At this point we would like to account for the topography or ground variations ($(x, y) \rightarrow \psi(x, y)$) in the prediction model presented above. Despite this plays an important role in the dispersion process, it is obviously hopeless to launch direct simulations using a Computational Fluid Dynamic (CFD) model, based on a detailed ground description .

[1] The four points trapezoidal rule is exact for numerical integration of bilinear functions $\int_\omega f(x, y) dx dy = \frac{1}{4} \sum_{j=1}^{4} f(q_j)$.

We should mention that ground variations effects are implicitly present in observation data for wind as mentioned in (4.3.4). However, as we said, wind observations are quite incomplete. In particular, wind measurements are available every few kilometers while topographic data are available on a metric basis. At each level i of the construction (see figure 5.2) we introduce a correction $\vec{u_t}^i$ to the restriction

$$\vec{U}_H = \sum_{i=0}^{n_{level}} (\vec{u}^i + \vec{u_t}^i)\chi(\omega^i) \tag{5.4}$$

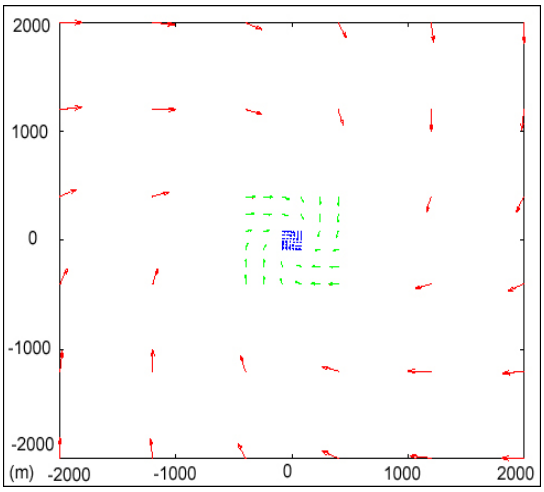

Figure 5.2: Example of three-level construction of an experimental rotating flow field.

Various local modeling can be considered for $\vec{u_t}^i$ going from simple algebraic expressions to more sophisticated local CFD models. We propose the following correction[2]

$$\vec{u_t}^i = -\frac{1}{\rho}\mathrm{sgn}(U_t)\nabla p^i, \quad p^i = p_r^{i-1}U_t^2 \tag{5.5}$$

where

$$U_t = \frac{\vec{u}^{i-1}}{\|\vec{u}^{i-1}\|}.\vec{n_t}^i \quad \text{and} \quad p_r^{i-1} = \frac{1}{2}\rho(\vec{u}^{i-1}.\vec{n}^i)_-^2$$

ρ is the density of the fluid. p_r is a local pressure reference based on averaged entering velocity into subdomain i:

$$(\vec{u}^{i-1}.\vec{n}^i)_- = \frac{1}{n_-}\sum_{j=0}^{4} \min(0, \vec{u}^{i-1}(q_j).\vec{n}_j^i)$$

$1 \leq n_- < 4$ being the number of entering flow corners. The normal to the ground evaluated from the digital terrain model restriction at level i is denoted by $\vec{n_t}^i$. This is different from the normal $\vec{n}^i$ to subdomain i. In absence of ground variations the two normals are orthogonal (see figure 5.3).

[2]This is the Bernoulli-Newton formula widely used in aeronautics and reproducing well the pressure distribution over a cylinder for a potential flow.

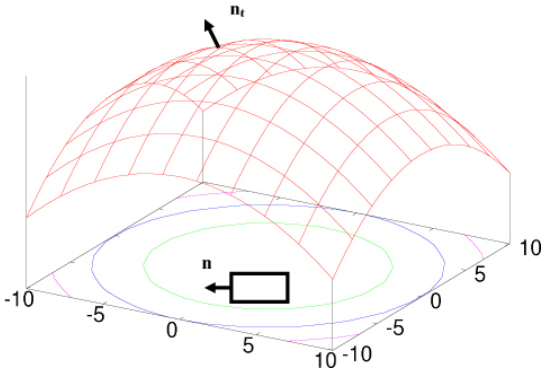

Figure 5.3: Sketch of topography variation and normals definitions

In case the topography is not constant, we have

$$\vec{u}^{i-1}.\vec{n_t}^{i-1} = 0, \quad \text{but} \quad \vec{u}^{i-1}.\vec{n_t}^{i} \neq 0$$

This multi-level correction improves the predictive capacity of the model introducing a dependency between ground variations and migration time. However, this is not sufficient to correctly account for ground variations in dispersion. For instance, it is indeed clear that even in a uniform flow,cross diffusion is not symmetric on a sloppy ground when dispersion is performed parallel to the iso-level contours (see figure 5.4).

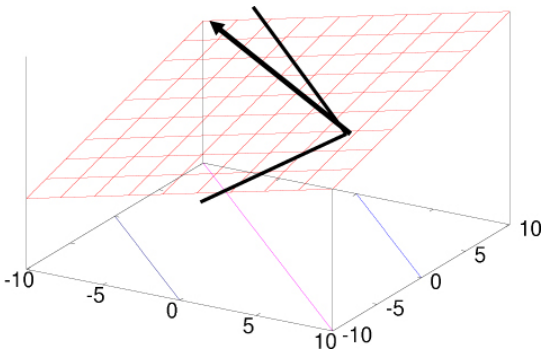

Figure 5.4: Sketch of topography variation and non symmetry in cross-definition for a constant velocity field

We also need to correct the functions a and b appearing in the dispersion modeling. As we have assumed the construction is only coarse to fine without feedback from fine to coarse levels, we assume the correction conservative in the sense that the incoming mass into subdomain i:

$$K^i = \left(c^{i-1} \frac{\vec{u}^{i-1}}{\|\vec{u}^{i-1}\|}.\vec{n}^i \right)_-$$

$$= \frac{1}{n_-} \sum_{j=0}^{4} \min \left(0, c^{i-1}(q_j) \frac{\vec{u}^{i-1}(q_j)}{\|\vec{u}^{i-1}(q_j)\|}.\vec{n}_j^i \right)$$

This defines the integral expression with or without topography changes:

$$K^i = \int_{\omega^i} c^i dV = \int_{\omega^i} c_t^i dV$$

where c_t is the modified expression for the concentration to account for topography changes and $\vec{n}_j^i$ is the normal to face $j = 1, .., 4$ of subdomain i. This implies a constraint on the modified expressions of a and b (e.g. correction on b can be deduced from a) through our analytical dispersion model.

$$K^i = \int_{\omega^i} c_t^i(a, b) dV \tag{5.6}$$

The correction in a is a scaling by a positive monotonic decreasing function worthing one in absence of topography changes. For instance, one can assume:

$$a_t^i = a^i \frac{\|\vec{u}^i + \vec{u_t}^i\|}{\|\vec{u}^i\|}$$

Hence, in case a change in topography increases the local velocity the dispersion goes further downstream with less cross-diffusion due to decreasing b through constraint (5.6).

Unsteadiness and uncertainties

Let us recall the multi-level dependency chain in our simulation from topography and wind measurements to the species distribution:

$$(\psi, \vec{u}_{obs}) \rightarrow \{\vec{u}^i, i = 1, .., n_{level}\} \rightarrow \{c^i, i = 1, .., n_{level}\}$$

For the sake of simplicity, we assumed the velocity field unchanged during the drift process and is therefore stationary. Let us now decompose the observation at a given point into a mean and a fluctuating part with zero mean:

$$\vec{u}_{obs} = \overline{\vec{u}_{obs}} + \vec{u}'_{obs}, \quad \overline{\vec{u}'_{obs}} = 0$$

where time average is performed over the time interval of interest T:

$$\overline{\vec{u}_{obs}} = \frac{1}{T} \int_0^T \vec{u}_{obs}(t) dt$$

If the flow is stationary $\vec{u}'_{obs} = 0$ and $\vec{u}_{obs} = \overline{\vec{u}_{obs}}$. If perturbations are weak the deviation from the mean tendency is small and can be represented by a normal law for instance:

$$\vec{u}'_{obs} = \mathcal{N}(0, \sigma_{obs}), \quad 0 \leq \sigma_{obs} << 1$$

As mentioned in (4.3.4), these deviations can be accounted for using Kriging interpolation [59, 60]. Another elegant way to account for small variations of observations while species are emitted and which is not subject to the limitations related to Kriging[3] is to take advantage of the low-complexity feature of the simulation platform and perform Monte Carlo simulations. Hence, we consider a set of observations (simulations) $j = 1, ..., n_{trials}$:

$$(\psi, \vec{u}^j_{obs}) \rightarrow \{\vec{u}^{i,j}, i = 1, .., n_{level}\} \rightarrow \{c^{i,j}, i = 1, .., n_{level}\}$$

where the trials are performed for 'admissible' random choices of $\vec{u}^j_{obs}$ through

$$\vec{u}^j_{obs} = \overline{\vec{u}_{obs}} + \vec{v}^j, \quad \vec{v}^j \in \{\mathcal{N}(0, \sigma_{obs})\}^2$$

One can then define ensemble averages for the calculated velocity field and species:

$$\overline{\vec{u}^i} \sim \frac{1}{n_{trials}} \sum_{j=1}^{n_{trials}} \vec{u}^{i,j}, \quad \overline{c^i} \sim \frac{1}{n_{trials}} \sum_{j=1}^{n_{trials}} c^{i,j}$$

For a given level i one can have an estimation of the deviation from mean tendency for the velocity field and species concentration:

$$\vec{w}^i = \vec{u}^i - \overline{\vec{u}^i}, \quad s^i = c^i - \overline{c^i}$$

and because $\overline{\overline{\vec{u}^i}} = \overline{\vec{u}^i}$ and $\overline{\overline{c^i}} = \overline{c^i}$, one has:

$$\overline{w^i} = 0, \quad \overline{s^i} = 0$$

with corresponding local standard deviations using for instance the maximum-likelihood estimate after assuming normal distribution for the results around their means:

$$\sigma^i_u \sim (\int_{\omega^i} \|\vec{w}^i\|^2 dV)^{1/2}, \quad \sigma^i_c \sim (\int_{\omega^i} (c^i)^2 dV)^{1/2}$$

Figure (5.5) shows an example of mean and standard deviation for a plume in an unsteady flow. The unsteady perturbations corresponds to $\sigma_{obs} = 0.1$. One sees that compared to an evaluation based on an instantaneous measurement the ensemble average based on Monte Carlo simulation introduces an eddy diffusion well known in turbulent flow calculations. Beyond unsteadiness, this approach can be used to analyze the effect of any randomness or uncertainties in data.

In the same way, time evolution of concentrations can be analyzed. Indeed, the following definition of the distance (4.7) permits to access to the concentration distribution at time τ: *If A is upwind with respect to B then*

$$d(B, A) = \infty \quad \textit{and} \quad d(A, B) = \min(\tau, T_{AB}) \tag{5.7}$$

with T_{AB} defined in (4.7). Hence, on can realizes snapshots of the concentration distribution evolution in time as shown in figure 5.6.

[3] Mainly one needs to know the variogram to establish the covariances.

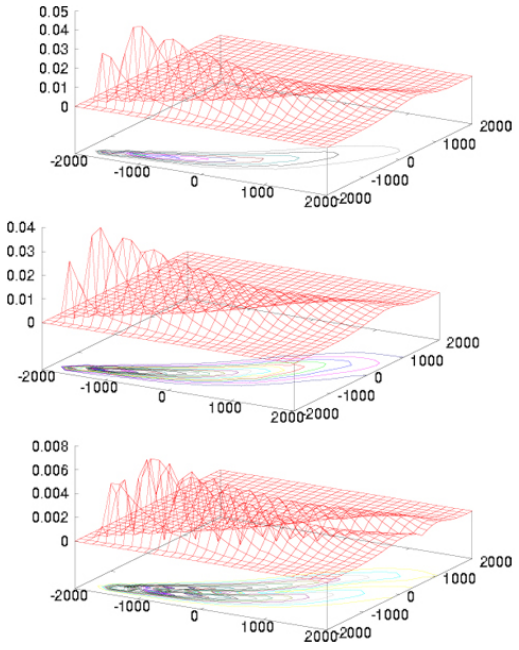

Figure 5.5: Drift based on a flow field evaluated from an instantaneous measurement (top), mean drift based on ensemble average and Monte Carlo simulation (middle) and drift standard deviation (bottom).

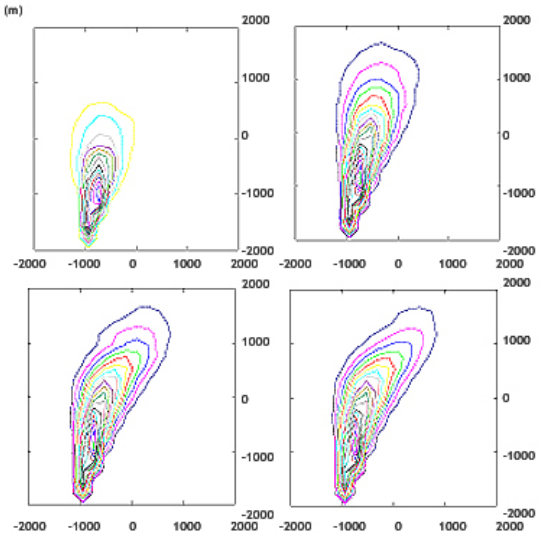

Figure 5.6: Example snapshots of the concentration distribution evolution in time

Chapter 6

Numerical results

This chapter aims to present some GIS-based numerical results of the modeling presented in chapters 4 and 5. The Drift-x model and GIS are used as isolated applications at that stage, and this implies input/output processing as we mentioned in section 3.1.1. Simple Drift-X simulations will be presented in the first section to show how the ouputs can be used in a GIS environment. The topographic impact on the dispersion calculation is then highlighted through simulations over a relevant topographic profile. The Drift-X sensitivity to DEM resolution is then studied by launching the same simulation with a reference DEM layer resampled according to different resolution. The scalability of the model is finally presented and linked to its multi-leveled capabilities.

6.1 Simple simulations

Here is a first Drift-X example simulation of dispersion from a vineyard plot to a $8km^2$ domain. The input parameters used are listed below.

Input parameters

- The domain for calculation is $8km^2$.
- The cartographic projection is extended Lambert 2 (EPSG:27572)
- The number of points for the output grid is 900.
- The used input DEM layer is SRTM 90m resolution.
- The source plot is 1 ha with 33 rows to treat.
- The sprayer treats 3 rows at the same time at the average speed of 1 m/s.
- The spraying nozzle output velocity is 7 m/s with an output flow of 0.001 kg/s.
- Two wind points are used to calculate the flow field.
- The first measurement point indicates a N 60° and 5 m/s wind.
- The second measurement point indicates a N 30° and 4 m/s wind.

Figure 6.1: A close-up of the resulting tractor's trajectory within the treated plot.

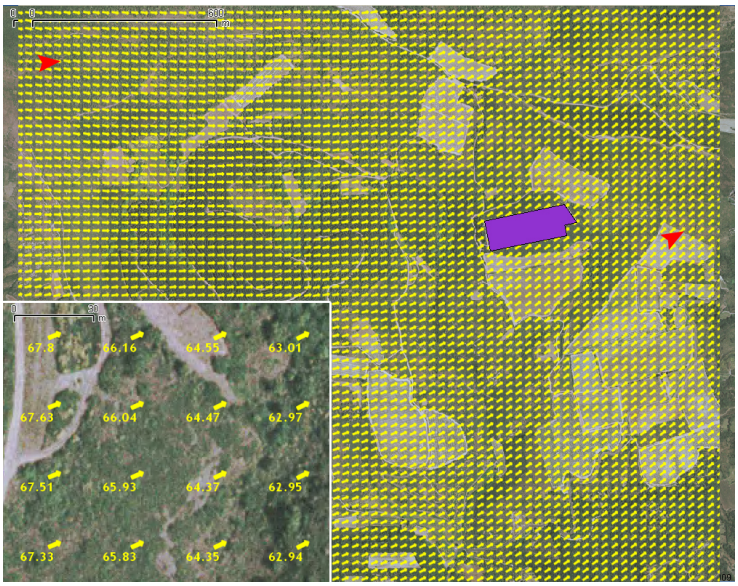

Figure 6.2: The flow field constructed using the modeling detailed 4.3.4 with an example close-up (bottom left)

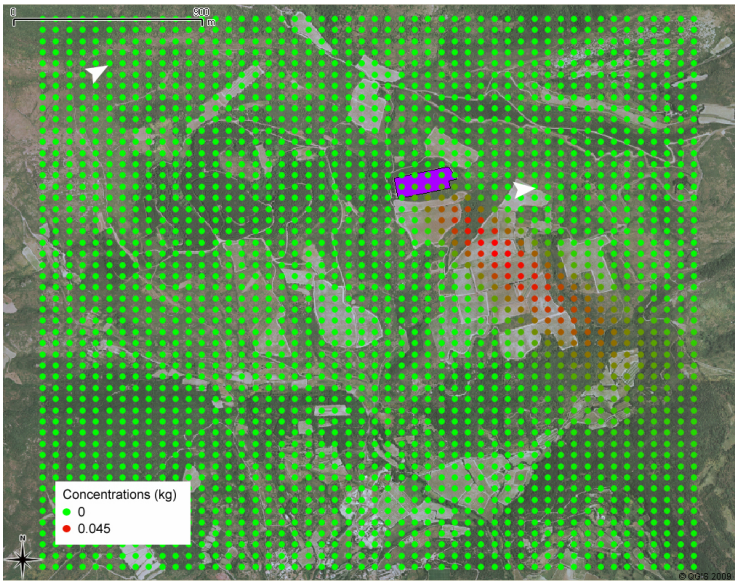

Figure 6.3: The resulting point shapefile (.shp) pesticide cloud using the calculated flow field of figure 6.2 and the source plot.

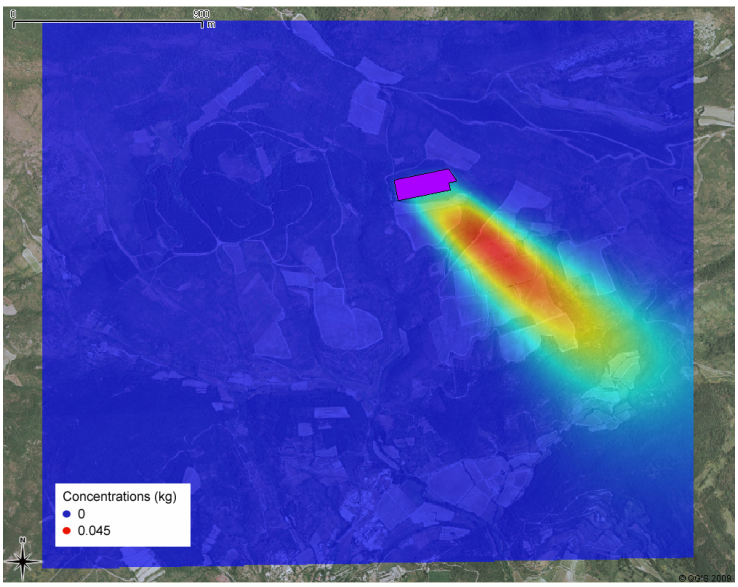

Figure 6.4: the same pesticide cloud as presented in figure 6.3 but displayed as a triangular interpolated raster layer (.tiff).

6.2 Topographic impact

Here are two other Drift-X simulation of dispersion aiming to highlight the topographic effects on the dispersion calculation. Referring to the topographic profile of the used SRTM 90 m layer, the first simulation is performed using a plot located at the top of the plateau according to a north downhill wind and the second one from another plot located at the bottom of the watershed according to a south up-slope wind, as shown by figure 6.5.

Input parameters

The same parameters as for the simulation performed in section 6.1 are used, but with different wind points.

- The first simulation is based on down-hill wind points:
  - X=680712.3899 - Y=1837974.8530 - wind speed 5.0 m/s - wind direction 360°
  - X=681855.1828 - Y=1838138.1090 - wind speed 4.0 m/s - wind direction 360°.
- The second simulation is based on two up-slope wind points:
  - X=680712.3899 - Y=1837974.8530 - wind speed 5.0 m/s - wind direction 180°
  - X=681447.0425 - Y=1837974.8530 - wind speed 4.0 m/s - wind direction 180°.

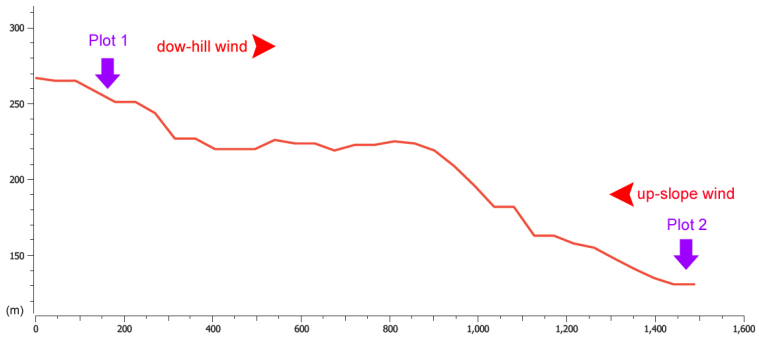

Figure 6.5: Topographic profile and plot and wind points location for simulations

The two simulations present the same quantity of sprayed pesticide on the domain because the same spraying parameters are used, but the resulting clouds have very different shapes. The first simulation shows a long and rather thin cloud as the wind field and the dispersion are accelerated by the slope. On the contrary, the second simulation provides a smaller and larger cloud as it is stopped by the bank but the concentrations are much higher because the cloud is concentrated on a smaller area.

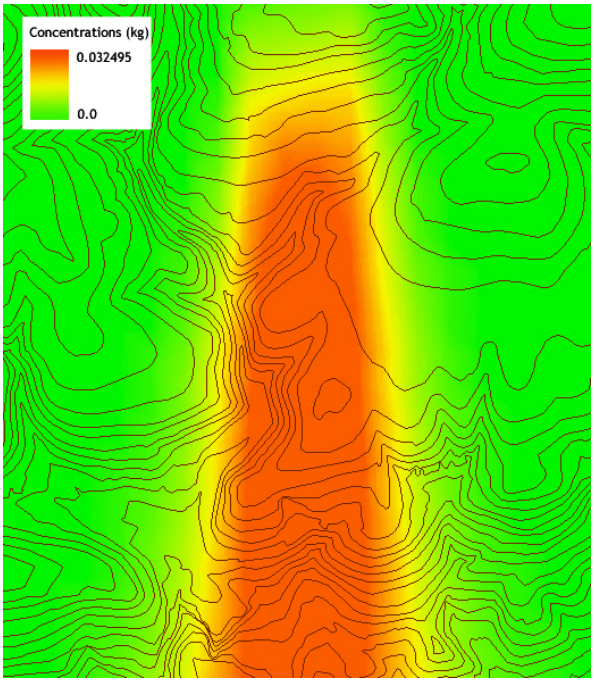

Figure 6.6: Resulting raster pesticide cloud from the plateau treatment with a down-hill wind.

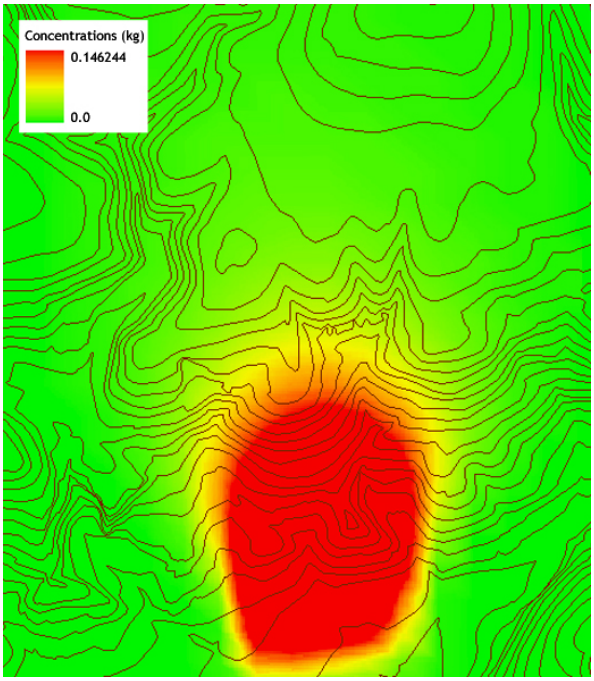

Figure 6.7: Resulting raster pesticide cloud from the bootom of the bank with an up-solpe wind treatment

6.3 Sensitivity to DEM resolution

The impact of topography on calculation has been proven in the previous section using a standard SRTM DEM, and it is then of high interest to study the influence of DEM resolution on the calculation. A simulation is performed on the same extent over a standard IGN 50 m DEM which then has been resampled to 100 m, 200 m and 400 m resolutions, as shown by figure 6.8. The same extent and input parameters listed bellow are used for the four simulations, in order to compare the resulting concentration curves according to the topographic profiles properly.

- The domain for calculation is $12km^2$.
- The DEM layer projection is extended Lambert 2 (EPSG:27572).
- The number of points for the output grid is 2500.
- The source plot is 0,5 ha with 50 rows to treat.
- The sprayer treats 3 rows at the same time at the average speed of 1 m/s.
- The spraying nozzle output velocity is 7 m/s with an output flow of 0.001 kg/s.
- Two wind points are used to calculate the flow field (N 60°-5 m/s and N 30°-4 m/s)

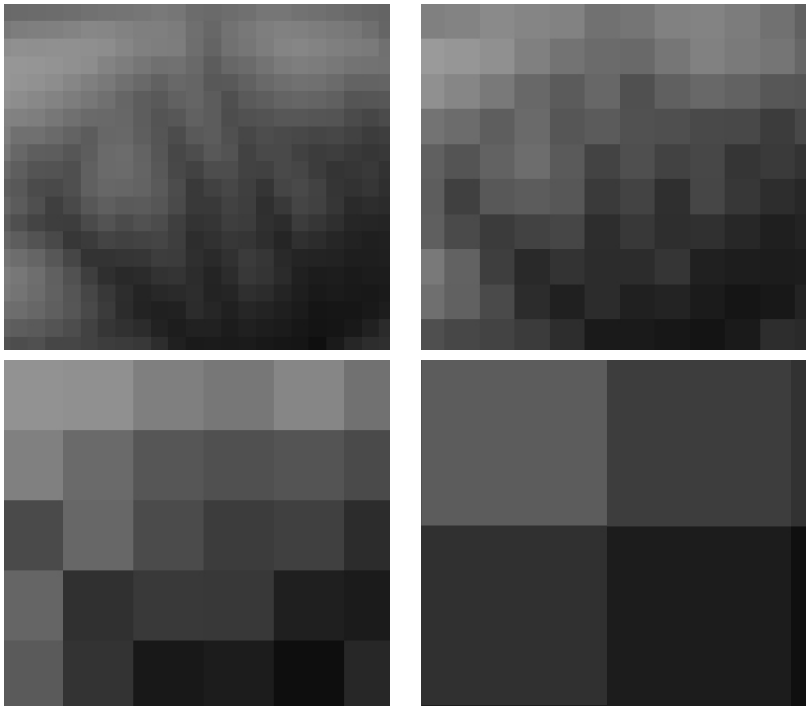

Figure 6.8: Standard IGN 50m DEM layer (top left) resampled at 100 m (top right), 200 m (bottom left) and 400 m (bottom right) resolutions

The resulting pesticide clouds presented in figure 6.9 appear to be rather like-looking although we can observe noticeable differences in their shapes especially at the thresholds of the concentration classes. The total quantity sprayed on the domain is the same for the four simulations, but the cloud i sspreading differently according to the density of elevation points read by Drift-X.

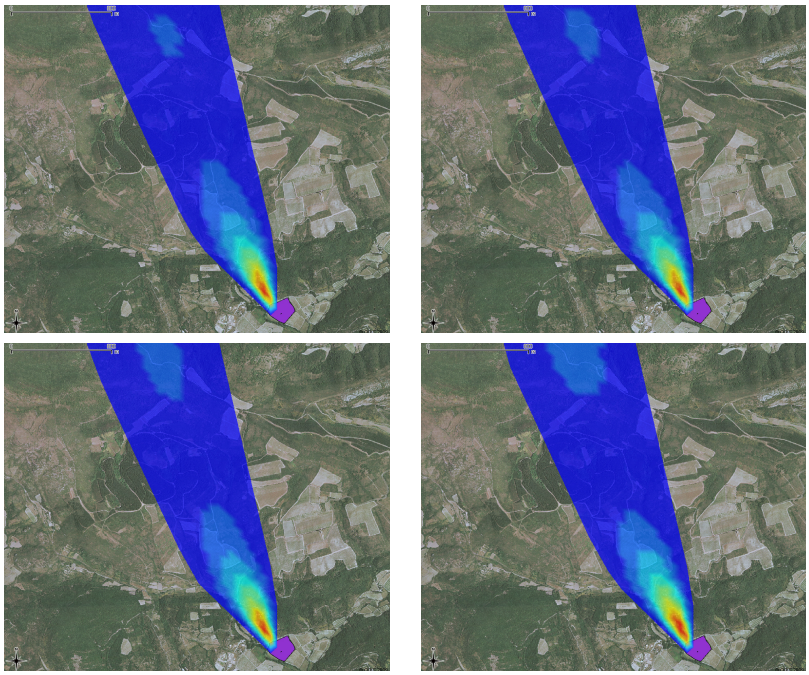

Figure 6.9: Resulting pesticide clouds with IGN 50m DEM layer (top left), 100 m (top right), 200 m (bottom left) and 400m (bottom right).

Comparing first the DEM layers profiles along the plume's x axis on figure 6.10, one can see that they are almost parallel during the first 500 meters of the dispersal (i.e at the bottom of the bank). The profiles then fluctuate on the next 1000 meters which correspond to the plateau zone, on which the 50m DEM provides more details on the topographic depressions whereas the 400 m DEM is much smoother and provides an average slope profile. At the top of the plateau, between 1500 and 2000 meters, we can also observe a peak which corresponds to the continental divide. 0bserving the corresponding concentration curves along the plume's x axis, figure 6.11 shows that a simulation over a 50 m or a 100 m resolution DEM provides almost unchanged concentrations curves. Focusing now on figure 6.12 and comparing concentration curves with the topographic profiles of figure 6.10,one can notice that small variations of concentrations occur on the areas where the topographic profiles are diverging. The concentration peak just next to the source term also presents variations. The 50 m and 200 m resolution resulting curves present higher concentrations as the height values are lower in the profiles and so the pesticide cloud is held back, whereas the averaged 400m resolution profile presents higher values and the cloud is a bit more led back so concentrations increase.

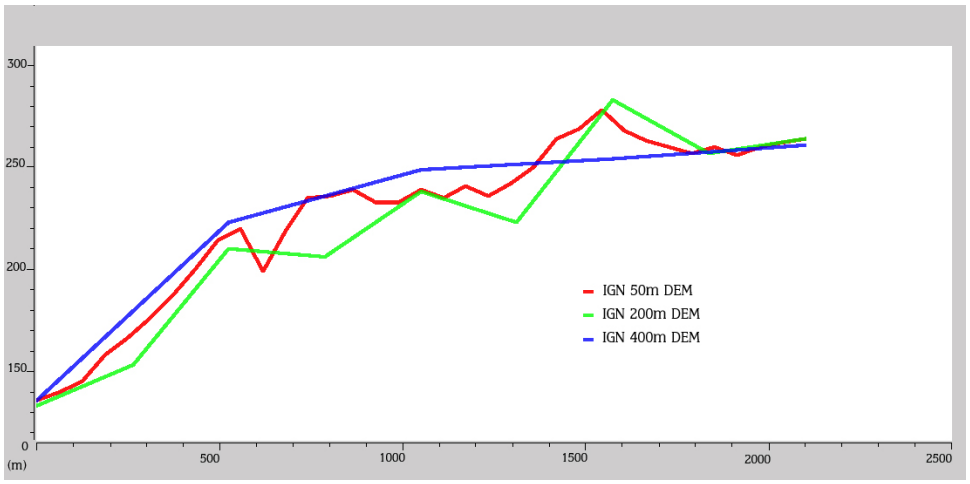

Figure 6.10: Comparison of the 50 m, 200 m and 400 m DEM layers topographic profiles

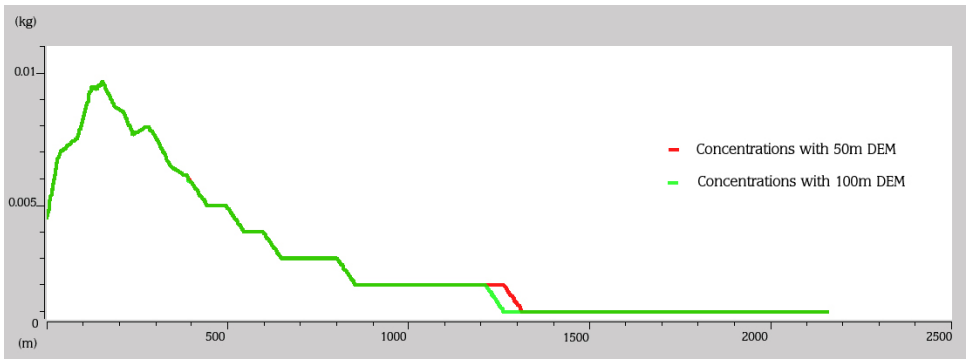

Figure 6.11: Comparison of the Drift-X concentrations curves over the 50 m and 100 m DEM layer.

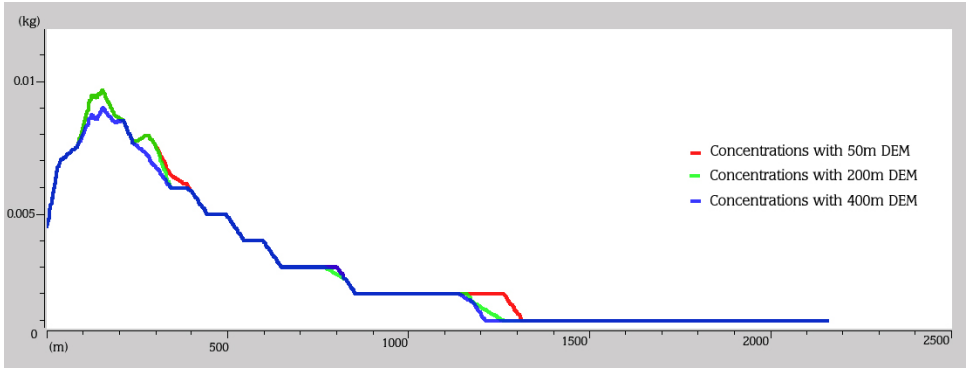

Figure 6.12: Comparison of the Drift-X concentrations curves over the 50 m, 200 m and 400 m DEM layer.

6.4 Multi-leveled simulations

6.4.1 Scalable simulations

As it has been said in chapter 4, the Drift-X model is able to forecast the pesticide concentrations from the plot to the watershed scales. The domain extent for calculation is defined by the user in the input parameters, and so Drift-X simulations can be performed at different scales. Indeed, the two following simulations show that simulations can be launched in either within the plot's surrounding extent (i.e a few ha) as shown by figure 6.13 or on larger domains (i.e several km^2) like in figure 6.14

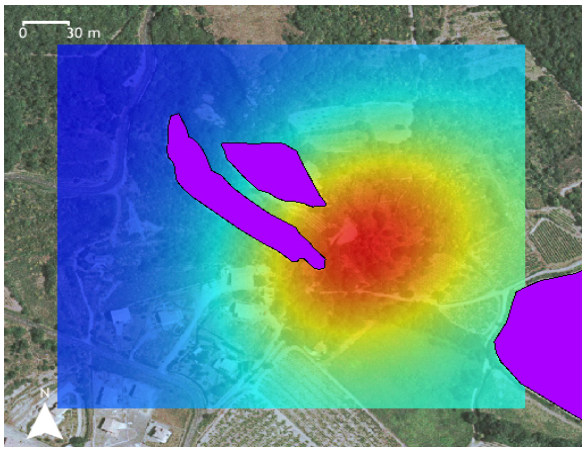

Figure 6.13: Drift-X simulation on a 12 ha domain with two wind points at 1m/s

However, the Drift-X scalability is limited and depends above all on the ratio between the size of the domain and the input wind speed and direction measurement points. Indeed, if the wind flow is strong and the extent too restricted, then the plume will be truncated at the domain's border and the concentrations outside it will be ignored.

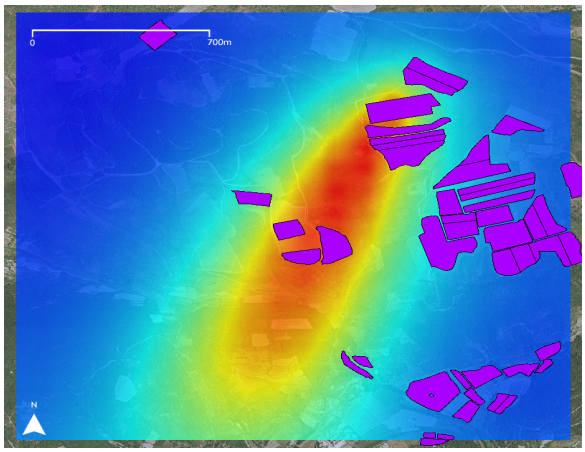

Figure 6.14: Drift-X simulation on a 6km^2 domain with two wind points at 5m/s

6.4.2 Multi-leveled pesticide cloud

As we said in chapter 5, the multi-leveled algorithm permits to locally add some accuracy by resampling the grid on a smaller domain and interpolating the topographic data. This way we can easily compute more detailed flow field and concentrations on any defined area.

The following simulation aims to present a 2 leveled simulation with the following input parameters.

- The coarser domain for calculation is $6km^2$.
- The finer domain is $3ha$ on the center of the treated plot.
- The used input DEM layer is IGN 50m resolution in EPSG:27572 projection.
- The source plot is $4ha$ with 250 rows to treat.
- The sprayer treats 3 rows at the same at the average speed of 1 m/s.
- The spraying nozzle output velocity is 7 m/s with an output flow of 0.001 kg/s.
- The first measurement wind point indicates a N 60° and 5 m/s wind.
- The second measurement point indicates a S 30° and 5 m/s wind.

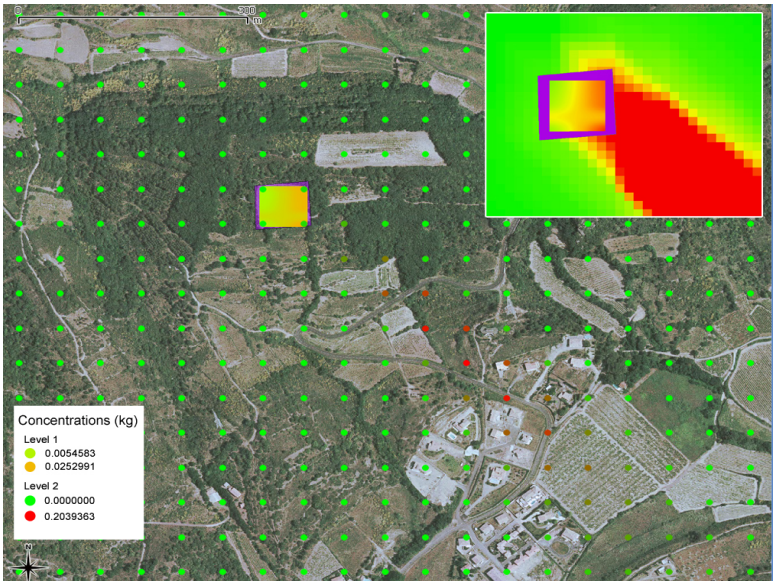

Figure 6.15: Example of two-leveled construction of a pesticide cloud with the finer level located on the treated plot. Close-up on the finer level in raster mode (top right).

This other simulation presents a 2 leveled simulation on a larger domain with a coarser DEM. The 50m IGN DEM layer used in the previous simulation has been extrapolated to a 400m resolution and the wind input parameters modified. The result is presented in figure 6.16.

- The coarser domain for calculation is $10km^2$.
- The finer domain is $60ha$ on a local hill.
- The used input DEM layer is IGN 400m resolution in EPSG:27572 projection.
- The source plot is $2ha$ with 110 rows to treat.
- The sprayer treats 3 rows at the same at the average speed of 1 m/s.
- The spraying nozzle output velocity is 7 m/s with an output flow of 0.001 kg/s.
- The first measurement wind point indicates a N 90° and 5 m/s wind.
- The second measurement point indicates a S 120° and 5 m/s wind.

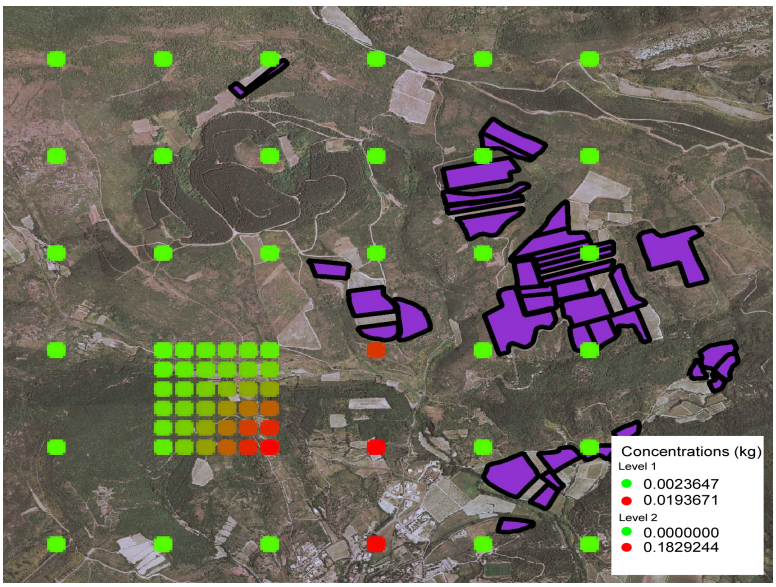

Figure 6.16: Two-level simulation on a larger domain

These two multi-leveled simulations show that the number of levels and their spatial extent can vary. For the sake of simplicity, only two levels were used. Figure 6.15 presents the finer level on the treated plot on only 3 ha, whereas the finer level of figure 6.16 is set-up on a much larger extent covering a local hill located on the cloud's trajectory. In both cases, the higher concentrations values presented in the finer levels are matching the ones of the coarser level which are located at the border between the two levels.

Chapter 7

The Drift-X simulation platform

This chapter presents the simulation platform that has been built in order to transcribe the mathematical modeling into a fast-solving computer program on the first hand, and to couple it with a friendly-user GIS software on the other hand. The main goal of this platform is to automate the set up of the Drift-x parameters and to easily perform numerous DEM based simulations. The Fortran program and its input/output will be presented in the first section and the Quantum GIS python plugin development will then be detailed in the second section. The use of open source GIS for ADM is especially emphasized.

7.1 Fortran ADM

The reduced order modeling approach used for the modeling made the programing aspects easier. The equations composing the model presented in chapters 4 and 5 have been transcribed in Fortran language, including the former local spray drift model, the wind flow calculation and the travel-time based transport model as routines. The choice of Fortran was made because it is one of the languages that is best suited to compute complex mathematical expressions.

The fastness of the Fortran compiler [63] and the mesh free approach allows us to compute the solution in only a few seconds depending on the size of the domain and on the elevation data resolution. Indeed, the DEM values are extracted for the domain and then sent to Drift-X, which computes the solution using the x, y, z triplets as base topography. The results are then written to output files which contain point-based information for the whole domain.

The program has not been transformed into a independent GIS class yet as the integrated approach would suggest, but is used as a standalone and fast executable program. Both input and output datasets will then have to communicate with Quantum GIS as explained in section 7.2. Despite the fact that a more integrated GIS oriented ADM class will greatly enhance the coupling, there is a major advantage in the resulting coupling which is that the Fortran program stay independent of the GIS software, which will

make any modification in the model easier as we will only need to re-compile the Fortran program.

7.1.1 The Drift-X inputs

Every parameter of the model is read by the Fortran program from input ASCII files. These are listed below:

Domain definition

- The spatial extent on which to compute $(X_{min}, Y_{min}, X_{max}, Y_{max})$
- The resolution of the resulting grid (ex: 100 x 100 to create 10000 points)
- The number of level wanted (when using the multi-leveled version)
- The X and Y values corresponding to the smallest level (it often corresponds centroid of the plot)

Vehicle definition

- The tractor's starting point (X, Y)
- The tractor's speed during the spraying application (generally 1 m/s)
- The tractor's direction angle in comparison with the X axis (45 ° for example)
- The tractor's direction at the end of the first treated row (left / right)

Sprayer definition

- The number of rows treated at the same time (generally 3 rows at each passage)
- The spraying nozzle output velocity (m/s)
- The spraying nozzle output flow (Kg/s)

Wind definition

- The number of wind measurement points on the domain
- The location of each wind points (X, Y)
- The wind speed at each point (m/s)
- The wind direction at each point (-180° / 180°)

Topography definition

- The path and name of the DEM layer to use for calculation

7.1.2 The Drift-X outputs

Once the program has been executed, three output results are written to output ASCII files. These are listed below:

- The tractor's trajectory as a line on the treated plot
- One or several calculated flow field as a point grid on the whole domain
- One or several pesticide dispersion as a point grid on the whole domain

7.2 Open source geospatial software for ADM

Open source GIS appeared in the early eighties with the birth of GRASS GIS which was initially developed by the U.S Army. With the broad use of non-proprietary and open data formats, as well as the adoption of Open Geospatial Consortium (OGC) standards in many GIS projects, the development of open source GIS software continues to evolve, bringing the best of open source to the geomatics community. New software and libraries such GDAL/OGR or QGIS were born and are continually improved by the open source community. Such softwares are also more and more used in various spatial related scientific projects and serve a lot of explorations of new algorithms, approaches and applications. They are sometime also used to couple GIS data models with numerical simulation models, which motivated our choice to use open source GIS libraries.

7.2.1 Quantum GIS API

Quantum GIS (QGIS) is an open source GIS licensed under the GNU General Public License. QGIS is a volunteer driven project that is officially featured by the Open Source Geospatial Foundation (OSGeo). It is multi-platform one and supports numerous vector, raster, and database formats and functionalities. Quantum GIS provides a continuously growing number of capabilities provided by core functions and plugins and has become one of the most highly capable and stable open source GIS.

Indeed, QGIS is based on a robust C^{++} API that presents plenty of spatial algorithms and native GIS functions. QGIS has been designed according to an extensible plugin architecture. This allows new features and user-oriented functions to be easily added to the application and that's why QGIS offers advanced programming possibilities. Plugins can be created using C^{++} or the related Python bindings, which allow a simpler programming environment for developing specific plugins that directly interact with the C^{++} source code.

As we did not want to develop a completely home made ADM dedicated GIS, but rather take advantage of existing stable GIS APIs to perform our coupling, the decision to use QGIS and to build a pesticide ADM plugin in it was made. The steps of the development are detailed in the next section.

7.2.2 Drift-x plugin development

The QGIS python bindings allows to develop plugins easily using PyQt library and Qt Designer to build cross-plateform user interfaces and PyQgis bindings to access the complete *C++* API classes and use them directly from python code. Once install in the local plugin folder (or on a distant repository), the plugin is registered at QGIS startup and must be activated using the plugin manager to be active in the plugin toolbar.

QGIS as an input data provider

The first role of QGIS deals with the automatic DEM extraction, needed by the model to compute the effects of ground variations on the atmospheric dispersion. As the multi-leveled approach has been conceptualized to gain in topographic accuracy, one has to work with several DEM resolutions and be able to extract pixel values from any loaded DEM in the GIS. Using the Python bindings, this can simply done using some common GDAL (Geospatial Data Abstraction Library) commands. In our case we used two successive *gdal translate* commands [64], as described bellow:

```
gdal_translate -ot Float32 -projwin "str(xmin) + str(ymax) + str(
   xmax) + str(ymin)+" input_dem.tif output_dem.tif
\label{gdal1}
```

This first command is run to clip the loaded DEM according the user-defined extent in which the calculation must be launched.

```
gdal_translate -of AAIGrid clip.tif clip.asc
\label{gdal2}
```

And this one is run to extract the elevation value of each pixel of the extent to an ESRI grid file. The grid thus obtained is then converted into x,y,z triplets [65] needed by the model as topography input, using the *grd2xyz* python class [65]. These successive commands enable the user to get the topographic input data for the dispersion model, overriding the user's DEM resolution and spatial projection as the Fortran program is then able to convert Cartesian metric into the same values it reads in input.

DEM as cross-platform datasource

The DEM layer of the studied area is required by the model and can be displayed and processed using QGIS API. This appears as useful and allows us to tend to a tight coupling approach. Indeed, the input DEM is clipped and parsed by the QGIS raster engine as shown by **??**, and then sent to the Fortran model. The DEM layers are thus used by the two systems and appear as a cross-platform data source, enabling the model to handle geographic coordinate systems.

Indeed, the mathematical model works on a Cartesian metric basis, which is not readable as is by QGIS. As one wants the plugin to be able to read any resolution in any geographic projection, the spatial properties of the DEM image have to be read and understood by the model. This can be achieved by sending the resulting file of the *gdal translate* commands to the Fortran program, which then reads the given tabular x,y,z file by accessing the standard Comma Separated Values (CSV) format [64].

The generated DEM is sent to Fortran using simple Fortran *open* and *read* commands: Each triplet (i.e each line of the former raster matrix) is then understood by Fortran which converts the x,y,z values from Cartesian to Geographic and so provides the elevation data on which the calculation has to be computed, for every point of the domain. The data flow which formalize the relationship between Drift-X and QGIS is detailed below in figure 7.1.

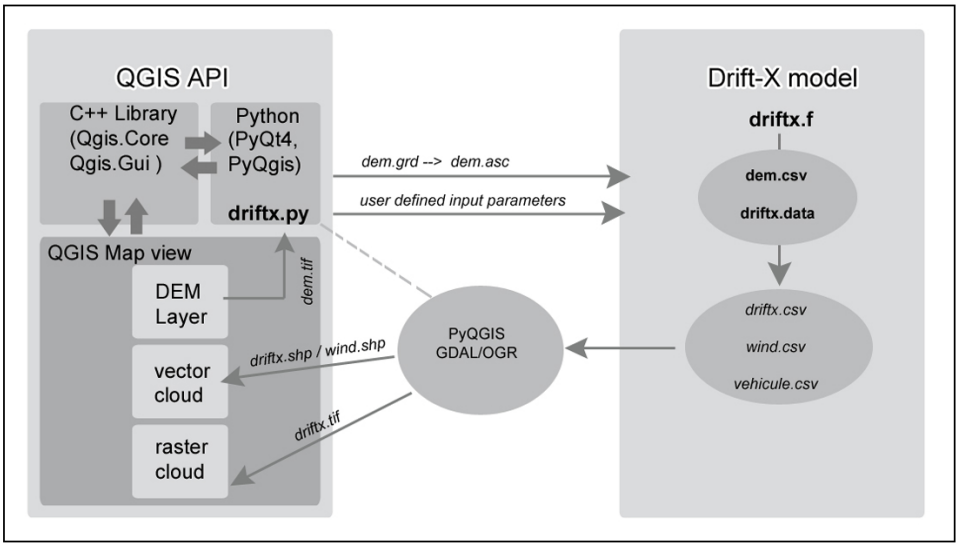

Figure 7.1: Scheme of the data flow used for coupling Drift-X model and Quantum GIS.

In this development approach, the Drift-X Fortran executable is embedded into the plugin directory and called by the main python class *driftx.py*. The latter writes input parameters and the user-defined DEM and send them to the model, which one computes the solution and sends the results back to QGIS. API classes are then used to convert the results into standard GIS vectorial and matricial formats, as explained in section 7.4.

As we have already explained, the main goal was to automate the model setup, to use it in a georeferenced framework and to build a coupling as tight as possible. This is achieved by using QGIS API and by managing the input/output in a single GIS program. However, tending to a more integrated approach can be imagined by translating *driftx.f* into a QGIS C^++ or python class. That way, several steps regarding coordinate transformations and output processing could be performed natively and this would greatly minimize the inputs/outputs exchanges.

7.3 The multi-level algorithm implementation

7.3.1 Scales and extents

The multi-leveled correction for ground variations lets the user choose the number of levels wanted (i.e *nlevels* in equation 5.1), as well as their spatial extent (see figure 5.2). This enables us to define the local area where the grid resolution must be finer in order to compute ground variations and the flow field more precisely. This "micro-scale" area can be defined just around the source plot considered for example, or any other area that presents particular topography or significative obstacles to the spray drift (like local depression, small hill or other interesting rock-formings). This is achieved in QGIS by using an adaptation of the *Region Tool* algorithm [66] applied in a recursive way:

```
def doneRectangle(self):
    level = self.iface.getMapCanvas().setMapTool(self.saveTool)
    self.updateBounds(self.r.bb)
```

This first function makes it possible to draw and save a rectangle on QGIS map view (map canvas) that defines the new extent for calculation.

```
def updateBounds(self,bb):
    self.xmindomain.setText(str(bb.xMin()))
    self.ymindomain.setText(str(bb.yMin()))
    self.xmaxdomain.setText(str(bb.xMax()))
    self.ymaxdomain.setText(str(bb.yMax()))
    newLevel = bb.xMin(),bb.yMin(),bb.xMax(),bb.yMax()
```

Then, the previous code allows to update the four corners of the extent and thus to determine a new level for calculation. This way *Region Tool* can be used as many times as needed, in order to set up the right number of levels for the calculation.

7.3.2 Limitations and perspectives

The multi-leveled approach appears as very useful in order to compute more accurate grids on small domains but displays some limitations. First of all, the algorithm do not interpolate elevation values in order to resample automatically the input DEM for each level. This could be done directly from Fortran using some down-sampling techniques, as presented in [67], but would imply modifying the model. Indeed, the multi-level correction for ground variations (see section 5.2.2) allows us to optimize locally the calculation on a finer grid, but does not provide more accurate elevation values as a precise DEM would do.

Given that Drift-X is well suited to take continuous ground variations into account but remains limited to handle big topographic variations, it is hopeless to use it on too complex topographies with metric accuracy DEM or even with Digital Surface Model (DSM) and to account for precise vertical obstacles.

7.4 Standard GIS formats rendering

A major asset of the coupling is the ability of QGIS API to render numerous different standards GIS formats as it is based on the GDAL/OGR library. The use of standard formats also makes it possible to use the Drift-X outputs in an independent GIS software. The last step of the plugin development deals with the conversion of CSV output into vector and raster layers, but also with identifying good practices to enhance the cartographic rendering of the output. The vector representation is first explained regarding pesticide clouds and windflows, and the raster creation and interpolation will then be detailed.

7.4.1 Vector representations

Pesticide clouds rendering

Using the QGIS API, we can first easily generate the model output results as an ESRI shapefile (.shp) or any other OGR supported GIS vector format. This is done using the QGIS *QgsVectorFileWriter* class as presented bellow:

```
uri="plume.csv?delimiter=%s&xField=%s&yField=%s"%(";","longitude","
   latitude")
v=QgsVectorLayer(uri,"vectorial␣plume")
QgsVectorFileWriter.writeAsShapefile(v,"vectorial-plume.shp"')
```

Where plume.csv is the input CSV file that include longitude, latitude and atmospheric concentrations fields, and vectorial-plume.shp is the created point shapefile. Once this has been done, one can instantaneously apply some styling options to the created layer, in order to emphasize the concentrations values. This can be done using the QGIS *QgsContinuousColorRenderer* class, by alloting a symbol type to the geometries and a couple of minimum and maximum colors for the continuous color rendering.

```
v=QgsContinuousColorRenderer(v.vectorType())
v.smin=QgsSymbol(v.vectorType(),"0","","")
v.smax=QgsSymbol(v.vectorType(),"1","","")
v.smin.setPen(QPen(Qt.green,1.0))
v.smax.setPen(QPen(Qt.red,1.0))
```

Moreover, Drift-X generates point values on the whole domain but it can be useful to delete the points where no concentrations are calculated (i.e GIS layers "no-data"). Accessing the *QgsFeature* class and the related *QgsMapAttributes* and *deleteAttributes* public member functions, this can be done using simple SQL request on the right field like in our case:

```
SELECT Features WHERE Field(deposition) = 0
```

This returns the same result as the QGIS search functionality would do [68] using the search query builder. This way, only points that contain information are displayed, as shown by figure 7.2

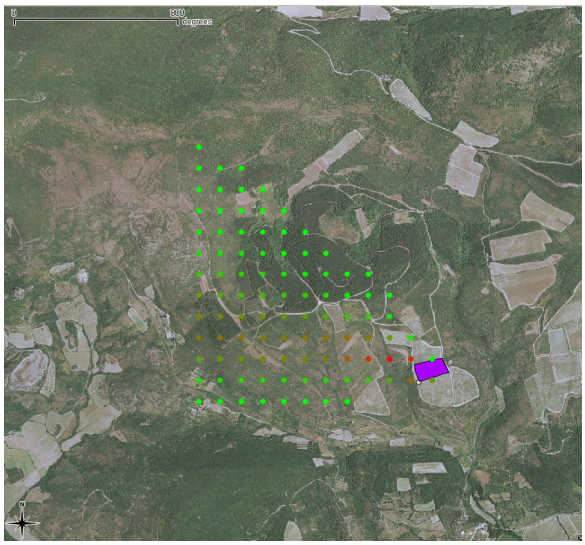

Figure 7.2: Point shapefile pesticide cloud but with no data features deleted

Wind fields mapping

According to the same principle (i.e *QgsVectorFileWriter*), we can also generate the associated wind field. Using the *setRotationClassificationField*, it is easy to render point symbol as oriented arrows according to the direction field contained in the wind attribute table, as shown in figure 7.3

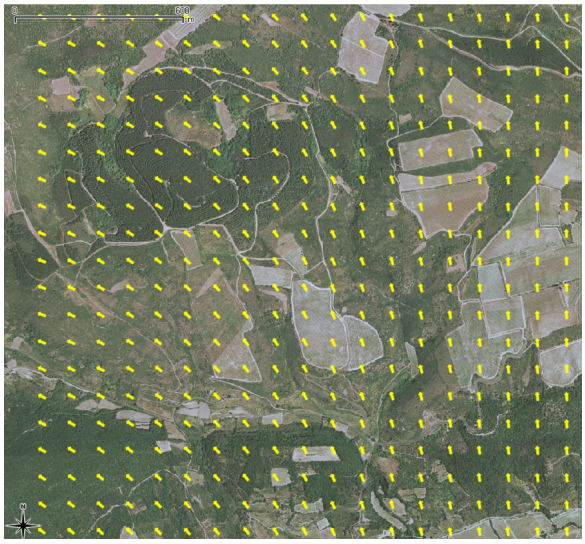

Figure 7.3: Generated point shapefile wind field with arrows oriented according to direction values

7.4.2 Raster representation

Raster creation

Another point of interest for mapping generated pesticide clouds is the raster generation, as the spray drift is a diffuse phenomenon and that a surfacic representation is much more readable than points in this case. The raster creation can greatly improve the cartographic message. This can be done using the *gdal grid* capabilities, using the GDAL virtual format (i.e VRT driver) in which the CSV file generated by Drift-X is addressed [64]:

```
gdal_grid -of GTiff -ot Float64 -l driftx driftx.vrt output.tif").
   readlines()
```

The generated raster can then be loaded with the *QgsRasterLayer* class and added to QGIS map using the *QgsMapLayerRegistry.instance()*. Several style settings can also be specified with the *setColorShadingAlgorithm* and *setTransparency* functions.

```
fileName = output.tif
fileInfo = QFileInfo(fileName)
baseName = fileInfo.baseName()
rlayer = QgsRasterLayer(fileName, baseName)
QgsMapLayerRegistry.instance().addMapLayer(rlayer)
```

Raster interpolation

The point-based information related to atmospheric pollution is usually represented using interpolation techniques. Interpolation predicts values for raster cells from a limited number of sample data points. It can be used to predict unknown values for any geographic point data. Most common methods to perform interpolation of atmospheric pollution point-based information are known to be Kriging, Inverse Distance Weighting (IDW) or Triangulating Irregular Network (TIN). Other methods are also possible such as the use of Spline or Natural Neighbors techniques. A comparison of interpolation techniques is proposed in figures 7.4

In the Drift-X plugin, we can acces the native interpolation plugin [69], which propose IDW or TIN methods, by accessing the $C^{+}+$ function from Python using SWIG [70]. It is also possible to do it in a simpler way using the GDAL interpolation algorithms. Here is an example using a IDW method:

```
gdal_grid -a invdist:power=1.0:smoothing=50.0 -txe"+str(xmin)+str(
   xmax)+"-tye"+str(ymin)+str(ymax)+"
-of GTiff -ot Float64 -l driftx driftx.vrt output.tif").readlines()
```

Where *-txe* is the spatial extent in which to interpolate (i.e the user-defined extent via the Region Tool class), *-of* is the desired output format and *-ot* the raster type. As the point-based values are interpolated over the whole domain, one has to apply a vectorial

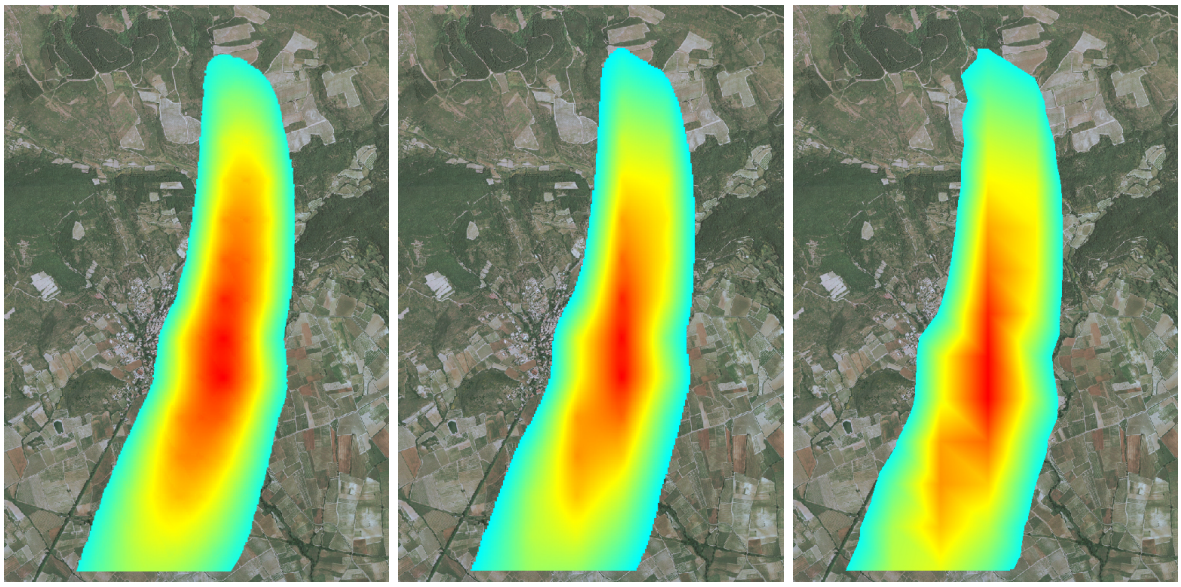

Figure 7.4: Raster pesticide cloud generated using Kriging (left), Natural Neighbors (middle), and TIN (right) interpolation methods

mask, in order to account only for points with values and so to delete the raster nodata. This can be done using the clipping functions of GDAL, using a *gdal translate* command line with clipping option. Finally and as for the vector ouput, one can apply coloring schemes and transparency values, using the QGIS *QgsRasterLayer* optionnal arguments, as suggested below:

```
rlayer.setDrawingStyle(QgsRasterLayer.SingleBandPseudoColor )
rlayer.setColorShadingAlgorithm(QgsRasterLayer.PseudoColorShader)
rlayer.setTransparency(90)
```

7.4.3 Drift-X plugin GUI

The Drift-X plugin graphical user interface (GUI) is designed to make Drift-X input setup as simple as possible. It is built with Qt Designer software which is Qt dedicated integrated development environment (IDE). It makes it possible to design GUI visually using every graphic widgets from the Qt library and making them interact. The Drift-X plugin GUI is organized according to a simple tabbed layout (see figure 7.5) in which each tab gathers the groups of input parameters cited in section 7.1.1.

Thus, the "Domain" tab allows to dynamically complete the wanted extent for calculation, thanks to *Region Tool* call (see section 7.3.1). The "Terrain" tab then enables to choose the DEM layer to use for calculation, by browsing the disk or getting the full path of any loaded DEM layer by clicking on it in the map view. The "Wind" tab lets the

user choose wind points location as well as their corresponding measurements (direction and speed). The "Sprayer" tab enables users to indicates the vehicle starting point and its speed during the treatment as well as the width of the spraying device and the nozzle outlet velocity. The "Output" tab finally asks for the wanted output format to the user, namely vector (.shp), raster (.tiff) or spreadsheet (.csv). General view of the QGIS GUI is given in figure 7.5 and an example tab is shown in figure 7.6.

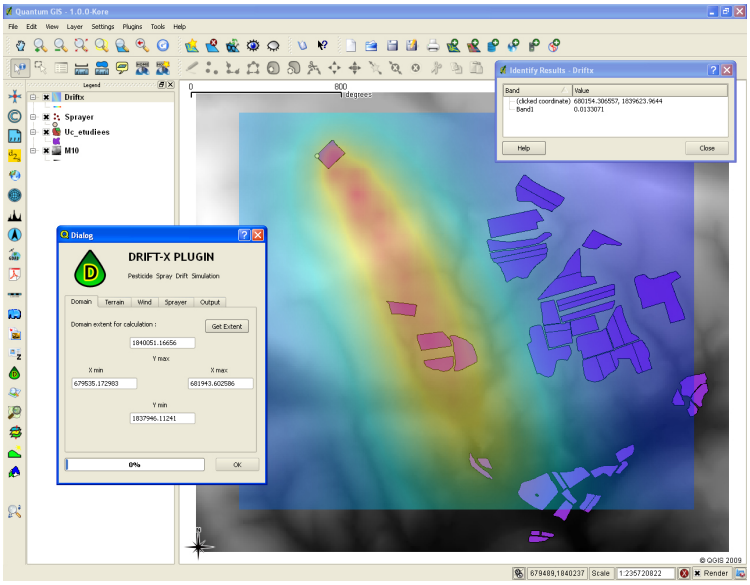

Figure 7.5: Quantum GIS user interface with Drift-X plugin activated

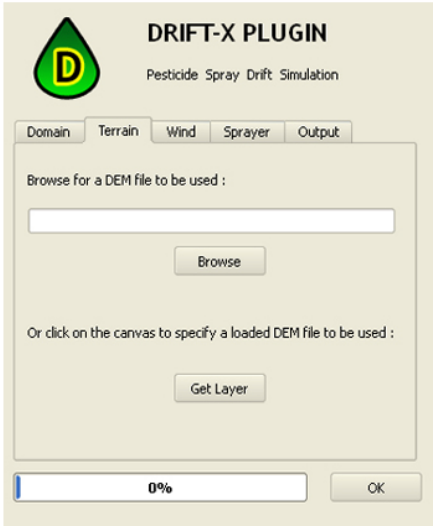

Figure 7.6: An example plugin tab to choose the input DEM on which to compute

Part III

Neffiès watershed: A case study

Chapter 8

A typical southern French wine-growing area

This chapter aims to present the Neffiès watershed which is the chosen area for this case study. Our goal is to give a general presentation regarding both the geographic context and the wine-growing activities first, and then to present the available datasets that will be used for the study in the second hand.

This chapter sets up the context of the case study and notably introduces the Aware project and its possible connections with Drift-X model. The linkage with an agro-meteorological database and an example of Drift-X use for risk assessment are explained in the next two chapters.

8.1 The geographic context of the study area

Neffiès is a small village in the department of Herault in the southern part of France. It is approximately located 50km west of Montpellier, at the crossroad of the Cevennes mounts and the Mediterranean scrublands. The village is $11km^2$ and has 700 inhabitants, most of them being located in the burg at the south of Neffiès. The area is surrounded by vineyards, scrublands and small wooded areas and scattered with numerous small water courses. A general view of the village and a map of the watershed are presented in figures 8.1 and 8.2 .

The Neffiès watershed is interesting for our concern as it presents a rather smooth topographic profile made of small hills and local depressions, but with sufficient topographic variations for the wind flow calculations to be modified. Vineyards are located both on the plateau and down the valley which provides an ideal study area to perform several simulations on various topographic configurations. Moreover, Neffiès is a typical southern French windy place where the tramontana wind prevails all the year long. Indeed, a meteorological station had been installed in the watershed and recorded a 1 m/s mean wind for 2008 with maximum speeds approaching 12 m/s according to the available meteorological backups. [71].

Figure 8.1: Neffiès watershed general view

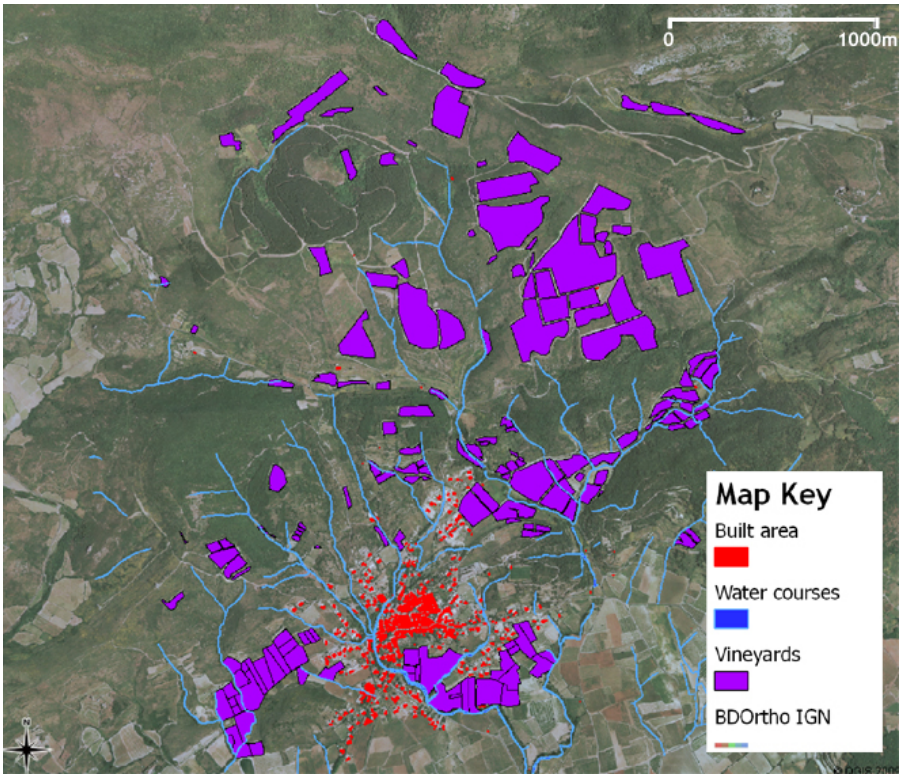

Figure 8.2: Neffiès vineyards map

8.2 The Life Aware project

Besides the number of vineyards and the representative topographic and meteorologic conditions, Neffiès was also chosen for the huge amount of available spatial and meteorological datasets provided by the Life Aware project, among others. The Life Aware project, co-funded by the European Union and 9 partners in France, Spain and Italy, focuses on the impacts of agricultural activity on water resources in rural areas. It was set up to demonstrate how the optimisation of agricultural practices and equipments related to pesticide spraying for viticulture helps the farmers to preserve the quality of water entities and to maintain a high quality production. This project is coordinated by the Cemagref and based on a partnership between public organizations such as the Conseil Général de l'Hérault and the Chambre d'Agriculture de l'Hérault, public research and training centers like Montpellier SupAgro and INRA but also private companies. One of the key actions of the project is to introduce high-technology sensors on the tractors and sprayers in order to assess their acceptability and to figure out how they can help wine-growers to better use their machine. The Aware system aims to measure a number of relevant datasets during the spraying applications and then to process the recordings into reports to be delivered to the farmers of the Neffiès wine cooperative.

The Aware system is made up of two parts:

- The Aware mobile device which, is an electronic system gathering a GPS device, a anemometer and several other sensors, and which is embedded on tractors and measure and record spraying parameters.

- The Aware Server on which a PostGIS database has been installed in order to backup and process both GPS and statistical records sent to the server by the mobile device. Indeed, PostGIS allows to add support for geographic objects to the PostgreSQL object-relational database. It spatially enables the PostgreSQL server, allowing it to be used as a backend spatial database for GIS.

The Aware PostGIS database thus appeared as an interesting resource to provide realistic wind input data to Drift-X, as it stores thousands of georeferenced wind points for each spraying application thanks to the anemometers and GPS devices. Details of the database are given in section 9.1.

8.3 Avalaible datasets

The richness of both the geospatial and meteorological information available made the Neffiès watershed an ideal place to perform simulations with realistic topographic and meteorological input datasets. This allowed to apply the Drift-X model to the reality of a typical wine-growing area, and to propose applications for the risk assessment of pesticide pollution, using simple spatial analysis. The available datasets used for this case study are listed bellow.

8.3.1 Geospatial data

Different types of raster and vector geospatial datasets are used for the study in the following chapters. As Neffiès is located in the southern part of the "New French Triangulation" (NTF) geodesic system, all the datasets have been converted into the corresponding Lambert 2 extended projection (EPSG:27572) [1] They can be classified as the following:

Reference DEM layer

- The reference IGN © 50 m DEM layer.

Vineyards related layers

- The studied vineyards geometries as a PostGIS polygon layer.
- The vehicules trajectory as a PostGIS point layer.

Reference data layers

- The Neffiès IGN Scan 25 © (topographic map).
- The Neffiès IGN BD Ortho © (ortho-images).
- The Neffiès land use as a Corine Land Cover (CLC) raster.

8.3.2 Meteorological data

The available meteorological datasets for the case study can be described as the following for each plot of the Aware database.

Wind datasets

- Wind speed measurement points linked to GPS way points for each spraying application (m/s).
- Wind direction measurement points linked to GPS way points for each spraying application (degree).

Nozzle related datasets

- The spraying nozzle output velocity (m/s) for each recorded point of a treatment (m/s).
- The spraying nozzle output flow (Kg/s) for each recorded point of a treatment(degree).

[1] the NTF coordinate system and the related Lambert projection systems are the reference frame for French map. Although it will be soon replaced by the "French Geodesic Reference" (RGF93), the EPSG:27572 is used for the study as it is the more accurate system for the Neffiès area.

Chapter 9

Linking Drift-X to an agro-meteorological database

This chapter aims to present the linkage of the Drift-X model with the Aware agro-meteorological database. The PostGIS database architecture is first described regarding its tables and their relationships, and basic SQL queries are used to reach spraying applications statistics over a given temporal window in the second hand. Then, the use of PostGIS within the Drift-X plugin is explained. Indeed, a special version of the plugin has been built in order to truly couple it with the Aware database using the QGIS API. This is done with the QGIS PostGres Data Provider as explained in section 9.2.

9.1 The Aware PostGIS database

9.1.1 Spraying applications as a relational database

The Aware PostGIS database is made of 16 tables all linked by an "id traitement" primary key. For our concern, we will only focus on the "traitement", "import parcelle" and "uc machine" tables, as they contain the required information that we want to provide to Drift-X. Those three tables are shown in figure 9.1.

The "uc machine" table stores the geometries of the plots as well as other interesting parameters for Drift-X inputs such as the plot's area, the number of rows and the distance between rows. As for the "traitement" table backups the raw data are related to all the treatments that occur on "uc machine" plots. This contains a GPS point per second with all the associated measurements such as date, time, wind speed and direction and the spraying nozzle output flow and velocity. The third relevant table is called "import parcelle" and gathers the same data as "traitement" but filtered by plot using "code uc" primary key. The raw data is also processed in this table in order to obtain mean values from raw data. This provides all the treatments performed on each plot and the mean values of wind and nozzle measurements for each treatment.

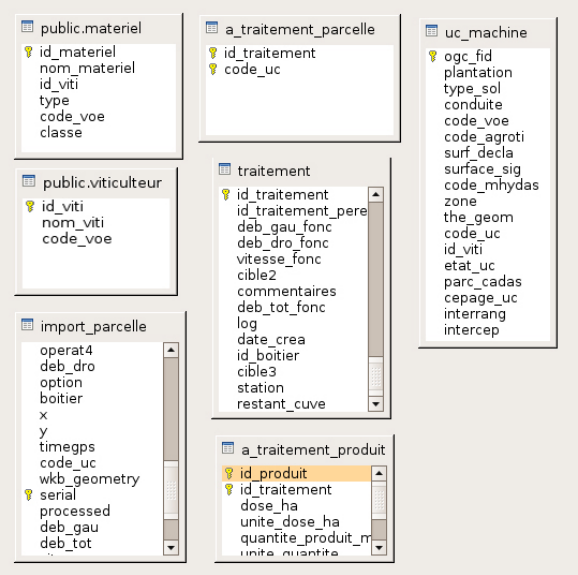

Figure 9.1: simplified scheme of the Life Aware PostGIS database

9.1.2 Spraying applications statistics

Querying the database using the nomenclature cited above, we can reach simple statistics about spraying applications. For example, we can determine the total number of treatments for all the plots in 2008 using the following query.

```
SELECT count(id_traitement)
FROM traitement
WHERE date_traite >'2008-01-01'
```

This returns 143 treatments for the 40 registered plots so an average number of 3,575 treatment per plot for a year. Using a more complex query, we can determine the exact number of treatments per plot ("code uc") and group them by date ("date traite").

```
SELECT
to_char(date_traite,'YYYY-MM-DD') as date_traitement,
count(code_uc) as nombre_parcelles
FROM traitement
WHERE date_traite >'2008-01-01'
GROUP BY date_traite
```

Then, we can also select plots where treatments occurred at given dates, group them by plot identifier and by date and order the results according to hour, as shown bellow:

```
SELECT code_uc,
MIN(TO_TIMESTAMP(dat_loc||heu_loc,'YYYY-MM-DD HH:MI:SS')) as
   heure_min,
MAX(TO_TIMESTAMP(dat_loc||heu_loc,'YYYY-MM-DD HH:MI:SS')) as
   heure_max,
```

```
FROM import_parcelle
WHERE(dat_loc='2007-06-09')
GROUP BY code_uc,dat_loc
ORDER BY heure_min
```

This example for June the 9^{th}, 2007 returns three plots where treatments occurred at the same time (between 4:18 am and 5:15 am), as presented bellow:

```
"03E";"2007-06-09 04:18:26+02";"2007-06-09 05:28:56"
"10A";"2007-06-09 04:29:48+02";"2007-06-09 05:15:37"
"10C";"2007-06-09 04:38:41+02";"2007-06-09 05:04:37"
```

Once simultaneous spraying applications have been identified, we can finally identify the recorded points within the three plots that have identical time slots, and extract the corresponding mean wind datasets from the "import parcelle" table:

```
SELECT
dat_loc,heu_loc,for_ven,dir_ven,code_uc
FROM import_parcelle
WHERE
dat_loc='2007-06-09'
AND TO_TIMESTAMP(dat_loc||heu_loc,'YYYY-MM-DD HH:MI:SS') > '
   2007-06-09 04:18:26'
AND TO_TIMESTAMP(dat_loc||heu_loc,'YYYY-MM-DD HH:MI:SS') < '
   2007-06-09 05:15:37'
AND ( code_uc='03B' OR code_uc='10A' OR code_uc='10C')
ORDER BY heu_loc
```

This finally provides three simultaneous realistic wind measurement points located at the centroid of plots 03E, 10A and 10C that are listed bellow and mapped on figure **??**.

```
"03E";"2007-06-09";"04:18:26";"05:28:56";"4.0";"301"
"10A";"2007-06-09";"04:29:48";"05:15:37";"3.0";"350"
"10C";"2007-06-09";"04:38:41";"05:04:37";"6.5";"323"
```

Figure 9.2: Plots 03E, 10A and 10C with the corresponding simultaneous mean wind points extracted from the Aware PostGIS database

9.2 Using PostGIS from Drift-X plugin

9.2.1 Neffiès dedicated Drift-X plugin

As the Aware PostGIS database provides realistic wind measurements, as shown in section 9.1, a special version of the Drift-X plugin has been built for the Neffiès study area. It has been designed to let the user consult any plot of the "uc machine" PostGIS layer and to automate the extraction of wind data to be sent to Drift-X. That way we can perform Drift-X simulations within QGIS using realistic winds points and topographies thanks to the database and to DEM layers.

The main differences from the former plugin presented in section 7.2 are listed bellow:

- The plugin automatically sets the map extent to the watershed area at start-up.
- The plugin automatically loads the "uc machine" PostGIS layer on the QGIS map canvas.
- The wind values and tractor's starting point are automatically extract from the database with a click event on the chosen plot.

9.2.2 Querying PostGIS from Python

This section presents some python code that allows the Drift-X plugin user to setup Drift-X wind and sprayer input data in a simple click. The connection to PostGIS is achieved using the *PyGreSQL* [72] python package which is imported into Drift-X source code header.

Connection to PostGIS

The permanent connection to the database is ensured with an "aware" variable which calls a *pg.connect* command that gathers the database name, the server URL and port and the authentication informations.

```
aware = pg.connect("aware_gps", "localhost", 5432, "login", "
   password")
```

Map Canvas initialisation

When the plugin is launched, the QGIS Map Canvas is firstly set to the Neffiès watershed extent. Accesing the *QgsMapCanvas* class, this is simply done by using the *setExtent* public function, as the following:

```
setExtent(677965.7039, 1836645.3068, 682539.7111, 1841257.2202)
```

Then, we must connect the plugin to the Aware PostGIS database using the QGIS API *QgsDataSourceURI*, as suggested below:

```
uri = QgsDataSourceURI()
uri.setConnection("localhost", "5432", "aware_gps", "login", "
   password")
```

Once the connection has been set, we can easily choose the "uc machine" layer and add it to map canvas at plugin activation like this:

```
uri.setDataSource("public", "uc machine", "the_geom", "cityid =
   2643")
vlayer = QgsVectorLayer(uri.uri(), "uc machine", "postgres")
```

Querying PostGIS

Once the map canvas initialization is done, the user only has to choose an extent for calculation and then click on the wanted plot for source term. At the click event, the x/y coordinates are captured and the python code then loops through all the "uc machine" layer's features looking for intersects. Once the feature identifier has been found and encapsulated into a "id uc" variable, we can then query the database directly using some *pg* commands, as specified bellow:

```
query1= "SELECT date_traite, code_uc,force_vent_moy, direc_vent_moy
    FROM traitement WHERE code_uc='"+ str("id_uc") + "'"
result1=db.query(query1)
```

This query returns the wind statistics for all the dates where spraying applications were performed on the chosen plot. The resulting dates can then be stored in a list in order to let the user choose one date and put it in a "id date" variable, and then launch another query like this to get the wind data for the chosen date:

```
query2= "SELECT force_vent_moy, direc_vent_moy FROM traitement
   WHERE code_uc='"+ str("id_uc") + "' AND date_traite='"+ str("
   id_date") + "' "
result2=db.query(query2)
```

We can finally reach the plot's centroid using PostGIS *ST Centroid* function, and assign the mean wind values to it using the following command:

```
query3= "SELECT x(ST_Centroid(the_geom)) as centroX, y(ST_Centroid(
   the_geom)) as centroY FROM uc_machine WHERE code_uc='"+ str("
   id_uc") + "' AND date_traite='"+ str("id_date") + "' "
result3=db.query(query3)
```

The chaining of these three queries thus makes it possible to get the mean wind speed and direction at the centroid of the plot, which is then sent to Drift-X in the usual way as specified in section 7.1.1.

Chapter 10

Drift-X for pesticide exposure risk assessment

This final chapter aims to show how the Drift-X model can be used to perform simplified risk assessment regarding the exposure of the environment to deposited pesticide. A scenario for simulations is proposed using the example given in section 9.1.2 and the available datasets listed in section 8.3.

10.1 Simultaneous Drift-X simulations

Using the example of June 9th, 2007 (see section 9.1.2), three simultaneous Drift-X simulations can be performed in relation to the same flow field. Plots 03E, 10A and 10C have been identified to get simultaneous wind measurements, which are used to calculate the flow field for this given time (between 4:18 am and 5:15 am). The input parameters for the three simulations are listed below.

10.1.1 Input parameters

Domain and topography

- The domain for calculation is $38km^2$.
- The cartographic projection is extended Lambert 2 (EPSG:27572)
- The number of points for the output grid is 900.
- The used input DEM layer is IGN 50m resolution.

Sources plots

- Plot 03E is 2 Ha with 70 rows to treat.
- Plot 10A is 4 Ha with 120 rows to treat.
- Plot 10C is 1 Ha with 30 rows to treat.

- The sprayer treats 3 rows at the same time at the average speed of 1 m/s for each plot.

- The spraying nozzle output velocity is 7 m/s with an output flow of 0.001 kg/s for each plot.

Wind flow field

The flow field is calculated using the mean wind values of each plot located at centroids of 03E, 10A and 10C. The values resulting from the PostGIS queries cited in section 9.1.2, are recalled below:

- Plot 03E wind point is 4m/s and 301°.

- Plot 10A wind point is 3m/s and 350°.

- Plot 10C wind point is 6m/s and 323°.

Numerical results

The three resulting pesticide clouds are then interpolated using the IDW method and added up using GRASS GIS *r.mapalgebra* function. This mean that overlapping pixel values are added up and that the three clouds are in a single raster layer. The nodata values have been removed using *r.null.val* function. The result is presented in figure 10.1.

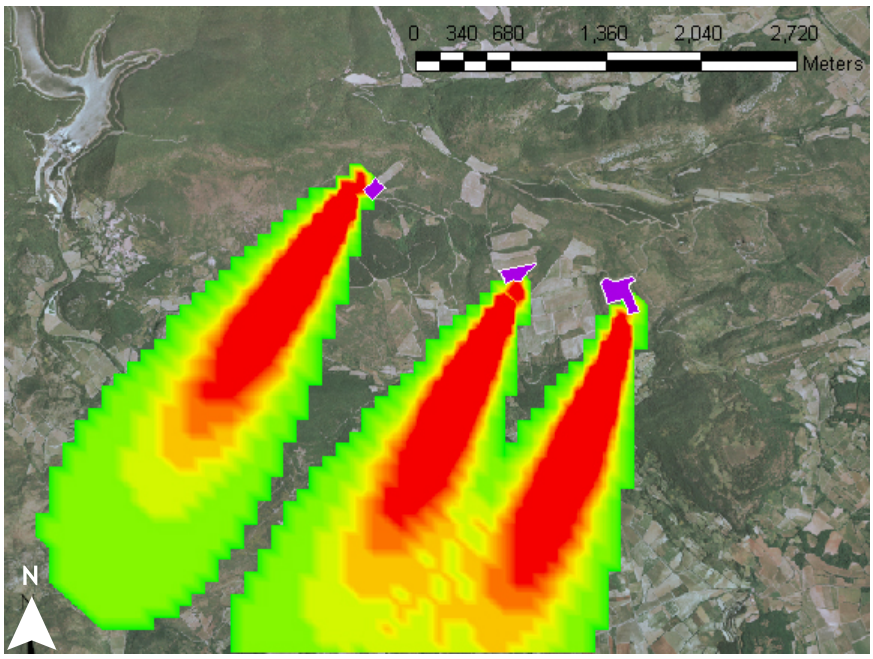

Figure 10.1: Resulting three simultaneous pesticide clouds

10.2 Using GRASS GIS for exposure risk assessment

10.2.1 GRASS GIS presentation

The Geographic Resources Analysis Support System, commonly called GRASS GIS, is a Geographic Information System (GIS) used for data management, image processing, graphics production, spatial modeling, and visualization of many types of data. It is an open source software and an official project of the OSGeo. GRASS support was recently added to QGIS as a suite of C++ plugins, and that provides a lot more functionalities to QGIS, notably about raster analysis. Those functionalities are used below.

10.2.2 Land use data description

Corine Land Cover (CLC) is used to get the land use classes of the Neffiès area. This is the European land use reference database, which is driven and maintained by the European Environmental Agency. At Neffiès, CLC provides a simplified classification of soils according to the nomenclature shown by figure 10.3

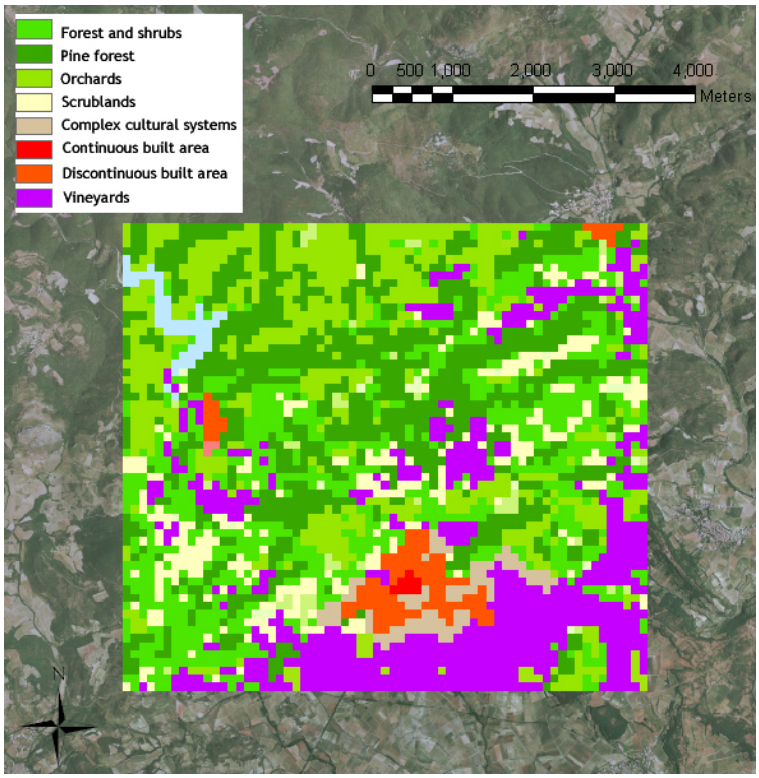

Figure 10.2: Neffies CLC layer classes

The Neffiès area land use is mainly composed of vineyards, scrublands and wooded areas. The built areas are located south of the watershed, and we can already notice that the village is in the way of the three simultaneous pesticide clouds, as shown by figure 10.1.

10.2.3 Intersecting CLC and Drift-X raster layers

Using GRASS GIS, we can simply isolate the CLC layer pixels which intersect the pesticide clouds. This is done with *r.mask* with the pesticide cloud layer as analysis mask, as presented in figure 10.3. The affected CLC classes can thus be identified.

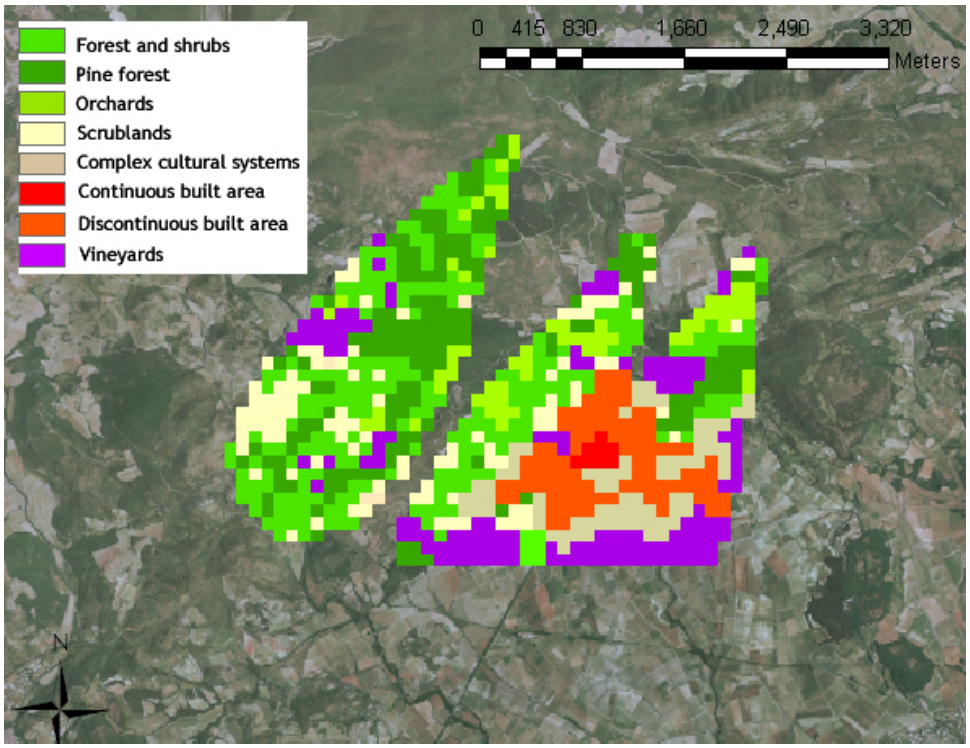

Figure 10.3: Neffies CLC layer classes intersecting the Drift-X layer

10.2.4 Zonal statistics

It is now possible to affect the concentration values to the selected CLC pixels. As the Drift-X layer has a finer resolution than the CLC one, we must sum the Drift-X values within each CLC class using the *r.sum* function (see figure 10.4). We can also calculate an average concentration value for each class using the *r.average* function (see figure 10.5).

According to the same principles but using local vector datasets, we can reach more accurate zonal statistics at larger cartographic scale. For example, figure 10.6 shows the sum of concentrations that have reached the village, obtained by intersecting the pesticide clouds layer with the Neffiès built area vectorial layer. As to figure 10.7, it presents the same calculation but using the Neffiès water courses vectorial layer. Those zonal statistics can then be used to quantify the total amount of pesticide that has been deposited on the built areas or on the water courses. This could constitute an interesting basis for more complex pollution risks analysis.

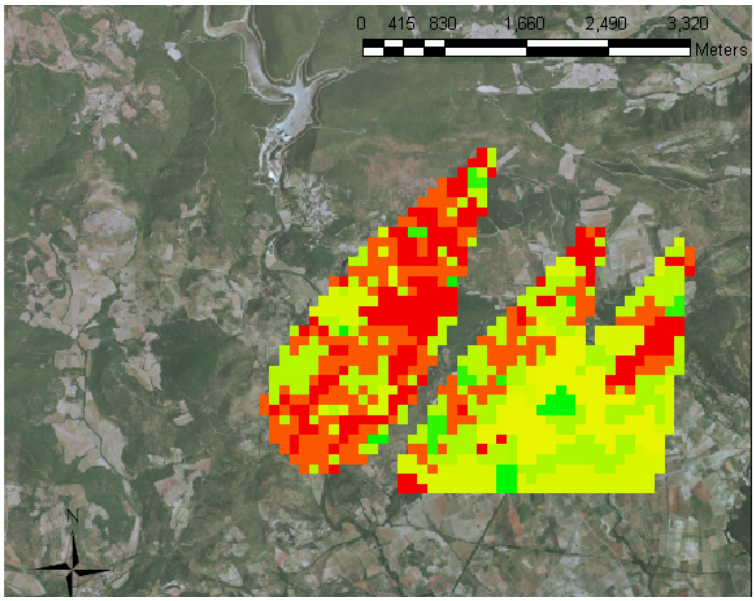

Figure 10.4: Clipped CLC layer presenting the sum of concentrations values per classes

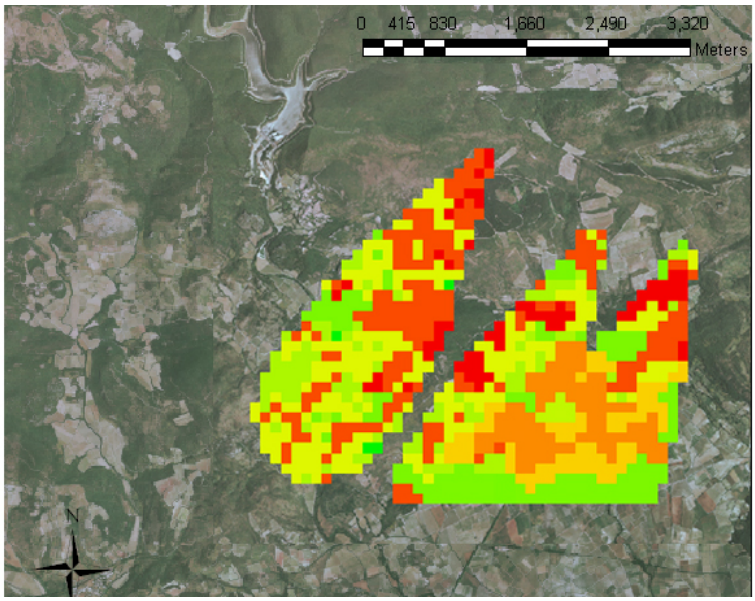

Figure 10.5: Clipped CLC layer presenting the averaged concentrations values per classes

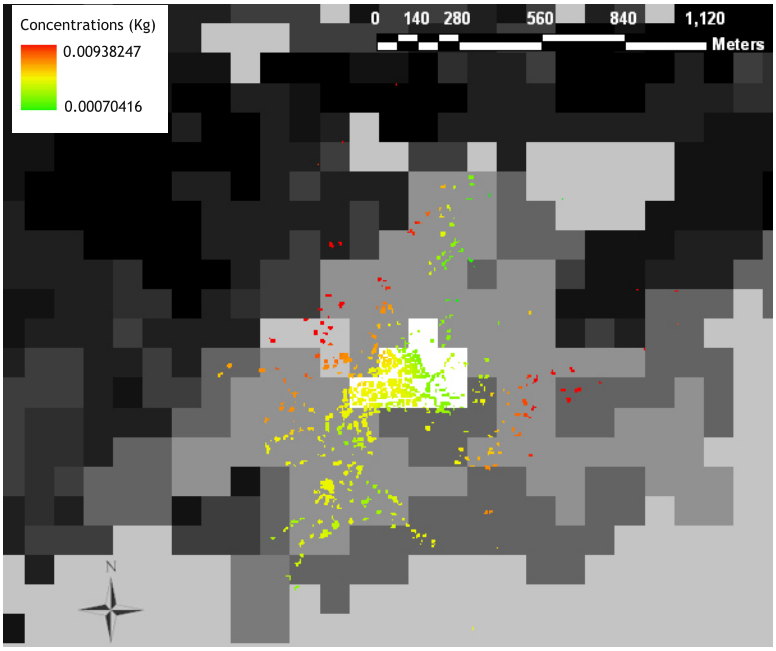

Figure 10.6: Neffiès built area layer presenting the sum of concentrations values per classes

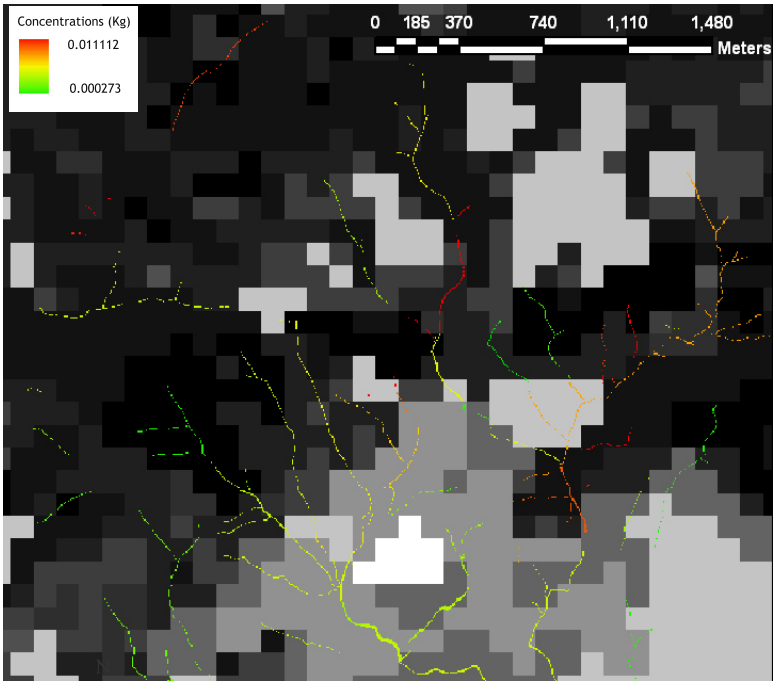

Figure 10.7: Neffiès water courses layer presenting the sum of concentrations values per classes

Conclusion and perspectives

The coupling of a reduced-order atmospheric dispersion model with GIS has been presented and applied to the spatial modeling of agricultural pesticide spray drift. This thesis has gathered some agro-meterological facts, an original mathematical modeling approach and some GIS knowledge and development, leading to a simulation platform able to forecast and map georeferenced wind flows and pesticide clouds.

The multi-disciplinary aspects of this thesis have highlighted a kind of duality in our coupling. Indeed, some theoretical improvements of the former Drift-X model have first been implemented, according to identified ADM and GIS cross-cutting thematics. Parts of the GIS data model like coordinate systems, layered information or the vector/raster differences have been used to adapt the mathematical modeling to the GIS-based representation of space. The use of DEM layers as a cross-platform data source has made it possible to tend to a tight coupling, as it is shared by the model and the GIS both for calculation and visualization. Furthermore, DEMs have supplied some different topographies on which to simulate dispersion and this has provide some terrain reality to the Drift-X model. Scale changes have been modeled according to the same principle of getting more accuracy and to tend to more realistic simulations.

The other side of the coupling deals with the inherent technical aspects of GIS, that have been notably shown by the development steps of the Drift-X simulation platform within the Quantum GIS environment. The latter has made it possible to automate the model setup in a projected frame and to simplify its execution thanks to the Python language and the QGIS plugin architecture. Although GIS development constitutes the technical part of the coupling, it is intimately related to the theoretical enhancements that have been proposed. Indeed, the input/output data flows are needed by Drift-X but generated by the plugin core functionalities. As an example, the DEM layer must be processed by QGIS before being sent to the model that computes the ground variations. That's the same principle for the extent or the multi-extent which are defined by QGIS and then sent to Drift-X. Without any DEM and extent, the model would not work.

Regarding the use of DEM for the coupling, several conclusions must be given. As we already said, the DEM first provide more reality to the dispersion process modeling as it allow to handle realistic topographies in the modeling. But the input DEM layer also provide its resolution and its projection that are implicitly contained in the x,y,z triplets understood by the model. This a key element of the coupling as the geospatial support is

added to Drift-X only using DEM properties. That makes the georeferenced simulations possible and allows to map directly the outputs. However, the user must be aware of the integrity of the input DEM according to this coupling approach.

The model takes many advantages from the use of DEM, and the impact of the provided topographic values on the flow field construction and the pesticide cloud transport has been proven in section 6.2. We have also shown that the DEM resolution influences the accuracy of the results. Nevertheless, it has been recalled that the Drift-X model is especially suited to large topographic variations that makes no sense to use very accurate metric DEM, as the small variations would not be taken into account. This should be improved because some of the small variations matters in the dispersion process, especially for simulations at finer scale. Moreover, the vineyards surrounding environment can presents significant obstacles to the spray drift, but these are visible only with high resolution DEM. The transport model should ideally be modified to handle Digital Surface Models (DSM) as the latter can for example provide building heights, but also tree lines properties or any other feature that can modify the pesticide cloud behavior. This would greatly enhance accuracy but would imply strongly modifying the model, as the reduced order modeling approach would have to deal with much more complex geometries. This would also affect the calculation costs due to the huge number of triplets that Fortran would have to read.

On the other hand, the Drift-X model scalability has been introduced and its limits identified. Thus, the multi-leveled approach appeared as judicious to split the domain in several sub-domains and to gradually account for smaller topographic variations around the main point of interest. This also allows to resample the output grids and to obtained more finer-grained wind flows and pesticide clouds at bigger cartographic scales. The DEM values are interpolated in the smaller domain but no topographic information is added, in the sense that accurate small variations cannot be identified from the loose DEM used at the coarser scale. Inspite downsampling techniques and powerful DEM interpolation techniques exist and could be applied, the best configuration for our concern would be to use a DEM per level (from coarse to fine) but this has not yet been implemented in the coupling.

Several other conclusions can be reached about the Drift-X simulation platform. The QGIS API has provided a powerful open source GIS platform to achieve the technical coupling. The plugin architecture and the Python language have also offered flexibility and many development resources in order to embedded the Drift-X model into QGIS. It is now possible to setup meteorological inputs, spraying parameters and topographic inputs through Drift-X plugin GUI, to launch the model in an easy way and to map and visualize the georeferenced outputs directly on the QGIS map canvas. Thus, pesticide spraying applications can be quickly simulated in their digital geographic reality, and many scenarios can be tested thanks to the plugin. More over, once the outputs loaded onto the map, tens of other native QGIS functionalities can be used from the most basic ones (i.e interrogate a pesticide cloud pixel to get its concentration value) to more complex

ones (i.e create a buffer around the vectorial cloud for example), which improves the dispersion analysis and can help to use the Drift-X outputs for more complex spatial analysis.

On the other hand, the Neffies watershed case study and its dedicated version of the plugin has proven that such a platform can communicate with spatial relational databases and greatly take advantage of spraying applications statistics. The linkage with the Aware agro-meteorological PostGIS database has allowed to construct wind flows from real wind measurements and this provides some more reality to the model. Thus, the scenario proposed in section 10.1 has thus been based on real topography and wind measurements and allowed to set up a simple risk analysis of pesticide exposure of the surrounding environment.

The coupling of Drift-X model and QGIS has finally lead to a detailed exploration of the open source GIS capabilities to integrate and enhance complex environmental models. Indeed, the QGIS plugin development has allowed to test several methods to perform the coupling, and this has provided a deep knowledge of the QGIS API and its dependencies or related tools such as the GDAL/OGR library or the PostGIS database. As for the GRASS environment, which has enabled the advanced use of the Drift-X outputs within the QGIS environment. Open source GIS has thus a great role to play for spatial-based scientific modeling and can be considered today as an alternative to the use of proprietary GIS softwares.

Future research for the coupling should be composed of different studies that need to be detailed. Talking about the model itself, several enhancements have been identified as possible in the near future. First, the Drift-X inner dispersion model has been used as a "black-box" in this study but could be greatly improved. It could be coupled for example to some more accurate models established at different scales once again. Droplets size and spraying nozzle models could first be used in order to obtain more precise quantities of pesticide reaching the plant rows. Some more accurate analysis of the inner plot dispersion could also be performed using CFD or LES tools, that would allow to set up elaborated pesticide flow model within the vineyards. Some volatilization models could also be coupled to Drift-X in order to reach more realistic quantities of pesticide leaving the plot. This would provide better inputs to the Gaussian transport model. The latter should also be subjected to several enhancements regarding wind flows construction and the topographic recognition. Indeed, more complex wind processes must be studied in order to minimize errors, especially on unsteady rotating flow fields. DSM or metric DEM implementation through a more complex multi-leveled algorithm could by the way greatly help to model finer turbulences due to obstacles on the pesticide cloud trajectory. Compromises will have to be done between modifying the model to improve the accuracy of outputs at each scale, and keeping the calculation costs as low as possible in order to perform fast GIS simulations.

Moreover, huge research and field experiments will have to be done to validate the model on the terrain reality. Several identified projects guided by the CEMAGREF Lab may allow to install anemometers and air samplers on the Neffiès area. This would allow to collect accurate wind measurement on larger areas and over longer time-series, and tend to the validation of the flow field construction. As for the air samplers, they would provide numerous air samples at different distances from the treated plot. Those could be analyzed thanks to chromatography techniques and provide real pesticide concentrations that could be compared to the simulations numerical results. The Drift-X model validation will be a long and expensive research and the use of GIS is once again heartily recommended in this work, as it could be used to determine the best locations for anemometers and samplers, using both DEM and slope analysis and the knowledge of local prevailing winds.

More over, several other possible enhancements deal with the Drift-X simulation platform. As we said, the best configuration would be to transcribe the Fortran program into a native C++ or Python QGIS class. This would provide a full integrated coupling between the model and QGIS and would probably increase the perspectives of using much more advanced QGIS functionalities from the plugin. This way, pesticide cloud based spatial analysis could be automated and the platform would tend to a real decision support tool for pollution prediction and analysis. Additionally, other GIS development tasks have already started in order to adapt the coupling for a Web-GIS architecture. Using open source tools and libraries once again, it will be soon possible to run Drift-X simulations on the Internet using a simple web browser. The use of the well known "open source GIS stack" is suggested to perform this task. Thus, the Web-GIS platform will be built using MapServer,PostGIS and OpenLayers in a Web Processing Service architecture, in order to make the Drift-X model communicate with the Internet user through the chaining of common mapping standards such as Web Map Service (WMS) and Web feature Service (WFS).

We can finally conclude that the coupling made it possible to simulate the atmospheric dispersion of agricultural pesticide within a GIS environment, and that several other dispersion process could be modeled using Drift-X. Indeed, the reduced order modeling approach will allow to easily adapt the equations to the industrial dispersion process. That way, pollutant clouds emitted by the industrial chimneys could be simulated and mapped using the Drift-X platform.

Conclusion et perspectives

Le couplage d'un modèle de dispersion à complexité réduite avec un SIG a été présenté et appliqué à la modélisation spatiale de la dérive des pesticides agricoles. Cette étude a permis d'assembler des notions de viticulture, une approche mathématique originale ainsi que des aspects de programmation SIG, conduisant ainsi à la mise en place d'une plateforme de simulation capable de prédire et de cartographier des champs de vents et des nuages de pesticides géoreferencés.

Les aspects pluri-disciplinaires de cette thèse ont permis d'identifier une certaine dualité du couplage. En effet, des améliorations théoriques ont d'abord été apportées au modèle Drift-X initial, selon des thématiques communes à la modélisation de la dispersion atmosphérique et aux SIG. Certains aspects du modèle de données des SIG comme les systèmes de coordonnées, les couches d'informations ou encore les modes vecteur et raster ont été exploités afin d'adapter le modèle mathématique à la représentation de l'espace géographique des SIG. L'utilisation des MNT comme source de données communes a notamment permis de tendre vers un couplage fort, dans le sens où elle est partagée par le modèle et le SIG aussi bien pour le calcul de la dispersion que pour sa visualisation cartographique. De plus, les MNT nous ont donner la possibilité d'appliquer le modèle sur différentes topographies réelles, ce qui confère plus de réalité aux simulations. Les changements d'échelle ont été modélisés selon le même principe d'amélioration de la précision pour tendre vers des simulations plus réalistes.

Le second pan du couplage est lié aux aspects techniques inhérents aux SIG, qui ont été notamment abordés lors du développement de la plateforme Drift-X dans l'environnement Quantum GIS. Ce dernier a permis l'automatisation du paramétrage du modèle au sein d'un repère projeté et la simplification de son execution grâce au langage Python et à l'architecture de plugin de QGIS. Bien que le développement SIG constitue la partie technique du couplage, celui-ci reste intimement lié aux améliorations théoriques qui ont été proposées. En effet, les flux d'entrées/sorties sont nécessaires à Drift-X pour fonctionner mais générés par les fonctionnalités de base du plugin. Par exemple, le MNT doit être traité par QGIS avant d'être envoyé à Drift-X afin qu'il calcule l'impact topographique sur la dispersion pour une étendue spatiale donnée. Sans MNT ni étendue, le modèle ne fonctionnerait pas.

Par ailleurs, plusieurs conclusions peuvent être formulée vis à vis de l'usage des MNT pour le couplage. Comme il a déja été dit, les MNT confère plus de réalisme aux sim-

ulations de la dispersion car ils permettent de manipuler des topographies réelles. De plus, le MNT d'entrée procure également les informations relatives à sa résolution et à sa projection cartographique qui sont implicitement contenues dans les triplets x,y,z adressé au modèle. Il s'agit d'un élément clé du couplage car le support du modèle de données SIG est ajouté à Drift-X uniquement grâce aux propriétés du MNT utilisé. Celà rend possible les simulations géoréférencées et permet de cartographier directement les sorties de Drift-X. Par contre, cette méthode de couplage impose à l'utilisateur de vérifier l'intégrité des données d'entrée.

La modélisation tire donc avantage de l'utilisation des MNT, et leurs impacts sur la construction du champ de vent et sur le transport du nuage de pesticides ont été démontrés dans la section 6.2. Nous avons également montré que la résolution du MNT utilisé influence la précision des résultats. Malgré celà, il a été rappelé que le modèle Drift-X est spécialement adapté aux variations topographiques continues, et qu'il ne supporte donc pas des MNT très précis car les petites variations topographiques ne seront pas prise en compte. Cela doit être amélioré car les petites variations influencent également le processus de dispersion, surtout aux échelles plus fines. En effet, l'environnement des parcelles traitées peut présenter des obstacles significatifs à la dérive qui sont visibles uniquement grâce à des MNT à haute résolution. Le modèle de transport devrait idéallement être modifié de manière à pouvoir interpréter les Modèles Numériques de Surface (MNS) car ces derniers peuvent par exemple fournir des hauteurs de bâtiments, celles de rangées d'arbre, ou encore de tout autre objet à la surface terrestre pouvant modifier le comportement du nuage. De telles modifications amélioreraient grandement la précision des calculs mais impliquerait de modifier fortement le modèle, car l'approche à complexité réduite devrait alors gérer des géométries beaucoup plus complexes. Cela se répercuterait également sur les temps de calcul en raison du grand nombres de triplets que le programme Fortran devrait lire.

D'autre part, l'extensibilité du modèle Drift-X vis à vis de l'échelle des simulations a été introduite et ses limites identifiées. L'approche multi-niveaux est ainsi apparue comme judicieuse afin de pouvoir séparer le domaine en autant de sous-domaines souhaités, et de prendre en compte graduellement des variations topographiques plus fines autour de la parcelle traitée ou d'une zone intéressante du domaine. Ceci permet de rééchantilloner les grilles de résultats et d'obtenir des champs de vents et des nuages de pesticides plus denses aux échelles les plus fines. les valeurs altimétriques des MNT sont interpolées au sein des sous-domaines mais cela n'apporte pas plus de précision en z, dans le sens ou les petites variations ne peuvent pas être identifiées à partir du MNT à résolution grossière utilisé au sein du domaine initial. Bien que de puissantes techniques de rééchantillonage et d'interpolation de MNT puissent être appliquées, la meilleure configuration dans notre cas serait d'utiliser un MNT différent à chaque niveau, mais celà n'a pas été encore implémenté dans le couplage.

Plusieurs autres conclusions s'avèrent nécessaire vis à vis de la plateforme de simulations Drift-X. L'API QGIS a procuré une puissante plateforme SIG open source pour la

mise en oeuvre du couplage technique. L'architecture de plugin et le langage Python ont également offert de la flexibilité ainsi que de nombreuses ressources de développement de manière à embarquer le modèle Drift-X dans QGIS. Il est à présent possible de paramétrer les données météorologiques, les paramètres spécifiques liés à la pulvérisation et les données topographiques depuis l'interface utilisateur du plugin Drift-X, d'éxecuter le modèle en un simple clic et de cartographier les sorties géoréférencées directement dans la vue cartographique de QGIS. Ainsi, les traitements phytosanitaires peuvent être simulés rapidement au sein de leur réalité géographique numérique, et de nombreux scénarii peuvent être testés grâce au plugin. De plus, une fois le nuage de pesticide cartographié, des dizaines d'autres fonctionnalités de QGIS peuvent être utilisées, des plus basiques comme l'interrogation d'un pixel de nuage de pesticide afin d'obtenir sa valeur de concentration, aux plus complexes comme par exemple la création de buffer autour d'un nuage de pesticde en mode vecteur. Celà améliore l'analyse de la dispersion atmosphérique et peut aider à manipuler les sorties de Drift-X au sein d'analyses spatiales plus complexes.

D'autre part, l'étude de cas sur le bassin versant de Neffiès et sa version dédiée du plugin ont démontré qu'une telle plateforme peut communiquer avec les bases de données spatiales et ainsi tirer profit des statistiques issues des traitements phytosanitaires. Le lien avec la base de données PostGIS du projet Aware a permis de construire des champs de vents à partir de mesures de vent réelles, ce qui ajoute encore de la réalité aux simulations. Ainsi, le scénario proposé dans la section 10.1 est basé sur des données topographiques et météorologiques réelles et à permis de mettre ne place une analyse de risques simplifiée de manière à quantifier l'exposition de l'environnement aux pesticides.

Le couplage de Drift-X et QGIS a d'autre part conduit à l'exploration du potentiel des SIG libres pour intégrer et améliorer les modèles environnementaux complexes. En effet, le développement du plugin QGIS à impliqué de tester plusieures méthodes de couplage , ce qui a apporté une profonde connaissance de l'API QGIS et de ses dépendances comme par exemple GDAL/OGR et PostGIS. Il en est de même à propos de l'environnement GRASS qui a permis un usage avancé des sorties de Drift-X au sein de l'environnement QGIS. Il est ainsi apparu que les SIG libres ont un grand rôle à jouer dans la modélisation scientifique à composante spatiale, et qu'ils peuvent aujourdh'ui être considéré comme une sérieuse alternative aux logiciels SIG propriétaires.

Les futures recherches devraient logiquement être composées de plusieurs études qu'il convient de détailler. A propos du modèle lui même, plusieurs améliorations possibles ont été identifiées. Premièrement, le modèle de dispersion intra-parcellaire a été utilisé en tant que "boîte noire" dans ce travail mais pourrait être amélioré. Il pourrait par exemple être couplé à d'autres modèles établis à différentes échelles. Les modèles de buses de pulvérisation et de tailles des gouttes des pesticides pourraient premièrement être utilisés afin d'obtenir des résulats plus précis quant aux quantités de pesticides atteignant la végétation. Des analyses plus fines de la dispersion intra-parcellaire pourraient également être menées grâce aux outils de CFD ou de LES, qui permettraient de simuler des champs de vents élaborés au sein des parcelles de vignes. Des modèles de volatilisation

pourraient d'autre part être couplé à Drift-X dans le but d'améliorer la précision des quantités de pesticides s'élevant au dessus de la parcelle. Cela procurerait de meilleures données d'entrées au modèle de transport. Ce dernier devrait aussi être assujetti à des améliorations notamment à propos de la construction des champs de vents et de la prise en compte de la topographie. En effet des processus éoliens plus complexes doivent être étudiés de manière à minimiser les erreurs, spécialement sur les champs de vents instables et tournants. L'implémentation de MNS au sein d'une architecture multi-niveaux plus complexe pourrait d'ailleurs concourir à la modélisation des turbulences dues aux obstacles se trouvant sur la trajectoire du nuage. Des compromis devront être établis entre la modification du modèle pour améliorer la précision des résultats, et l'augmentation des temps de calculs, qui doivent rester les plus faibles possible pour mener des simulations SIG rapides.

Par ailleurs, d'importantes recherches et des expériences aux champs devront etre menées pour tendre vers la validation du modèle. Plusieurs projets initiés par le Cemagref permettront peut-être d'équiper le bassin-versant de Neffiès d'anémomètres et de collecteurs. Ceux-ci permettraient de collecter des mesures de vents précises et sur de longues périodes, et de les confronter avec les champs de vents simulés par Drift-X. Il en est de même pour les collecteurs d'air qui procureraient de nombreux échantillons d'air à différentes distances de la parcelle. Ceux-ci seraient ensuite analysés grâce aux techniques de chromatographie et les valeurs de concentration observées pourraient être comparées aux valeurs simulées. La validation du modèle Drift-X sera une recherche longue et coûteuse, et l'utilisation des SIG est à nouveau fortement recommandée pour ce travail, car ils permettraient de déterminer au mieux les positions des anémomètres et des collecteurs en utilisant des MNT, des analyses de pentes ainsi que la connaissance des vents dominants locaux.

De plus, d'autres améliorations possibles sont à formulées quant à la plateforme de simulation Drift-X. Comme il a été dit, le meilleur scénario serait de convertir le programme Fortran en une classe QGIS, pouvant être écrite en C++ or Python. Cela procurerait un couplage intégré entre le Drift-X et QGIS et permettrait d'utiliser des fonctionnalités de QGIS bien plus avancées depuis le plugin. Ainsi, l'analyse spatiale basée sur les couches de nuages de pesticides pourraient être automatisée et la plateforme tendrait ainsi vers un véritable outil d'aide à la décision dédié à la prédiction et à l'analyse de la pollution atmosphérique. Par ailleurs, d'autres travaux de développement SIG ont déja commencé dans l'optique d'adapter le couplage à une architecture de webmapping. L'utilisation des outils et librairies open source permettra bientôt de réaliser des simulations Drift-X depuis un simple navigateur Internet. La plateforme de webmapping sera construite grâce aux logiciels MapServer, PostGIS et OpenLayers qui seront réunis au sein d'une architecture Web Processing Service (WPS), afin de pouvoir faire communiquer Drift-X avec l'internaute à travers le chainage de webservices standards tels que Web Map Service (WMS) et Web Feature Service (WFS).

Enfin, nous pouvons conclure que le couplage a permis de simuler la dispersion atmosphérique des pesticdes agricoles dans un environnement SIG, mais que d'autres processus

de dispersion atmopshérique pourraient être modélisés en utilisant Drift-X. En effet, la compléxité réduite permettra par exemple d'adapter les équations à la dispersion atmosphérique d'origine industrielle. Ainsi, les nuages de pollution émis par les cheminées industrielles pourront être modélisés et cartographiés grâce à la plateforme Drift-X.

List of Figures

1 Pulvérisateur typique utilisé dans les vignobles du sud de la France 2
2 Nuage de pesticides observé tôt le matin à Neffiès (34) 2
3 Typical sprayer used in southern French vineyards 7
4 Early morning pesticide cloud observed at Neffiès (34) 7

1.1 Atmospheric layers 14
1.2 ABL and BSL layers 15

2.1 GIS Vector and Raster data models 22
2.2 Cartesian (left) and Geographic (right) coordinate systems 23

4.1 Map of European territory (left) and its distorted isochronic representation (right) based on driving travel times. 38
4.2 Sketch of the plume model in a cartesian metric for a uniform flow field . . 40
4.3 Sketch of the plume in a travel-time based metric for a rotating flow field . 40

5.1 Sketch of the multi-leveled construction 44
5.2 Example of three-level construction of an experimental rotating flow field. . 46
5.3 Sketch of topography variation and normals definitions 47
5.4 Sketch of topography variation and non symmetry in cross-definition for a constant velocity field 47
5.5 Drift based on a flow field evaluated from an instantaneous measurement (top), mean drift based on ensemble average and Monte Carlo simulation (middle) and drift standard deviation (bottom). 50
5.6 Example snapshots of the concentration distribution evolution in time . . . 50

6.1 A close-up of the resulting tractor's trajectory within the treated plot. . . . 52
6.2 The flow field constructed using the modeling detailed 4.3.4 with an example close-up (bottom left) 52
6.3 The resulting point shapefile (.shp) pesticide cloud using the calculated flow field of figure 6.2 and the source plot. 53
6.4 the same pesticide cloud as presented in figure 6.3 but displayed as a triangular interpolated raster layer (.tiff). 53
6.5 Topographic profile and plot and wind points location for simulations . . . 54
6.6 Resulting raster pesticide cloud from the plateau treatment with a downhill wind. 55

6.7 Resulting raster pesticide cloud from the bootom of the bank with an upsolpe wind treatment . . . 55
6.8 Standard IGN 50m DEM layer (top left) resampled at 100 m (top right), 200 m (bottom left) and 400 m (bottom right) resolutions . . . 56
6.9 Resulting pesticide clouds with IGN 50m DEM layer (top left), 100 m (top right), 200 m (bottom left) and 400m (bottom right). . . . 57
6.10 Comparison of the 50 m, 200 m and 400 m DEM layers topographic profiles 58
6.11 Comparison of the Drift-X concentrations curves over the 50 m and 100 m DEM layer. . . . 58
6.12 Comparison of the Drift-X concentrations curves over the 50 m, 200 m and 400 m DEM layer. . . . 58
6.13 Drift-X simulation on a 12 ha domain with two wind points at 1m/s . . . 59
6.14 Drift-X simulation on a 6km^2 domain with two wind points at 5m/s . . . 59
6.15 Example of two-leveled construction of a pesticide cloud with the finer level located on the treated plot. Close-up on the finer level in raster mode (top right). . . . 60
6.16 Two-level simulation on a larger domain . . . 61

7.1 Scheme of the data flow used for coupling Drift-X model and Quantum GIS. 66
7.2 Point shapefile pesticide cloud but with no data features deleted . . . 69
7.3 Generated point shapefile wind field with arrows oriented according to direction values . . . 69
7.4 Raster pesticide cloud generated using Kriging (left), Natural Neighbors (middle), and TIN (right) interpolation methods . . . 71
7.5 Quantum GIS user interface with Drift-X plugin activated . . . 72
7.6 An example plugin tab to choose the input DEM on which to compute . . . 72

8.1 Neffiès watershed general view . . . 76
8.2 Neffiès vineyards map . . . 76

9.1 simplified scheme of the Life Aware PostGIS database . . . 80
9.2 Plots 03E, 10A and 10C with the corresponding simultaneous mean wind points extracted from the Aware PostGIS database . . . 81

10.1 Resulting three simultaneous pesticide clouds . . . 85
10.2 Neffies CLC layer classes . . . 86
10.3 Neffies CLC layer classes intersecting the Drift-X layer . . . 87
10.4 Clipped CLC layer presenting the sum of concentrations values per classes 88
10.5 Clipped CLC layer presenting the averaged concentrations values per classes . . . 88
10.6 Neffiès built area layer presenting the sum of concentrations values per classes . . . 89
10.7 Neffiès water courses layer presenting the sum of concentrations values per classes . . . 89

List of Acronyms

List of ADM related acronyms

ADM	Atmospheric Dispersion Modeling
ABL	Atmospheric Boundary Layer
CFD	Computational Fluid Dynamics
DNS	Direct Numerical Simulations
LES	Large Eddy Simulations
PDE	Partial Differential Equations
PSL	Planetary Surface Layer
VLES	Very Large Eddy Simulations

List of GIS related acronyms

API	Application Programmable Interface
GIS	Geographic Information Systems
GPS	Global Positioning System
GPX	GPS eXchange Format
DEM	Digital Elevation Model
DTM	Digital Terrain Model
DSM	Digital Surface Model
EPSG	European Petroleum Survey Group
IGN	Institut Géographique National
OSGeo	Open Source Geospatial Foundation
RGF	Réseau Géodésique Francais
SQL	Structured Query Language
SRTM	Shuttle Radar Topography Mission
SWIG	Simplified Wrapper and Interface Generator
TIN	Triangulated Irregular Network
QGIS	Quantum Geographic Information System
GRASS	Geographic Resources Analysis Support System

Bibliography

[1] Donaldson D. Kiely T. and Grube A. Pesticides industry sales and usage, 2004.

[2] Carpentier A. L. Guichard P. Lucas S. Savary I. Savini Aubertot J.N., Barbier J.M. and Voltz M. Reducing the use of pesticides and limiting their environmental impact, collective scientific expert report, 2005.

[3] F. De Leeuw, W. Wan Pul, F Van Den Berg, and A. Gilbert. The use of atmospheric dispersion models in risk assessment decision support system for pesticide. *Environmental Monitoring and Assessment*, 62, 2000.

[4] A. DaSilva, C. Sinfort, C. Tinet, D. Pierrat, and S. Huberson. A lagrangian model for spray behaviour within vine canopies. *Aerosol Science*, 37, 2005.

[5] M. Deluca. *Contribution à la modélisation de l'atomisation d'un jet liquide en vue de réduire les pollutions : Application à la pulvérisation de produit phytosanitaire.* PhD thesis, University of Méditerannée, 2007.

[6] Verboven P. Baetens K. Ramon H. Endalew A., Hertog M. and Nicolaï B. Modelling airflow through 3d canopy structure of orchards. *Aspects of Applied Biology - International advances in pesticide application 2006*, 77, 2006.

[7] C. Bedos, P. Cellier, and P. Gabrielle. Modélisation de la volatilisation des pesticides. In *Actes du 35ème congrès du Groupe Français des Pesticides*, 2005.

[8] F. Ferrari, M. Trevisan, and E. Capri. A lagrangian model for spray behaviour within vine canopies. *Journal of Environment Quality*, 32, 2003.

[9] Y. Gil Pinto. *Caracterisation expérimentale des émissions de pesticides vers l'air pendant les pulvérisations viticoles.* PhD thesis, Montpellier SupAgro, 2007.

[10] Patel N.R. Remote sensing and gis application in agro-ecological zoning. In *Proceedings of the Training Workshop Satellite remote sensing and GIS applications in agricultural meteorology*, 2003.

[11] Sivakumar M.V.K. and Hinsman D. Satellite remote sensing and gis applications in agricultural meteorology and wmo satellite activities. In *Proceedings of the Training Workshop Satellite remote sensing and GIS applications in agricultural meteorology*, 2003.

[12] M. Markiewicz. Modeling of air pollution dispersion. Technical report, 2006.

[13] U. Dragosits, C.J. Place, and R.I. Smith. The potential of gis and coupled gis/conventional systems to model acid deposition of sulphur dioxide. In *Third International Conference/Workshop on Integrating GIS and Environmental Modeling*, 1996.

[14] H. Karimi and B. Houston. Evaluating strategies for integrating environmental models with gis: current trends and future needs. *Computers, Environment and Urban Systems*, 20, 1997.

[15] L. Bernard, B. Schimdt, U. Streit, and C. Uhlenküken. Managing, modeling, and visualizing high-dimensional spatio-temporal data in an integrated system. *Geoinformatica*, 59, 1998.

[16] I.C. Agrawal, R.D. Gupta, and V.K. Gupta. Gis as modelling and decision support tool for air quality management: a conceptual framework. In *MapAsia Conferences*, 2003.

[17] N. Bozon and Mohammadi B. Gis based atmopsheric dispersion modelling forecasting the pesticide atmospheric spray drift from a vineyard plot to a watershed. *Applied Geomatics*, 6, 2009.

[18] N. Bozon, Mohammadi B., and C. Sinfort. Similitude and non symmetric geometry for dispersion modelling. *Proceeding of STIC and Environment 2007*, 5, 2007.

[19] R. Thompson. *Atmospheric Processes and Systems*. 1998.

[20] M. Beychok. *Fundamentals of Stack Gas Dispersion*. Beychok, 4th edition, 2005.

[21] Bruce Turner D. *Workbook of Atmospheric Dispersion Estimates: An Introduction to Dispersion Modeling*. CRC Press Inc, 2nd edition, 1994.

[22] Schnelle K. and Dey.P. *Atmospheric Dispersion Modeling Compliance Guide*. McGraw-Hill Inc., 1st edition, 1999.

[23] J-M. Brun. *Modèles à compléxité réduite de transport pour applications environnementales*. PhD thesis, Université Montpellier 2, 2007.

[24] A. Da Silva. *Modélisation numérique des dépôts de produits phytosanitaires*. PhD thesis, Université Montpellier 2, 2003.

[25] Ministère de l'écologie et du développement durable. La dispersion atmosphérique. Technical report, 2002.

[26] A. Fotheringham and M. Wegener. *Spatial models and GIS*. Taylor and Francis, 1st edition, 2000.

[27] R. Tomlinson. *Thinking about GIS*. ESRI Press, 1st edition, 2003.

[28] P. Wilson and J. Gallant. *Terrain Analysis: Principles and Applications*. John Whiley and Sons Inc., 1st edition, 2000.

[29] P. Snyder. *Map Projections: A working manual*. USGS Professional Papers, 1st edition, 2000.

[30] A. Quattrochi and M. Goodchild. *Scale in Remote Sensing and GIS*. Lewis Publishers, 1st edition, 1997.

[31] M. Duckham M., Goodchild and M. Worboys. *Fundations of Geographic Information Science*. Taylor and Francis, 1st edition, 2003.

[32] M. Jacobson. *Fundamentals of Atmospheric Dispersion*. Cambridge University Press, 2nd edition, 2005.

[33] G. Hart, A. Tomlin, J. Smith, and M. Berzins. Multi-scale atmospheric dispersion modelling by use of adaptive gridding techniques. *Environmental Monitoring and Assessment*, 52, 2004.

[34] T. Ott and F. Swiaczny. *Time-integrative Geographic Information Systems*. Springer, 1st edition, 2001.

[35] P. Wilson, J.and Burrough. Dynamic modeling, geostatistics, and fuzzy classification: New sneakers for a new geography? *Annals of the Association of American Geographers*, 89, 1999.

[36] T. Nyerges. Coupling gis and spatial analytic models. In *5th International Symposium on Spatial Data Handling : Charleston, S.C., USA*, 1992.

[37] B. Huang and B. Jiang. Avtop: a full integration of topmodel into gis. *Environmental Modelling and Software*, 17, 2001.

[38] Wong.D, Camelli.F, and Sonwalkar.M. Integrating computational fluid dynamics (cfd) models with gis: an evaluation on data conversion formats. volume 6753. SPIE, 2007.

[39] A.K.M. Chua, R.C.W. Kwokb, and K.N. Yua. Study of pollution dispersion in urban areas using computational fluid dynamics (cfd) and geographic information system (gis). *Environmental Modelling and Software*, 20, 2005.

[40] C. Sood and R.M. Bhagat. Interfacing geographical information systems and pesticide models. *Current Sciences*, 89, 2005.

[41] N.K. Hewitt, J. Maber, and J.P. Praat. Drift management using modeling and gis systems. In *World Congress of Computers in Agriculture and Natural Resources*, 2002.

[42] K.J. Allwine, F.C. Rutz, J.G. Droppo, J.P. Rishel, E.G. Chapman, S.L. Bird, and H.W. Thistle. Spraytran 1.0 user guide: A gis-based atmospheric spray droplet dispersion modeling system. User guide, U.S. Department of Agriculture Forest Service, 2006.

[43] K. Hoffmann, W.and Fritz and D. Martin. Agdisp sensitivity to crop canopy characterization. In *NAAA Convention and Exposition*, 2005.

[44] P. Rangel Sotter, A Hamersson Sánchez Ipia, Cely Pulido, and W. Libardo Siabato Vaca. Alternative analysis viewpoints for air pollutants in bogotá d.c. *Applied Geostatistics to Studies of Environmental Contamination*, unknown, 2003.

[45] L.D. Koffman. Integration of predicted atmospheric contaminant plumes into arcview gis. In *1st Joint Emergency Preparedness and Response and Robotic and Remote Systems Topical Meeting*, 2005.

[46] N.Kh. Arystanbekova. Application of gaussian plume models for air pollution simulation at instantaneous emissions. *Mathematics and Computers in Simulation*, 67, 2004.

[47] 0. Wilhelmi, T. Betancourt, J. Boehnert, S. Shipley, and J. Breman. Arcgis atmospheric data model. In *ArcGIS Atmospheric Data Model Reference*, 2005.

[48] O. Dassau, S. Holl, M. Neteler, and M. Redslob. *An introduction to the practical use of the Free Geographical Information System GRASS 6.0.* GDF Hannover, 2nd edition, 2005.

[49] A. Vitti, P. Zatelli, and F. Zottele. 3d vector approach to local thermally driven slope winds modeling. In *Proceedings of the FOSS/GRASS Users Conference 2004*, 2004.

[50] M. Ciolli, A. Vitti, D. Zardi, and P. Zatelli. 2d/3d grass modules use and development for atmospheric modeling. In *Proceedings of the Open source GIS - GRASS users conference*, 2002.

[51] Sinfort.C. Link between experimental research and modelisation for the optimisation of agricultural spraying processes, hdr memoir, 2006.

[52] Ciarlet P. *The finite element method for elliptic problems.* 1978.

[53] Patera A. and Veroy K. Certified real-time solution of the parametrized steady incompressible navier-stokes equations: Rigorous reduced-basis a posteriori error bounds. *Institute of Computational Fluid Dynamics Conference No8, Oxford*, 47, 2005.

[54] Cousteix J. *Turbulences et couche limite.* 1989.

[55] Simspson J. *Gravity currents in the environment and laboratory.* 1999.

[56] Frey P. Alauzet F., George P-L. and Mohammadi B. Transient fixed point based unstructured mesh adaptation. *International Journal of Numerical Methods in Fluids*, 43, 2003.

[57] Hecht F. and Mohammadi B. Mesh adaptation by metric control for multi-scale phenomena and turbulence. *Journal of American Institute of Aeronautics and Astronautics*, 97-0859, 1997.

[58] Borouchaki H. George P-L. and Mohammadi B. Delaunay mesh generation governed by metric specifications. *Finite Element in Analysis and Design*, 25, 1999.

[59] D.G. Krige. *A statistical approach to some mine valuations and allied problems at the Witwatersrand*. PhD thesis, Master's thesis of the University of Witwatersran, 1951.

[60] J.-P. Chiles and Delfiner P. *Geostatistics: Modeling Spatial uncertainty*. 1999.

[61] Mohammadi B. and Pironneau O. *Analysis of the K-Epsilon Turbulence Model*. 1994.

[62] Mohammadi B. and Puigt G. Wall functions in computational fluid mechanics. *Computers and fluids*, 35, 2006.

[63] Clive G. Page. Professional programmer's guide to fortran 77, June 2005. `http://www.star.le.ac.uk/ cgp/prof77.html`.

[64] Franck Warmerdam. Gdal/ogr project homepage, December 2008. `http://www.gdal.org/`.

[65] David Finlayson. grid2xyz gis scripts webpage, December 2007. `http://david.p.finlayson.googlepages.com/gisscripts`.

[66] Barry Rowlingson. Region tool homepage, December 2007. `http://www.maths.lancs.ac.uk/ rowlings/Software/regionTool/`.

[67] Y. Doytsher and J. Hall. Interpolation of dtm using bi-directional third-dgree parabolic equations with fortran subroutines. *Computers and Geosciences*, 23, 1998.

[68] G. Sherman. Shuffling quantum gis in the open source gis stack. In *Proceedings of the 2007 FOSS4G conference, Victoria*, 2007.

[69] Marco Hugentobler. Qgis interpolation plugin, January 2006. `http://homepage.hispeed.ch/hugis/`.

[70] David M. Beazley. Swig project homepage, December 2008. `http://www.swig.org/`.

[71] Pessl Instruments GmbH. Pessl instruments gmbh homepage, April 2009. `http://www.metos.at`.

[72] J.M D'Arcy. Pygresql homepage, February 2006. `http://www.pygresql.org`.